NTNU

Norwegian University of
Science and Technology

Characterisation of Feed and Produced Material in Screw Extrusion of Titanium

Jan Inge Hammer Meling

Materials Science and Engineering
Submission date: June 2016
Supervisor: Hans Jørgen Roven, IMTE
Co-supervisor: Kristian G. Skorpen, IMT
Oddvin Reiso, IMT

Norwegian University of Science and Technology
Department of Materials Science and Engineering

Abstract

A novel method of extrusion of materials with high viscosity is being developed at NTNU, the method is based on screw extrusion, which is more known in the plastic industry. The process, at the end of the development cycle will hopefully reduce cost in production of titanium and its titanium alloys, as well as open doors for new titanium alloys. The work will be based on characterisation of titanium sponge and corresponding screw extruded material. With the use of metallurgical methods such as elemental analysis, hardness testing, heat treatments, light microscopy and tensile testing the titanium sponge and screw extruded material will be evaluated and modified for optimisation of the process and a better quality product.

Heat treatments of titanium sponge showed a decrease in hardness and the presence of recrystallization. The effect of lowered strength in titanium sponge was tested in compression shear deformation experiments. The tests showed a correlation between lowered hardness of titanium sponge and an increased consolidation. However, the testing method needs further work and optimisation.

The screw extruded profiles show a relative large increase in chemical contamination and varying deformation over the cross section of the material. The material also showed inhomogeneity along the cross section parallel to the extruding direction. A protective atmosphere during screw extrusion is needed. Further processing of profiles should probably include compression of profiles at high temperatures to ensure enhanced diffusion bonding, removal of cracks and stress relief.

Sammendrag

En ny fremgangsmåte for ekstrudering av materialer med høy viskositet blir utviklet ved NTNU, fremgangsmåten er basert på skrue-ekstrudering, som er mer kjent i plastindustrien. Prosessen, ved slutten av utviklingssyklusen vil forhåpentligvis redusere kostnadene ved produksjon av titan og dets titanlegeringer, samt åpne dørene for nye titanlegeringer. Arbeidet vil være basert på karakterisering av titan svamp og tilhørende skrue ekstrudert materiale. Med bruk av metallurgiske metoder som elementanalyse, hardhet testing, varmebehandlinger, lysmikroskopi og strekkprøving vil titan- svampen og skrue ekstruderte materialet bli vurdert og modifisert for optimalisering av prosessen, og ett bedre kvalitet på produktet.

Varmebehandling av titan-svamp viste en reduksjon i hardhet og rekrystallisering. Virkningen av redusert styrke i titansvamp ble testet i kompresjons skjærdeformerings eksperimenter. Testene viste en sammenheng mellom senket hardhet av titansvamp og en økt konsolidering. Men testmetode må utvikles og optimaliseres.

Skrue ekstruderte profiler viser en relativ stor økning i kjemisk forurensning og varierende deformasjon over tverrsnittet av materialet. Materialet viste også inhomogenitet langs tverrsnittet parallelt med ekstruderingsretningen. En beskyttende atmosfære under skrue-ekstrudering er nødvendig. Videre behandling av profiler bør trolig inkludere komprimering av profiler ved høye temperaturer for å sikre økt diffusjons heft, fjerning av sprekker og spennings utjevning.

Preface

This work has been carried out at the Norwegian University of Science and Technology(NTNU) at the Department of Materials Science and Engineering.

I would like to thank my supervisor Hans Jørgen Roven for guiding my hand and giving me the opportunity to work on this project. I also want to express my sincere gratitude to Kristian G Skorpen for exciting discussions both technical and other. In addition, I would like to thank my co-supervisors Ola Jensrud and Oddvin Reiso for thoughtfully and intelligent input into the project. I would also like to thank Martin Borlaug Mathisen and Norsk Titanium for technical discussion and help, as well as many thanks to Pål Skaret, Torild Krogstad and Trygve Schanche in assistance with the experimental work.

Honourable mentions go to my classmates and friends, without you my concentration and grades would be a lot better. Finally, lots of love to Maren Elise, you are the coolest.

Trondheim, June 2016
Jan Inge Meling

Contents

1 Introduction

Titanium is a useful but expensive material. The high strength at high temperatures, high corrosion resistance and lightness make it an exciting material. However, the obstacle faced by titanium usage is high production cost and huge wastage. A continuous screw extrusion method for materials with high viscosity has been developed at NTNU over several years to lower these costs. With a lower working temperature and less energy input it should, at the end of the development cycle produce CP titanium and alloy profiles at a significantly lower price than former casting methods.

The screw extrusion process was originally constructed for aluminium. As research continued and milestones were past, a possibility in production of titanium was taken. Through use of metallurgical methods as hardness, microscopy, microstructure, chemical composition analysis and tensile test this thesis intends to ratify and determine the current state of the screw extrusion of titanium. The input material, titanium sponge, is examined for chemical composition and microstructure, as well as how a heat treatment will change its characteristics. With this information, an investigation into the effect of these heat treatments in a process designed to simulate the screw extrusion process is done. There is also an investigation into the already screw extruded material. Hardness, chemical composition as well as tensile test are used to determine the need for after treatment. With this information the state of the project and if the project should be continued will be determined and further work suggested.

Originally, several screw extrusion experiments of titanium were planned, where the focus on the characteristics of the input material, the efficiency of the process and the final product was placed. However, due to a delay in production of a new screw for the process, a different approach to the project was taken. A pressure torsion process is used to investigate what effect pre heated titanium sponge has on the screw extrusion process. Leading to two questions that will guide this thesis, will heat treatment of titanium sponge optimise the screw extrusion process and to what degree is the already produced material within industry specifications.

On the next page, a flow chart overview of the project is shown in Figure 1-1. The intent is to give a quick overview over paths and sequence of the thesis. The figure show two paths of inquiry designed to answer two simple questions, is the material that is already produced within or close to industry demands and will heat treatment of sponge increase efficiency for the screw extrusion process.

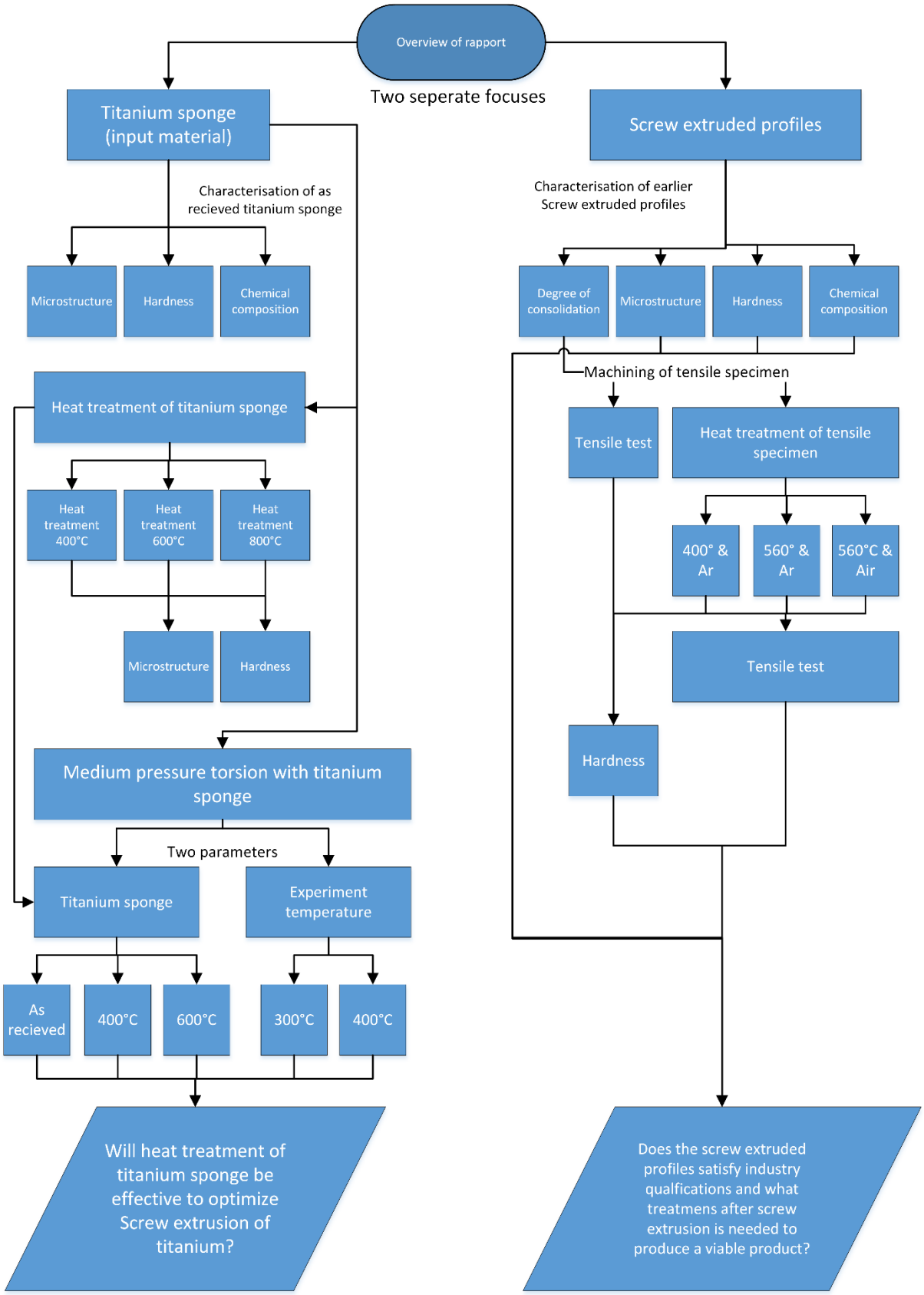

Figure 1-1. Flow chart representation of the project. Two paths designed to answer two questions.

1.1 Aim of work

This work is structured along two paths. The aim is to characterise the titanium sponge and screw extruded profiles. In the first path, titanium sponge is characterised through methods such as chemical composition, hardness and microstructure. A following study will focus on the effect of a heat treatment on titanium sponge using microstructural and hardness examinations. This will lead in turn to a testing of differently treated sponge in a medium pressure torsion(MPT) experiment designed to determine any change in consolidation in terms of input material.

The second path, i.e. characterisation of the screw extruded profiles will focus on chemical composition, hardness and microstructure as well as tensile test. These test will determine the amount of contamination spanning from titanium sponge to screw extruded profiles, the homogeneity, degree of deformation and overall consolidation behaviour.

2 Theoretical background

A general overview of the properties of titanium vs aluminium is shown in Table 2-1. The reason for this comparison lies in the screw extrusion process where the project already has reached several milestones with aluminium, and any further development of extrusion of titanium will be built upon this research foundation.

Table 2-1. Property table for titanium and aluminium, data gathered from ASM Handbook (1990), Boyer et al. (1994) and M.J. Donachie (1988)

Property	***Unit***	***Al***	***Ti***
Atomic number	-	13	22
Allotropic transformation	°C	-	$\alpha \overset{882}{\longrightarrow} \beta$
Crystal structure	-	fcc	$hcp \rightarrow bcc$
a	Nm	0.405	0.295
c	Nm	-	0.468
Melting point	°C	660.4	1668
Relative density (at 25°C)	-	2.698	4.507
Elastic modulus	GPa	62	100-145
Tensile strength	MPa	60	235
0.2% yield strength	MPa	20	140
Elongation in 50 mm?	%	45	54
Thermal conductivity (20 to 500°C)	$\frac{W}{mK}$	247	11,40
Cp at Room temperature	$\frac{Kj}{Kg * K}$	0.900	0.5223
Coefficient of thermal expansion (20 to 500°C)	$\frac{10^{-6}}{°C}$	27.4	8.41
Price, Metalprices.com (2016)	$/ton	1600	11500

The important aspects to take from Table 2-1, are titanium's melting temperature, its transus temperature and strength, as well as its low thermal conductivity. These are important aspects as the screw extrusion process today, is designed with aluminium in mind. Another critical aspects of titanium are its high affinity for oxygen and hydrogen, giving it excellent corrosion resistance(Roven, 1985), but at a huge cost as all forming processes and welding has to be done in a vacuum or inert atmosphere(M.J. Donachie, 1988).

2.1 Phases – the microstructure of titanium

Titanium can be classified into three simple types of phases, α-phases, β-phase and mixed α/β phase. These phases have a substantial influence on the properties of titanium and its alloys, such as: strength, diffusion, ductility, fracture strength, creep performance and hot workability. A titanium aluminium phase diagram is included as Figure 2-1.

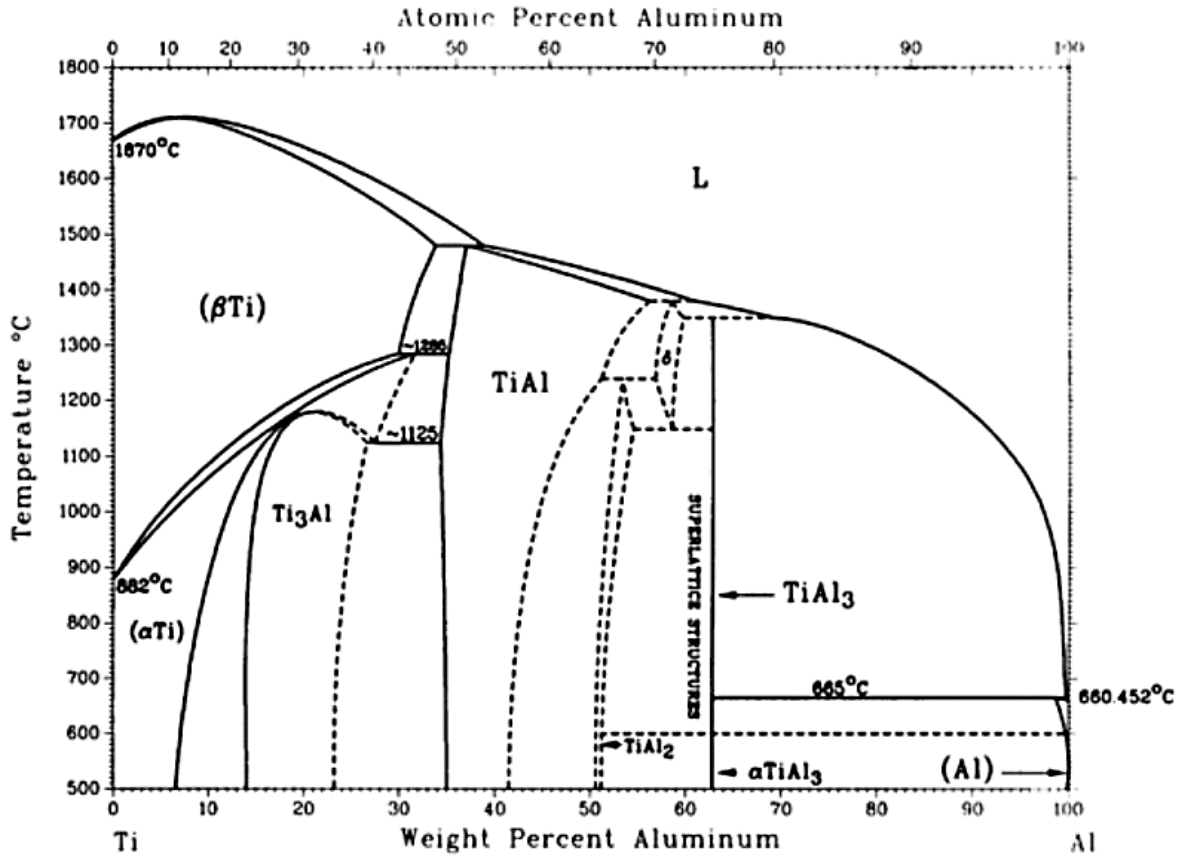

Figure 2-1. The phase diagram Ti-Al. At the far left the mentioned α & β phases are presented with a transus temperature at 882°C, gathered from ASM Handbook (2015).

For pure titanium, the α-phase is stable at temperatures up to 882°, here, the phase is arrange in a hexagonal crystal system(HCP). This arrangement causes poor deformability see chapter 2.2, as well as a low diffusion rate of $D^{\alpha\text{-}Ti} \approx 10^{-19}$ at 500°C(Peters et al., 2005). The HCP crystal system also has a pronounced anisotropy, were the Young's modulus of titanium single crystals consistently varies between 145GPa for a load vertical to the basal plane, and only 100GPa parallel to this plane.

Above 882°C is titanium β-phase, which is arranged as a body-centred cubic crystal(BCC). BCC has a much better deformability than HCP. It also exhibits a higher self-diffusion rate of $D^{\beta\text{-}Ti} \approx 10^{-18}$ at 500°C(Peters et al., 2005). This makes it the best phase to undergo work, and it is common practice to heat titanium to β-phase and form the product to its near final form before cooling.

2.1.1 The microstructure of titanium

The microstructure of titanium is of great importance and influence several characteristics. The categories are divided into either lamellar or equiaxed, as either coarse or fine. Lamellar microstructure is developed with slow cooling from above the β-transus temperature, see Figure 2-2 for a demonstration and Figure 2-4 for an illustration. The α-phase will nucleate along the grain boundaries and form into lamellar structure. The cooling rate will determine if it becomes either fine or coarse, where the lamellar microstructure becomes coarser with reduced cooling rate. Lamellar microstructure is a needle structure where all needles in the same grain are orientated in the same direction. Observe the orientation switch between the grain boundary in Figure 2-2, where a typical lamellar structure is shown from a Grade 5 Titanium. Another form of the lamellar structure is the Widmanstätten structure. Notice the 60° orientation relationship between the needles, this is the reason for the microstructure name basketweave, as is shown in Figure 2-3.

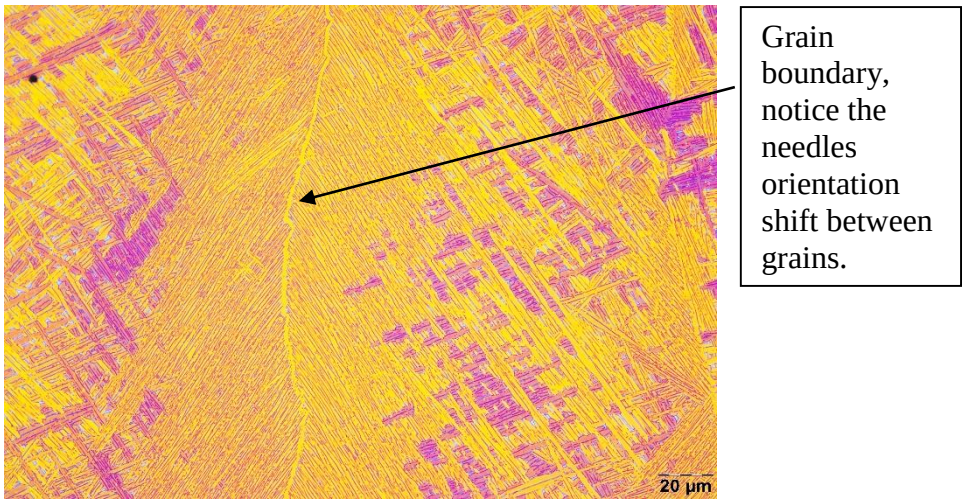

Figure 2-2. Demonstration of lamellar microstructure (curtesy of Norsk Titanium). The top picture shows lamellar microstructure at 500 magnification. The Titanium alloy is grade 5 (Ti-6Al-4V).

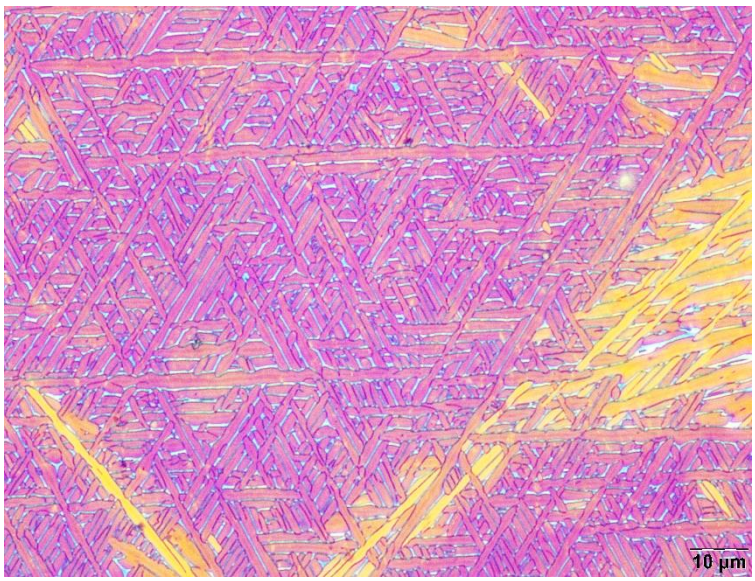

Figure 2-3. Demonstration of basketweave microstructure (curtesy of Norsk Titanium) at 1000 magnification. The titanium alloy is Grade 5 (Ti-6Al-4V).

At rapid cooling rates, it is possible to get a martensitic transformation of β-phase forming a fine needle-like microstructure. However, it is important to note that this martensitic transformation does not enhance the material at the same ratio as in steel, for titanium the increase in hardness and strength is only moderate. The volume fraction of α-phase is determined by the solution heat treatment, where lower temperature gives a higher volume fraction. There are also benefits of creating a bimodal microstructure, a mix of lamellar and equiaxed microstructure.

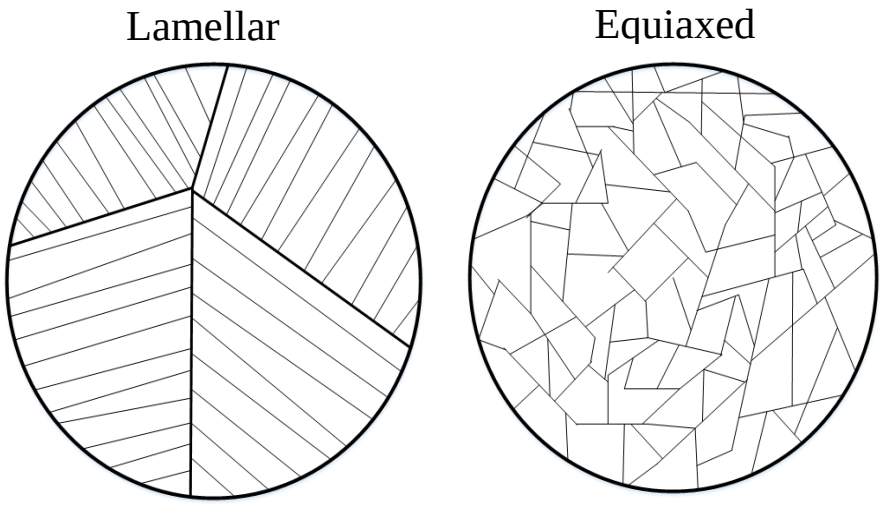

Figure 2-4. Lamellar microstructure is represented to the left, the characteristic microstructure of the equiaxed is shown to the right.

The equiaxed phase, illustrated in Figure 2-4, can be obtained through a recrystallization process, where the material has to be heavily deformed. This intends to create surface where nucleation can occur, a following solution heat treatment just below or in the α+β phase field will lead to a high nucleation rate and formation of many small grains. A rapid cooling prevents significant growth in grain size.

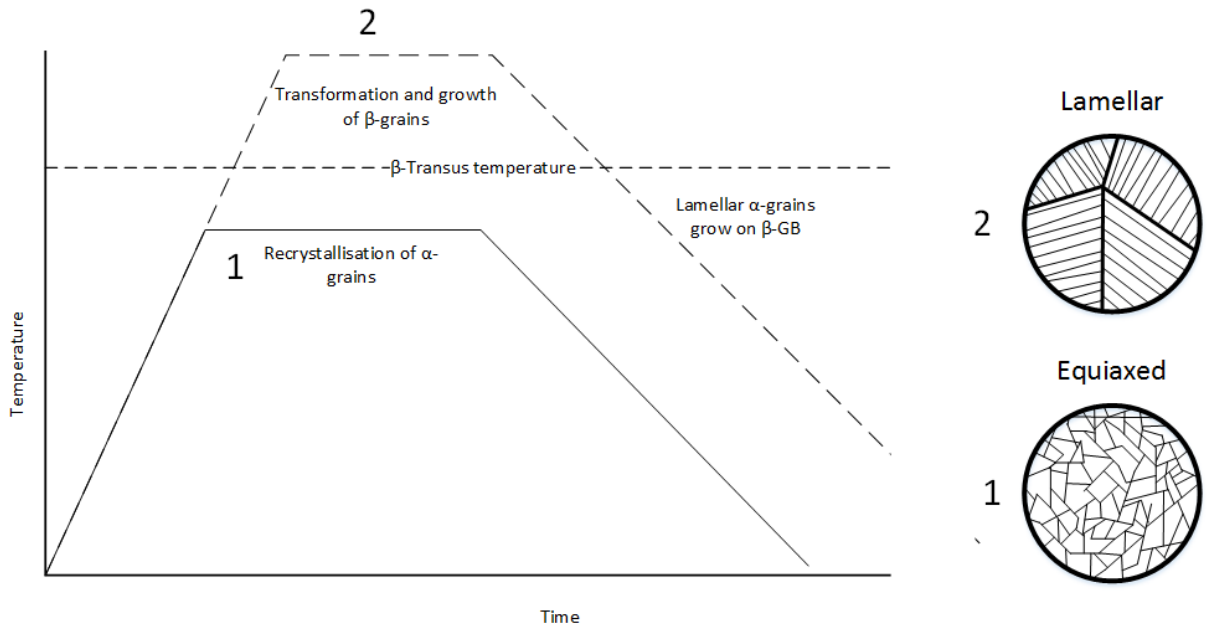

Figure 2-5. A simplification of the heat treatment needed to create the desired microstructure. Lamellar and equiaxed heat treatments are separated by the β-transus temperature.

An illustration of the process to produce the microstructures are presented below in Figure 2-5. The size, volume fraction of microstructure, as well as creation of basketweave vs lamellar structure are all temperature and time dependent. Slower cooling after recrystallization leads to large grains, slow cooling from above β transus temperature forms lamellar structure.

Table 2-2 has been included as an overview of the positive and negative sides of the lamellar vs equiaxed as well as a fine or coarse distribution. Equiaxed gives a stronger material as well as more ductile, the lamellar microstructure on the other hand has an improved fracture toughness and creep strength.

Table 2-2. Influence of microstructure on selected properties of titanium alloy, gathered from Peters et al. (2005)

Fine	Coarse	Property	Lamellar	Equiaxed
+	-	Strength	-	+
+	-	Ductility	-	+
-	+	Fracture toughness	+	-
+	-	Fracture crack initiation	-	+
-	+	Fatigue crack propagation	+	-
-	+	Creep strength	+	-
+	-	Super plasticity	-	+

2.1.2 Titanium alloys

Alloying of titanium is focused on the stabilisation of either the α- or the β-phase. These titanium alloys have varied properties depending on the dominate phase. The alloying elements are split into what phase they stabilize, which is related to the number of bonding electrons. Aluminium, oxygen, nitrogen, carbon are examples of α-phase stabilisers, the β-phase stabilisers are Va, Mo, Ta, Fe, Mn, Ni, Si, Cu. The stabilizing effect of each phase on titanium is illustrated in Figure 2-6.

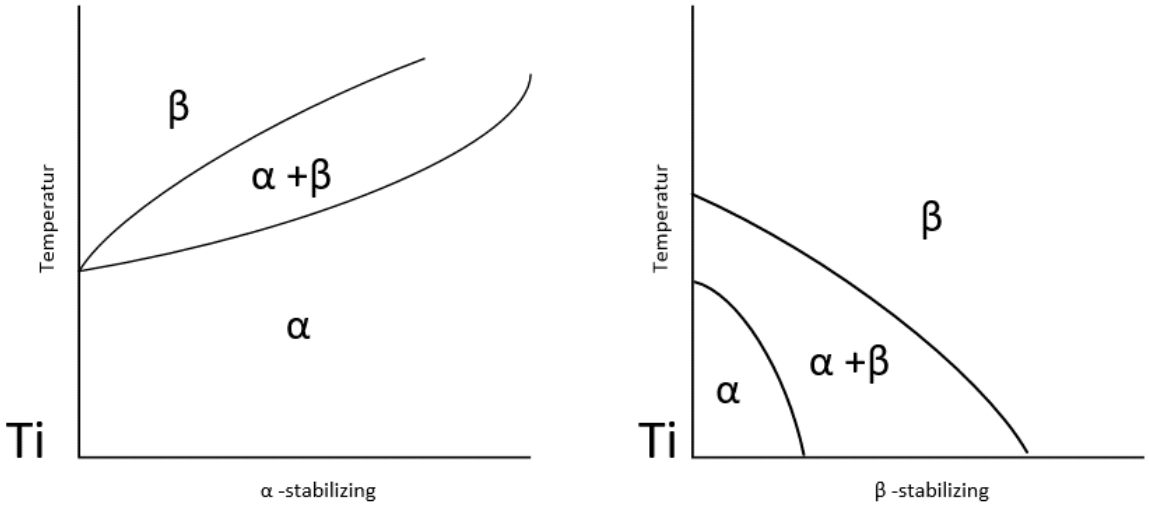

Figure 2-6. An illustration of the effect of stabilising alloy elements have on the phase diagram. The illustration show a pseudo phase diagram, with increase element composition along the bottom axis.

Another important alloying effect in titanium is solid solution strengthening mechanisms, possible due to titanium's large crystal system. Alloying elements as oxygen, nitrogen and aluminium have this effect on titanium (Liu and Welsch, 1988), as shown in Table 2-3. This strengthening effect is often accompanied with a reduction in ductility, where aluminium and oxygen hinders deformation twinning (Williams et al., 2002). Aluminium's has a max limit of 7 wt. % to hinder precipitation of the Ti_3Al phase. Table 2-3 is created to serve as a quick overview over the direct effect of elements found in commercially pure titanium.

Table 2-3. Overview of the effect common elements found in commercially pure titanium have on its properties. Data gathered from Conrad (1981)

Elements	***O***	***C***	***N***	***H***	***Fe***
α - stabiliser	+	-	+	-	-
β - stabiliser	-	+	-	+	+
Tensile Strength	+	+	+	+	+
Ductility	-	-	-	-	-
E-modulus	+	+	+	+	-

Iron and nitrogen is often considered an impurity and not alloying element because of their negative effect on ductility, fracture toughness and creep strength. Other common alloying elements are Aluminium, Vanadium and Silicon.

2.1.2.1 Overview titanium alloys

There are over hundred known titanium alloys today, however only a few are cost effective enough to be commercial(Peters et al., 2005). The high cost of production and development makes research into new titanium alloys difficult. Titanium and its alloys are usually divided into four categories, α – alloys, near α-alloys, α + β alloys and β-alloys, or often known as metastable β-alloys. Below in Table 2-4, a list is prepared to illustrate the positive and negative sides of the different phases.

Table 2-4. Properties of α, α +β and β Ti alloys, gathered from Peters et al. (2005).

	α	**α+β**	**β**
Density	+	+	-
Strength	-	+	++
Ductility	-/+	+	+/-
Fracture toughness	+	-/+	+/-
Creep strength	+	+/-	-
Corrosion behaviour	++	+	+/-
Oxidation behaviour	++	+/-	-
Weldability	+	+/-	-
Cold formability	--	-	-/+

There is a definite positive side of having a mix of α + β phases as both strength and ductility increases, with good creep strength, corrosion and oxidation behaviours as well as a positive weldability.

α – alloys are either commercially pure titanium of different grades 1 to 4, or titanium alloyed with α-phase stabilisers as aluminium and oxygen. Because of their excellent corrosion resistance and deformability these alloys are usually used in chemical and process engineering industry. Oxygen are its main alloying element, giving rise to the quick strength increase in titanium grades 2-4, however it also decreases the ductility at the same rate.

Near α – alloys are titanium's solution to high temperature application, the alloy combines excellent creep behaviour from the α-phase and the strength from the α + β. In these alloys the alloying element Si is important because of its remarkable creep resistance, believed to be from Si precipitating at grain boundaries and hinder dislocation climb.

α + β alloys is the most wildly used and research alloy of titanium, because of its high strength, ductility and overall good balance of properties, see Table 2-4. Its versatility in microstructure is also a reason for its success making it easier to tailor the right properties for its application. The titanium alloy Ti-6Al-4V which is a α + β alloy, is estimated by Peters et al. (2005) that 50% of all titanium alloys in use are Ti-6Al-4V. The prominent attributes of this alloy are its high strength and ductility at high temperatures.

The metastable β-alloys are the strongest of the titanium alloys reaching above 1400 MPa, as well as achieving a high toughness. Even though several low cost beta alloys have been developed these alloys still generally suffer from high cost in production and research compared to other titanium alloys. The metastable β alloys have great strength, fracture toughness and ductility, however its limited by a higher density, poor weldability and oxidation behaviour as well as a complex microstructure.

Table 2-5, with the intent to illustrate examples of different grades, their composition and tensile properties is shown below.

Alloy	***Chemical composition, wt. % max***						T_β	***Hardness***	***UTS***	***YS***	***Elongation at break***
	C	**H**	**O**	**N**	**Fe**	**Other**	**°C**	**HV**	**MPa**	**MPa**	**%**
α - alloys											
CP-TI ASTM grade 1	0.10	0.015	0.18	0.03	0.20	…	890	122	240	170	24
ASTM grade 2	0.10	0.015	0.25	0.03	0.30	…	913	200	340	280	20
ASTM grade 3	0.10	0.015	0.35	0.05	0.30	…	920	235	440	380	18
ASTM grade 4	0.10	0.015	0.40	0.05	0.50	…	950	260	550	480	15
Near α – alloy											
Ti-5Al-2,5Sn	0.08	0.02	0.20	0.05	0.50	5Al & 2.5Sn	1040-1090	349	790	760	15
α & β – alloy											
ASTM grade 5	0.10	0.015	0.20	0.05	0.25	6Al & 4V	995	300-400	900	830	13-16
Metastable β – alloy											
Ti-10V-2Fe-3Al	0.05	0.015	0.16	0.05	2.5	10V & 3Al	800	300-470	1170	1100	6-16

Table 2-5. General properties for pure titanium and various grades of titanium. Data collected from Peters et al. (2005), Boyer et al. (1994) and M.J. Donachie (1988).

2.2 Plastic deformation

HCP titanium lattice parameters are, a = 0.295 nm and c = 0.468 nm(Peters et al., 2005), which gives an c/a ratio of 1.587. An ideally HCP lattice would give 1.633. This reduced c/a ratio favours prism planes vs basal planes because of the lower spacing between prism planes, leading to a higher packing density. The c/a ratio can be changed with interstitial or substitutional atoms, increasing c with alloying of nitrogen and oxygen.

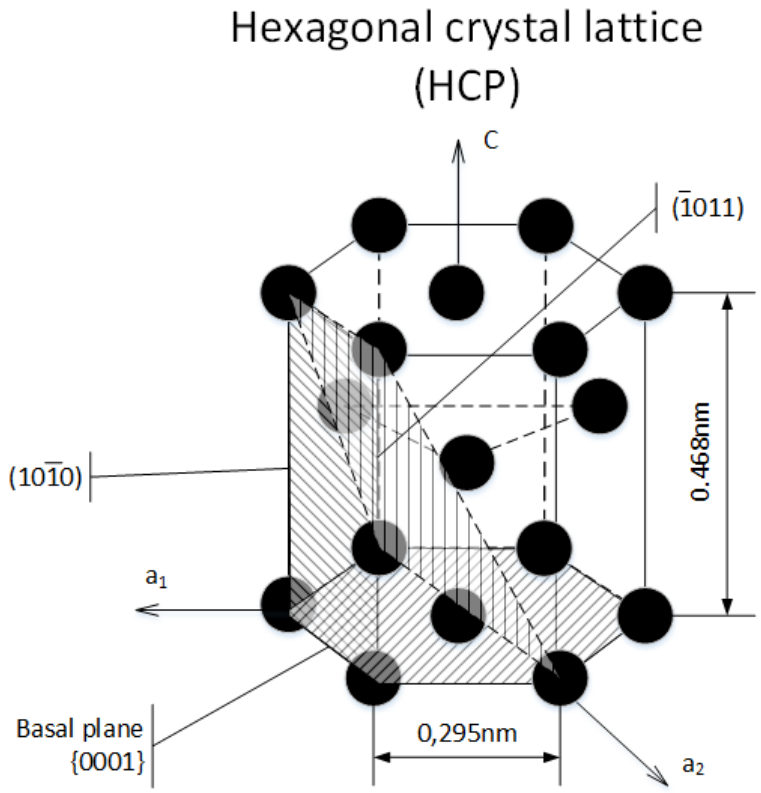

Figure 2-7. The figure illustrates the Hexagonal close packed crystal system and the standard slip systems in the HCP lattice. Titaniums lattice parameters are shown, where the a = 0.295 nm and c = 0.468.

Titanium is a difficult material for cold work as it has a limited plastic deformability in HCP titanium, were there are only 3 slip systems at room temperature, in contrast BCC has 12. On the other hand, HCP has a higher packing density in the basal plane, but the energy needed for plastic deformation is dependent on the length of minimal slip length, which again favours plastic deformation in BCC compared to HCP.

These three listed slip systems, shown in Table 2-6 for HCP, constitutes only four independent slip systems. Von Mises criterion demand five independent slip systems, for homogenous plastic deformation. This indicates a low ductility for titanium compared to BCC and FCC structures. The low possibilities of slip systems and low temperatures pushes the titanium HCP lattice into twinning, especially in shock loading as crushing, and make it susceptible to cleavage fracture. The tendency to twinning decrease with increasing interstitial content hindering movement, and increasing temperature, activating less favourable slip systems(Conrad, 1981).

Because of the anisotropic character of the hexagonal crustal structure of α, the elastic modulus of strongly textured structures can substantially vary with load direction. In the transverse direction, i.e parallel to the c-axis of the hexagonal crystal structure of α, the Young's modulus is higher than in the rolling direction. At temperatures above 882°C titanium transforms to the BCC-structured β-Ti. The body centred crystal systems, illustrated in Table 2-8, has 12 slip systems in the {110} slip plane in the (110) slip direction and deforms homogenously and easier, slip planes are shown in Table 2-6.

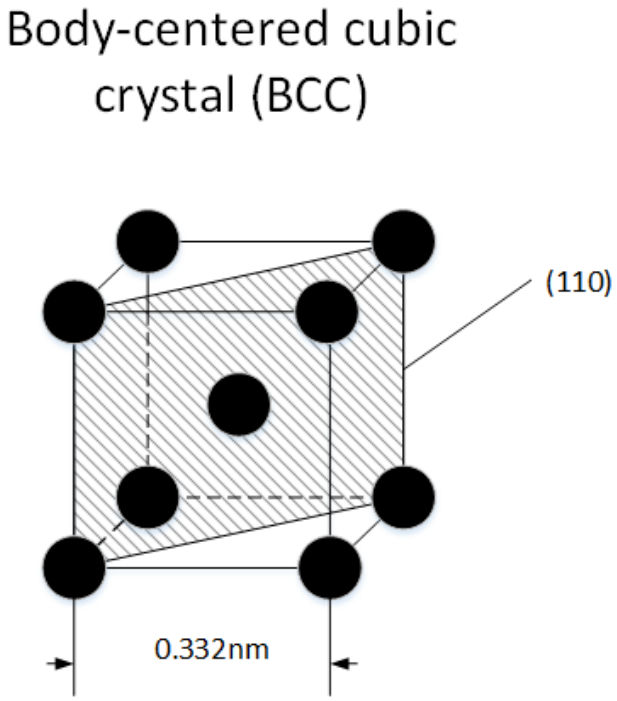

Figure 2-8. The figure illustrates the BCC crystal system with its favourite slip plane and slip direction. The titanium lattice parameter inn β phase is a = 0,332 nm.

Table 2-6. Overview of slip planes and slip direction for the HCP and BCC crystal systems.

Crystal systems	*Slip plane*	*Slip direction*	*Number of slip systems*
HCP	{0001}	<1120>	3
	{1010}	<1120>	3
	{1011}	<1120>	6
BCC	{110}	<111>	12

2.2.1 Response to heat treatment

Any heat treatment at temperatures above 427 °C should be done in a protective atmosphere to minimize surface oxidation and minimize the needed after treatments of machining away the oxidised surface. Stress relief of titanium and its alloys are a common heat treatment, however, care must be taken as the metallurgical response is contingent on the alloy. Both phases have a low diffusion rate having temperatures below 600°C give a diffusion rate less than 10^{-18}, see Figure 2-9, at high temperatures such as 600°-800°C, the diffusion rate is still low, giving titanium a good resistance against creep. Diffusion bonding is reported to work at 920° to 950°C, with a pressure of 2-6MPa and 2 to 3 hours. The pressure in screw extrusion are much higher, however the temperature and holding time is considerably lower. Which tells us that any fusion or welding of material will go slowly at the designed temperature of the screw extrusion process at 600°C.

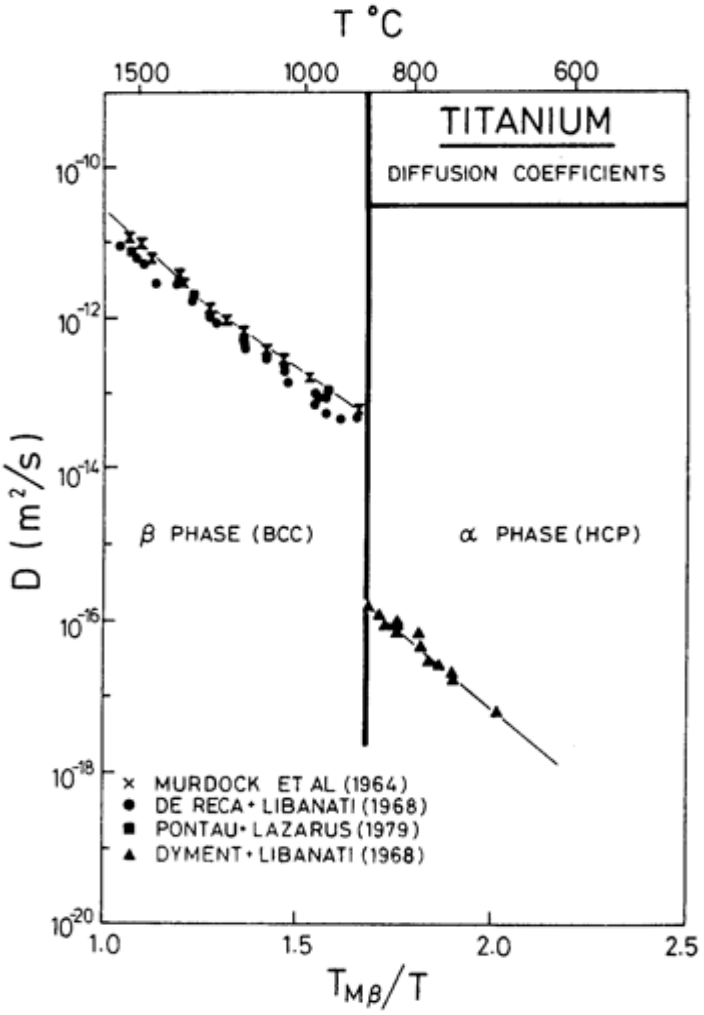

Figure 2-9. Self-diffusion coefficients for titanium, collected from Ashby (1982).

The general problem with heat treatment of titanium is that the low diffusion rate demands temperatures close to the recrystallization temperature, a solution to this are long holding times at low temperatures, however this again my not be cost effective.

Heat treatment and stress reliving depends heavily on the alloy, as composition will dictate the β transus temperature and amount of possible metastable β. α and near-α alloys can only be stress relived and annealed, but any aging cannot be obtained, and therefore any strengthening through heat treatment has not been found for these alloys. The α+β alloys have a large potential through heat treatment, and the heat treatment can dictate phase composition, sizes and distribution, as well as a number of different microstructures can be developed, specifically tailored for a purpose. Normally a solution treatment plus aging is done to create the strongest alloys. The metastable β alloys can be stress relieved and strengthen through heat treatments. At sufficiently high temperatures the retained β phase decomposes, and the alloy is strengthened. An overview of proposed stress relief treatments, collected from M.J. Donachie (1988), are displayed in Table 2-7.

Table 2-7. Recommended stress-relief treatments for titanium and titanium alloys, gathered from chapter 8 M.J. Donachie (1988).

Alloy	Temperature (°C)	Time (hours)
Commercially pure Ti (all grades)	480-595	0.25–4
α or near-α titanium alloys		
Ti-5Al-2.5Sn	540–650	0.25–4
Ti-8Al-1Mo-1V	595–705	0.25–4
Ti-2.5Cu (IMI 230)	400–600	0.5–24
α-β titanium alloys		
Ti-6Al-4V	480–650	1-4
Ti-6Al-7Nb (IMI 367)	500–600	1-4
Ti-6Al-6V-2Sn (Cu + Fe)	480–650	1-4
β or near-β titanium alloys		
Ti-13V-11Cr-3Al	705–730	0.08-0.25
Ti-11.5Mo-6Zr-4.5Sn (Beta 111)	720–730	0.08-0.25
Ti-3Al-8V-6Cr-4Zr-4Mo (Beta C)	705–760	0.15 – 0.5
Ti-10V-2Fe-3A	675–705	0.5 – 2

2.2.2 Hardness

Hardness is a realistic and relative inexpensive non-destructive method to track the results of heat treatment. However, it suffers from high variation because of titaniums HCP's anisotropy as well as poor correlation with strength(M.J. Donachie, 1988). Figure 2-10 shows the contribution contamination elements have on the hardness of titanium. It is calculated with equations shown in Figure 2-11.

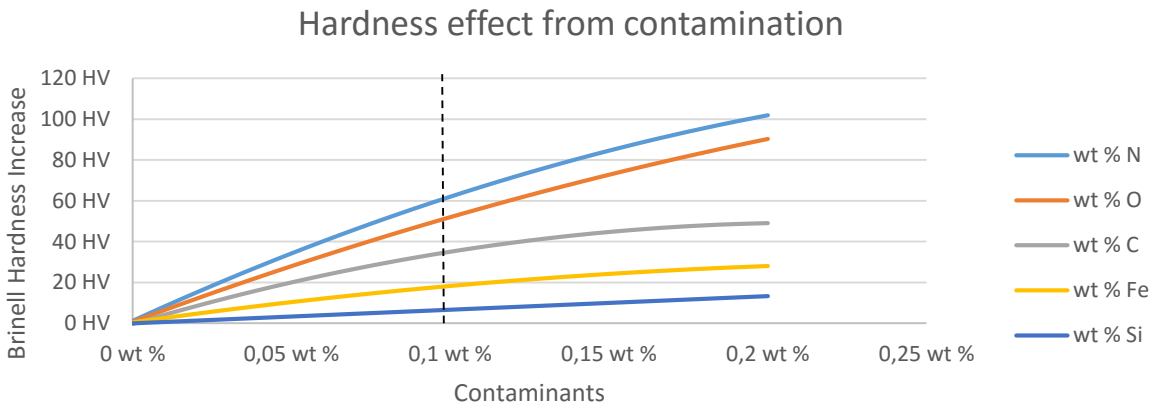

Figure 2-10. Hardness increase from contaminations, these are equations based upon empirical data. Equations are gathered from Sibum (2005) and shown in Figure 2-11.

It is clear that even a small contamination increases the hardness considerably, where 0,1 wt. % of nitrogen and oxygen leads to an increase in hardness of 60 HV and 50 HV respectively.

$BHN_N = -1100X_N^2 + 750X_N + 1.3$
$BHN_O = -680X_C^2 + 607X_C + 0.9$
$BHN_C = -1125X_C^2 + 485X_C - 0.35$
$BHN_{Fe} = -425X_{Fe}^2 + 230X_{Fe} + 0.55$
$BHN_{Si} = 70X_{Si}$

Figure 2-11. Shows equations used in Figure 2-10 to calculate curves, gathered from Sibum (2005).

The hardness increase in the equations in Figure 2-11, is given in BHN, Brinell hardness, as this rapport measures in Vickers a standard ratio of HV = 0,95 BHN has been applied to convert from BHN to HV. Figure 2-11 will only be a guideline for possible hardness increase from contamination, as the actual hardness of titanium is somewhat unclear. Table 2-8 has been included to serve as the assumed hardness values for pure titanium and subsequent grades of titanium.

Table 2-8, General hardness for pure titanium and various grades of titanium. Data collected from Boyer et al. (1994) and Peters et al. (2005).

Alloy	**Chemical composition (wt. %)**	**Hardness HV**
High Purity	99.98 % Ti	100
Grade 1	Cp-Ti: 0.2Fe, 0.18O	122
Grade 2	Cp-Ti: 0.3Fe, 0.25O	200
Grade 3	Cp-Ti: 0.3Fe, 0.35O	235
Grade 4	Cp-Ti: 0.5Fe, 0,40O	260
Grade 5	Ti-6Al-4V	349

2.3 Screw extrusion

The screw extrusion is a novel process developed at the Norwegian University of Science and Technology. The original patent can be found at Reiso et al. (2006), and more recent research written by Skorpen et al. (2014) and Widerø (2012) shows great potential in the method. Compared to the traditional extrusion methods, the screw extrusion method provides a way to produce material in a continuous process, simultaneously work harden the material, as well as reduce cost. The process versatility with feedstock for extrusion makes it an excellent way for future work within production of alloys.

The process is represented in Figure 2-12, where pellets or sponge are feed into the back of the container where it falls to the bottom between the screw and container wall. The material is then pushed to the extrusion chamber by the rotational movement of the screw, leading to a material build-up in zone 2. This leads to increased friction conditions which, with help from the high temperature, consolidates the sponge. The pressure build-up relies on four parameters: the geometry of the screw, the frictional conditions, size of the die opening and the material characteristics.

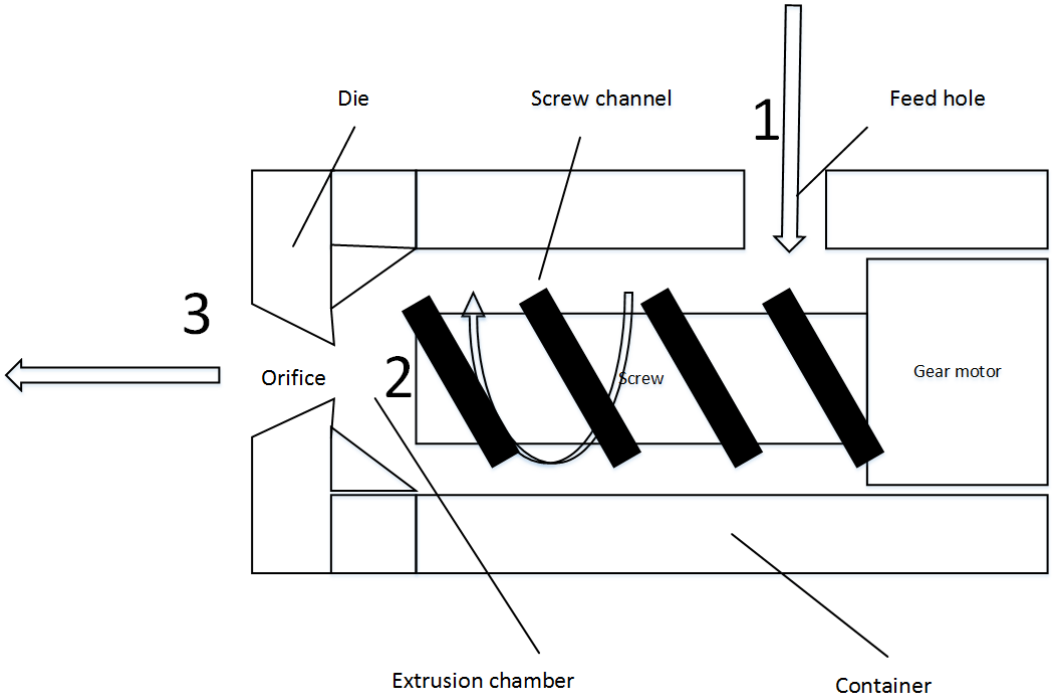

Figure 2-12. Schematic drawing of the screw extrusion process. Essentially it compresses and deforms granulates into a consolidated material at a much lower temperature than conventional extrusion. At zone 1, the titanium sponge is fed into the process, zone 2 is where the sponge consolidates and zone 3 is where the titanium exits the process in form of consolidated profiles.

When the extrusion chamber is filled and the pressure build up is high enough, extrusion starts. The profiles exit the container through the die, usually as a circular opening between 10 to 30 mm. The process produces a continuous profile that can either be cooled directly upon leaving the die or air cooled. A more detailed description of the setup can be found in Reiso et al. (2006) and Widerø (2012)

During the experiment, several parameters are logged, temperatures are monitored with 6 thermocouples placed strategically to register the temperature difference during the process and variation between zones. The feed rate of the material and screw speed can be varied, and moment of the screw is controlled through the desired screw speed.

Two samples from the screw extrusion were available for examination, one produced with a die diameter of 20 mm and one with a die diameter of 30 mm, respectively sample ϕ20 and ϕ30. The extruded ϕ20 sample had a length of 600 mm and a weight of 829 g, the extruded ϕ30 had a length of 490 mm and a weight of 1520 g. Both are produced in the same screw extrusion machine, which begins with heating the equipment up to temperatures above 550°C, with the experiment target temperature of 640°C. The heating is done with an induction ring powered at 6 kW, mounted on the front of the die. The feeding of the material is not begun until die temperatures are above 550 °C to ensure as little holding time as possible of the material inside the container to decrease oxidation of the titanium sponge. Figure 2-13 and Figure 2-14 presents the temperature variation and moment registered during each experiment. Notice the temperature variation during both experiments, during extrusion the temperature varies between 600°C and 670°C at the die opening. The chamber has a slightly steadier temperature variation at 550° to 590°C. Regrettably the beginning of extrusion and the speed of extrusion is not written down.

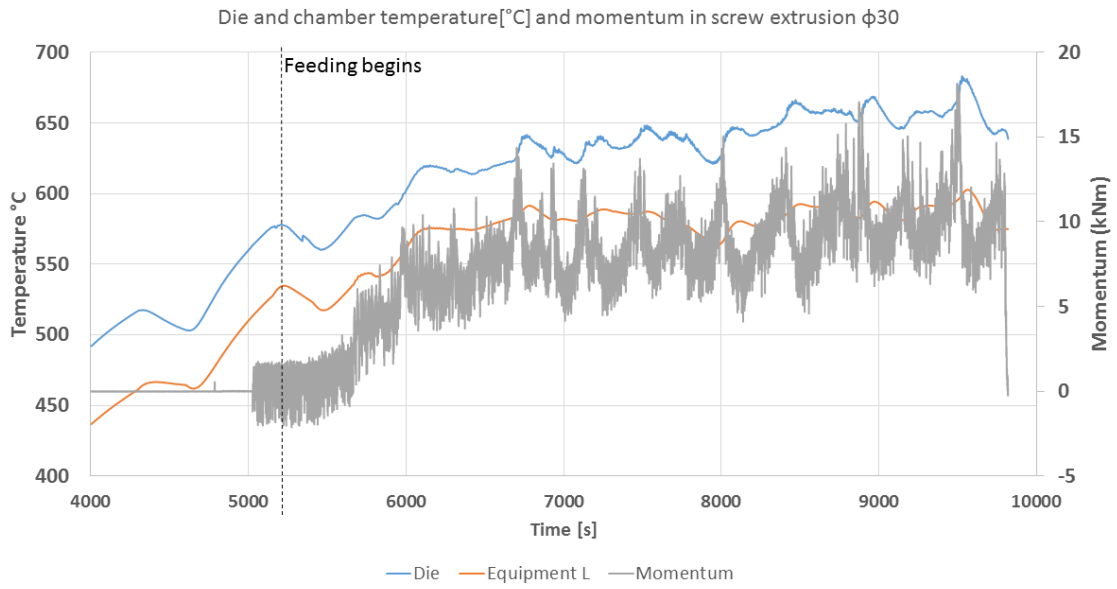

Figure 2-13. Overview of temperature and moment during screw extrusion of the φ30 sample. Feeding is noted in the figure, beginning after roughly 5600 seconds at a temperature of 575 °C. Screw speed at 3RPM.

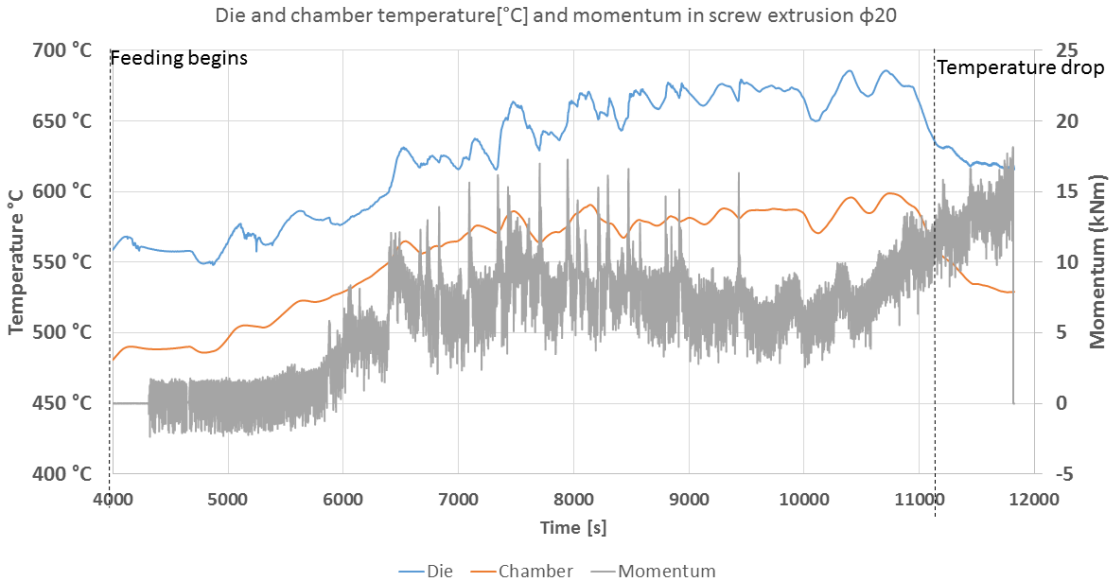

Figure 2-14. Overview of temperature and moment during screw extrusion of the φ20 sample. Feeding is noted in the figure, beginning after roughly 4100 seconds, at a temperature of 560 °C. Notice the temperature drop in the end, this was due to a relaxed heating scheme to stop temperatures going up to 700 °C. The effect of lower temperature increased the needed moment to turn the screw and the experiment ended with the screw stopping because of max moment.

2.4 Medium pressure torsion

An in-house designed hydraulics compressor designed for combined compression and shear is used to simulate the screw extrusion process. The area which it focuses on is where the titanium sponge consolidates to a more or less fully dense titanium. Below in Figure 2-15, this region in the screw extrusion and compression and shear deformation is presented in A) and B) respectively. In other words, the medium pressure torsion unit can be regarded as a physical simulation of the consolidation process taken place in the region where the screw ends into the extrusion chamber

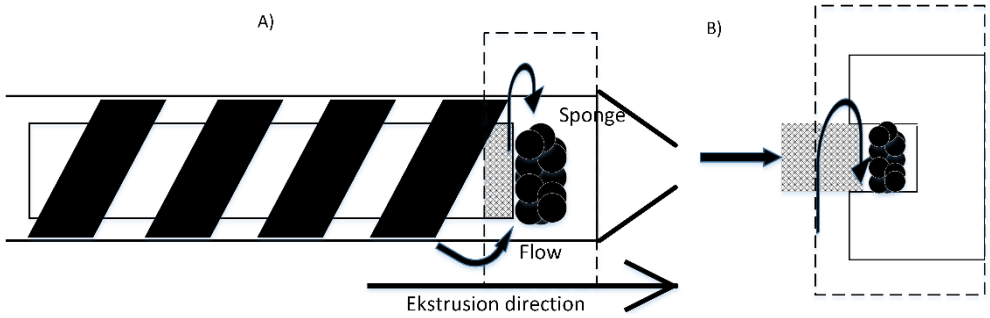

Figure 2-15. Illustrative comparison of the screw extrusion process and compression and shear deformation process (MPT). A) The screw extrusion is depicted with the head of the screw, mentioned as zone 2 in Figure 2-12. This is where the titanium sponge is consolidated. B) shows the compression and shear deformation that will serve as simulation to the screw extrusion process.

The medium pressure torsion will push down on titanium sponge in a sample holder, compress the sponge and rotate the holder while holding the piston still. It is assumed that the granulates touching the piston will be hindered from moving along with the holders due to large frictional forces and sticking. This introduces shear deformation in the material and increase the pressure conditions between sponges and deformation easing further consolidation and mixing. An equation designed to estimate the accumulated strain is presented in equation 1, described by Zhilyaev and Langdon (2008).

Formel 2-1. The equation relates the total accumulated strain during pressure and torsion. N is number of rotations, r is radius of disk and h is the thickness of the disk. The equation is designed for fully consolidated disk of material.

$$\varepsilon \approx \ln\left(\frac{2\pi N * r}{h}\right) \quad (1)$$

On the next page in Figure 2-16 the accumulated strain has been calculated in terms of the planned compression disk for the medium pressure torsion experiment. Notice the sharp climb in deformation during the first round, with further deformation evening out, but not showing any clear saturation point.

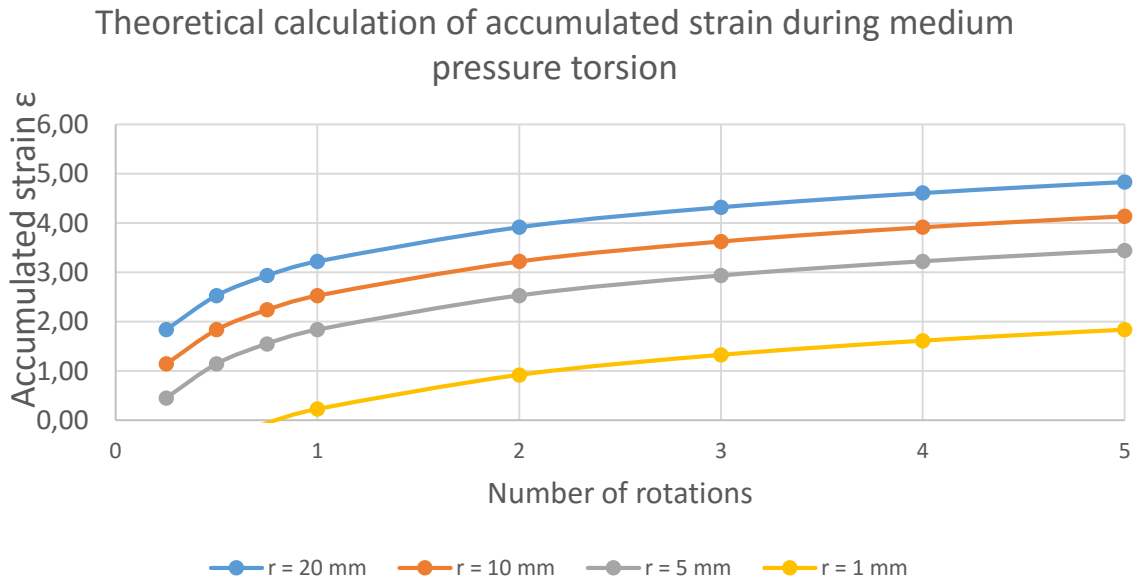

Figure 2-16. A theoretical calculation of the accumulated strain induced during the medium pressure torsion. The amount is calculated with equation 1. The planned dimension of the disk is a radius of 20mm and height of 5 mm. The figure shows the largest deformation gradient before the first round, with subsequent decrease in deformation gradient. The development over time shows large amounts of deformation.

3 Experimental

The experimental chapter is divided into three sections. The first two sections are the earlier defined two paths, i.e. titanium sponge and screw extruded profiles. The work is presented chapter by chapter in accordance with Figure 1-1. The last section is designed for describing details in applied techniques such as cutting, grinding, polishing and etching, machine used and other technical information.

3.1 Titanium sponge

The titanium sponge, see Figure 3-1, was examined with respect to chemical composition, hardness and size distribution, as well as an investigation into heat treatment of the sponge for the purpose of lowering the hardness and easing consolidation. There are two batches of titanium sponge, one labelled sponge above 4mm in diameter and one labelled below 4mm in diameter. The primary batch, the one formerly used in screw extrusion, is titanium sponge below in 4mm, and any research will mainly focus on this batch.

Figure 3-1. Picture of sponge, lain out on a A4 paper. The length scale is given in millimetres.

The origin of the titanium sponge is not certain, however a possible source may be the Xi'an Jinxin Technology Co, in China, who produced different grades of titanium sponge, where the Brand MHT-100 might be the titanium sponge that is used in the screw extrusion project. An independent elemental chemical analysis was carried out on the received sponge, on behalf of SINTEF, before the project. The elemental chemical analysis of the titanium sponge, on the behalf of SINTEF, has been executed by the Universidad Carlos III de Madrid. The compositional study was carried out using a LECO TC-500 instrument in order to determine the oxygen and nitrogen content, and LECO CS-200 to measure the carbon content.

These investigations mainly focus on the primary batch of titanium sponge, however due to large uncertainties in heat treatment and the hardness measurements the heat treatment and hardness testing were done on the secondary batch as well, reasoning being it will serve as a reference group.

3.1.1 Size distribution

The primary titanium sponges granules were measured in width and height, where the average of the two served as the sponge size. Figure 3-2 shows a single sponge, measured at a average size of 5 mm. The measuring was done by taking an overview picture of several sponges, measured length and width in pixels and then converted to millimetres. This was done using the MATLAB command imshow and its picturehandlebar. In all, 228 sponges were counted and characterised.

Figure 3-2. Close up picture of titanium sponge with an length of 7 mm and an width of 2mm, resulting in an average size of 5.5 mm.

3.1.2 Heat treatment of titanium sponge

Primary and secondary sponge were divided into three groups each and heat treated separately following the temperature profile in Figure 3-3, with a gradient of 200°C both up and down, holding the max temperature in 1 hour. Each group of the primary sponge batch consisted of 10 – 12 sponges, the secondary had 6 sponges per group. The heating was done using equipment described in chapter 3.3.3.

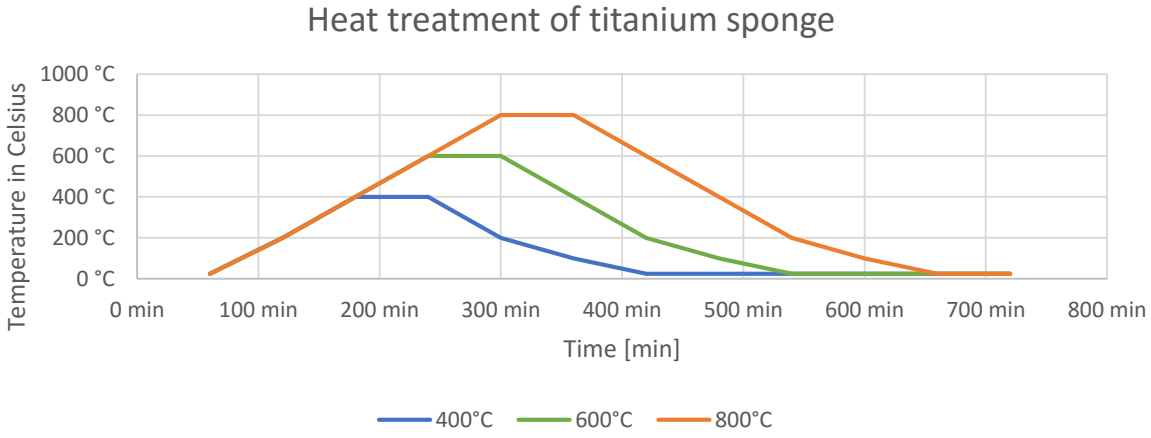

Figure 3-3. Illustration of the temperature time laps of the heat treatment of titanium sponge. The temperature lines show the heating schedule, holding time and cooling time of each heat treatment. They are labelled by colour indicating different heating programs.

After heat treatment the titanium sponge was filled into cylindrical moulds of 30mm and, whilst firmly making sure the grains were in contact with the bottom, filled with Streuers EpoFix.

3.1.3 Hardness testing

All samples were grinded and polished as explained in Section 3.3.2 and the hardness was tested as explained in Section 3.3.4. Each epoxy cast sample of the large titanium sponge had one sponge per epoxy cast, and indented 20 times per sample. The smaller titanium sponge, diameters below 4 mm, had between 3 and 5 sponges per epoxy cast, and 20 indentations per epoxy cast were spread out evenly between sponges. This resulted in 60 indentations or more per heat treatment, giving a minimum total of 360 indentations.

3.1.4 Microstructural images of titanium sponge

The microstructural images are taken of the already hardness measured samples, they are re-polished and etched as described in Section 3.3. To produced satisfactory results, the polishing and etching had to be repeated once to fully remove surface strain induced microstructure. The pictures are taken with a LEICA MEF4M light microscope with a JENOPTIK ProgRes C10plus camera.

The average grain size is calculated through the use of the line method. The line is drawn horizontally or vertically in the picture, positioned and given a specific length as not to cross any voids or cavity's. Three lines per picture is drawn and counted, two pictures per sample, counting more than fifty grains, specified by the ASTM E112-13.

3.1.5 Consolidation region and Medium Pressure Torsion (MPT)

Originally several screw extrusion experiments were planned, however due to lack of a screw capable of withstanding the pressure conditions under extrusion of titanium another method needed to be found to determine the effect of pre-heat treatment of titanium sponge. The medium pressure torsion equipment deemed sufficient as it has the capability to exert both compression and shear deformation on granulates/sponges, mimicking zone 2 in the screw extrusion process, as explained in chapter 2.4.

The current set-up of the machine has capabilities to deliver up to 500kN in compression and a torque effect of 1.65kN. The set-up available consist of an equipment holder, sample holder which can be mounted inside the equipment holder and a piston designed to fit into the sample holder with a clearance of 0,2 µm, see Figure 3-5 for clarification of dimensions and set up. A detailed description of the system can be found in Fredrik Widerøe (2011). Parameters for the test set up are displayed in Table 3-1 at the next page with a picture of the MTS 311, 1000kN hydraulics press.

Table 3-1. The parameters for the medium pressure torsion. The compressive force was set at 200MPa, the torque force is rotation speed controlled. The experiment was done at two different temperatures, 300°C & 400°C, and three differently heat treated sponge types were used. 29 to 30 grams of sponge was used for every experiment.

Parameters of test setup	
Compressive force	200 MPa
Torque force	Rotation speed controlled (1,33 rounds per minute), max 1.65kN
Equipment temperature	300° & 400°C
Input material, sponge	As received, heat treated at 400° & 600°C
Amount of sponge	29g-30g sponge

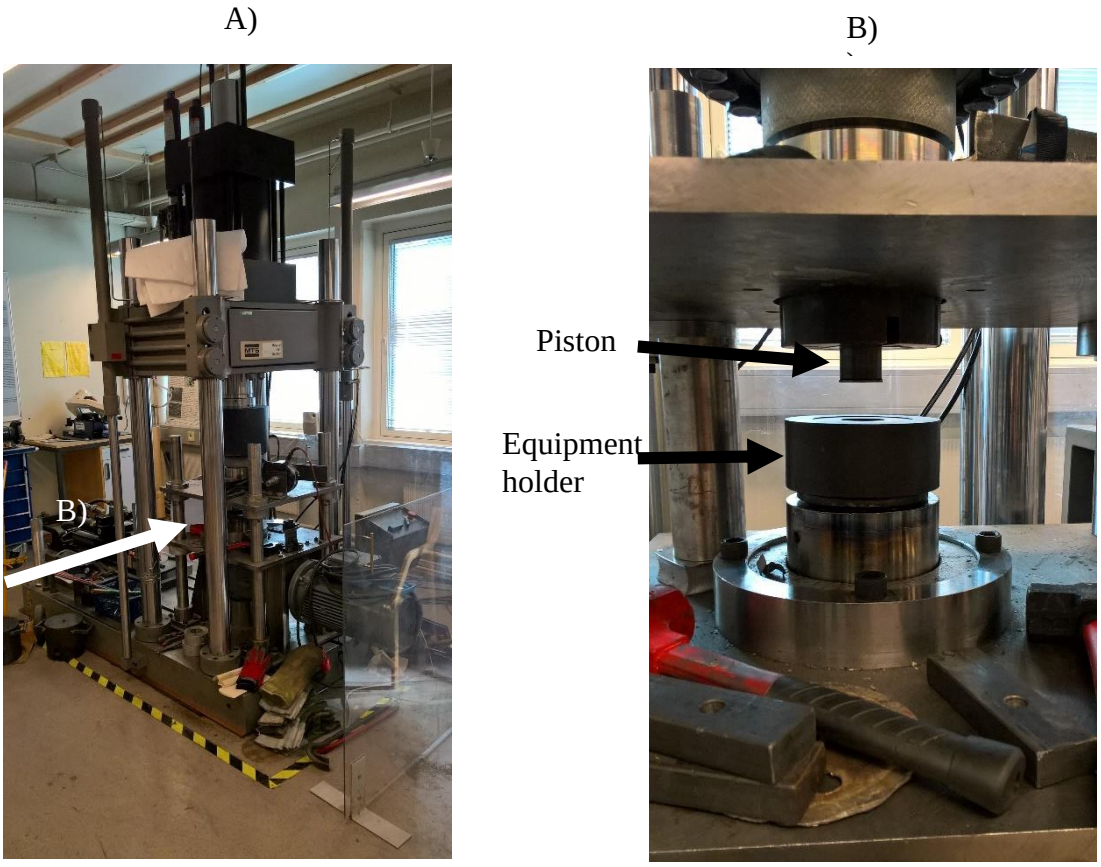

Figure 3-4. A) Picture of the MTS 311. The arrow indicates the angle for picture in B. B) Close up on the test setup. Notice the equipment holder and piston.

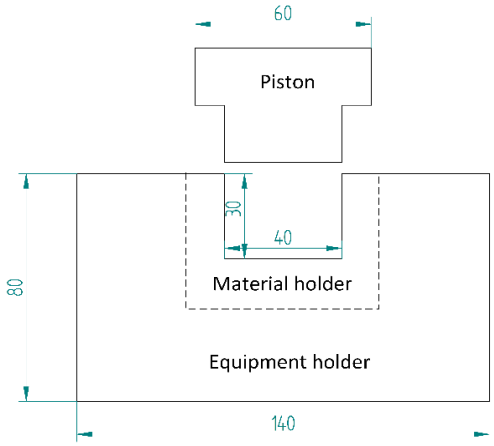

Figure 3-5. Overview over the three components mounted in the medium pressure torsion process. The equipment holder, with the sample holder within, and a piston designed to compress the sponge in the sample holder.

The equipment holder has a width of 140 mm and height of 80 mm, with a cavity width of 60 mm and depth 30 mm. The sample holder has a conical shape with a cavity with a diameter of 40 mm and depth of 30 mm. The piston has matching diameter of 40 mm, with a designed 0.2 mm clearance, shown in Figure 3-5. The equipment holder is equipped with a bottom cavity, easing removal of the sample holder.

The heat treatment of the primary sponge intended to be used in the medium pressure torsion experiments were done with the same furnace and temperature scheme as the former heat treatment of the sponge. One important difference was the amount of heat treated titanium sponge in one setting. To be able to produce enough heat treated primary titanium sponge for testing, the alumina boat crucible was filled with roughly 35 grams of primary titanium sponge, as shown in Figure 3-6. The alumina boat crucible is inserted into the tube furnace and heat treated.

Figure 3-6. The alumina boat crucible filled with primary titanium sponge. Ready for heat treatment, and subsequent use in medium pressure torsion.

Figure 3-7. A SCAN-FORM SF-2 furnace, with the equipment inside, and a thermocouple mounted through the furnace roof and into a thermocouple holder inside the piston.

The preheating of the equipment to the target experiment temperature is done in a SCAN-FORM SF-2 furnace, shown in Figure 3-7, and hot-mounted in the machine, giving source to errors in both exact temperatures of equipment and material during the experiment. It also led to a problem of having experimental temperatures above 400°C as the thermal expansion made the mounting of equipment difficult and damaging for the set and MTS 311.

The execution of the experiment is done by heating the set as described earlier. Then, when the piston had a 5° to 10° C above target experiment temperature the set was removed from furnace and mounted into the MTS 311, it needs to be reckoned that some heat is lost during mounting of the equipment, and therefore some variation in the experiment temperature are hard to avoid. When the equipment was mounted, the titanium sponge was poured into the sample holder, the piston was lowered and exert a compressive force of 50 tons, which amounts to 400 MPa. The compressive force of 400 MPa was held in 10 seconds to distribute the heat. Because of titanium's low thermal conductivity, a concern in the amount of holding time before it could be assumed that all the test material had the uniform target experimental temperature. Numerical calculation of the heat development in the titanium disk, shown and explained in Appendix A, gives a homogenous temperature distribution after 2 seconds, indicating 10 seconds is enough. The force is then lowered till 200 MPa and the shear deformation is begun. The shear deformation part is done through 5 complete rotations of the sample holder, this is timed to roughly 3minutes and 30 seconds, and monitored visually. The setup is then dismantled as quickly as possible and sample placed in air, this stage had time range of 5 minutes till 3 hours. The large deviation is due to the large amount of forces in play and thermal gradient, which creates large amount of friction in the holders making them difficult to separate, and made dismantling difficult.

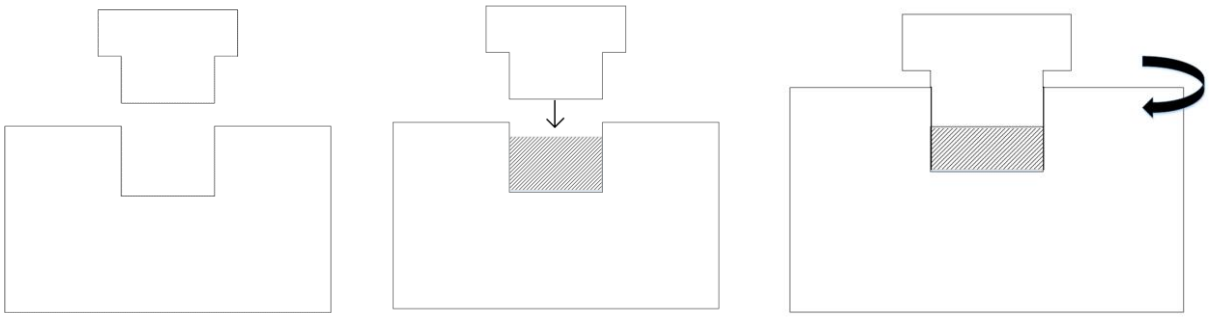

Figure 3-8.The equipment is placed preheated in the MTS 311. The holder is then filled with titanium sponge marked as the shaded area. The piston is lowered and the sponge is compressed at a 50 tons pressure. The compression is lowered till 25 tons, and the sample holder is then rotated at a speed of 1,33 rounds per minute.

Any cold welding of titanium onto the equipment had to be manually machined or grinded as chemical removal was not an option. The density of the samples are measured through measuring thickness and weight of the samples, the radius being the same.

The medium pressure torsion samples were also investigated in order to reveal their degree of consolidation. Each samples are examined at the centre cross sections, they are cut and prepared as discussed in 3.3, and then etched to enhance the state of the material. An overview picture is taken with a Reichert-Jung Univar microscope and ProgresC5, compiled in Image Pro Pluss. This overview picture is imported into PowerPoint, great care is taken to have the same size and equal treatment on all samples. A drawing onto the overview picture is done with simple line tools in PowerPoint, which is then imported into Microsoft Visio and measured the maximum depth of the consolidation through use of dimensioning tools. This length is then converted to true length using a ratio calculated using the height in Visio vs true height. The consolidation area is defined by no visual pores detected and clear macroscopic deformation.

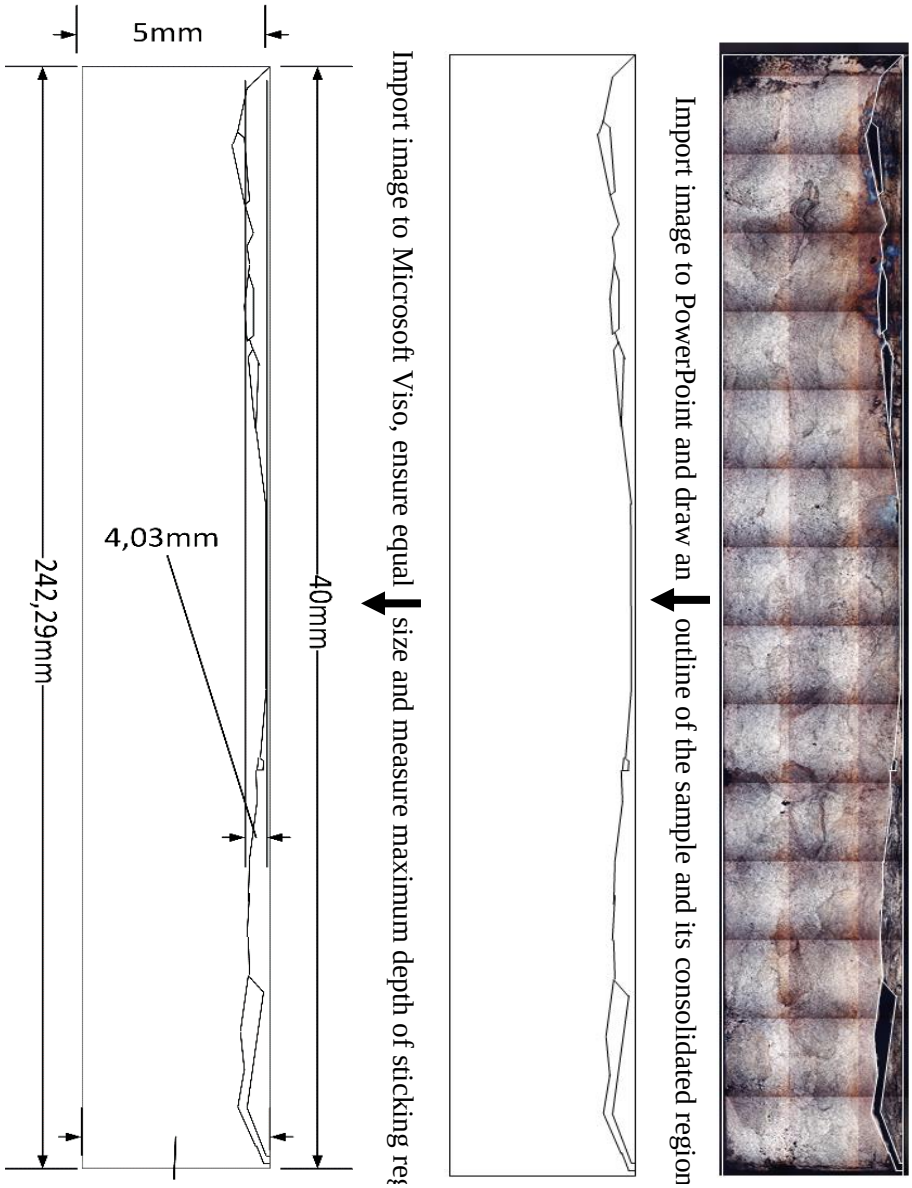

Figure 3-9. The figure illustrates the process through measuring the depth of the consolidated region. This is done through a series of three steps shown in the figure. First action is taking an overview image of the cross section. The image is then imported into PowerPoint and an outline of the area of interest is drawn. This outline is imported to Microsoft Visio to find the depth of consolidated area. The ratio used to convert to real height is found by dividing specimen thickness with the fixed out outline in Visio at 26.05mm

3.2 Screw extruded profiles

Already produced screw extruded profiles, shown in Figure 3-10, are examined in regard to its chemical composition, consolidation, hardness and homogeneity. The screw extrusion that produced these samples have been described in chapter 2.3.

Figure 3-10. Extruded profiles from the screw extrusion process, top sample have a diameter of 30mm, bottom sample have a diameter of 20mm. The screw extrusion processes are explained in chapter 2.3

The elemental chemical analysis of the extruded samples was as mentioned done by an external part, SINTEF Molab. The analysis of the φ30 sample was commissioned and produced in November, 2015, the φ20 sample was commissioned and produced in February, 2016. The methods are described in 3.3.5.

The homogenity of the samples are examined with extensive hardness measurements and microstructure examination of the cross sections. To examine the need for further processing, the degree of consolidation in the profiles need to be determined. The machining of tensile specimen from the screw extruded samples will serve as the investigative method, looking at the tensile characteristics as well as the amount of flaws in the material. Several tensile specimens are heat treated to examine if annealing would be a sufficient after treatment.

3.2.1 Hardness measurement and microstructure in screw extruded profiles

One sample of each extruded profile, φ20 & φ30, were cut as described in Section 3.3, an illustration of it is shown below in Figure 3-11.

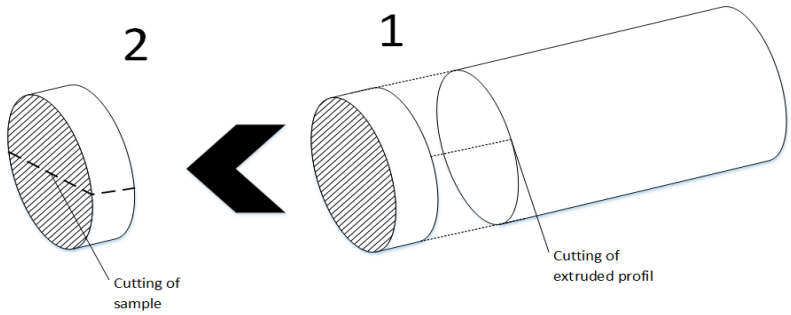

Figure 3-11. Illustrative example of cutting of the sample from the extruded profiles, step 1, and the subsequent cutting of the sample, step 2, to produce cross sections of the planes parallel and normal to the extruding direction.

Figure 3-11 shows the cutting of the sample from the extruded profiles and the subsequent cutting of the sample to produce a cross sections of the planes parallel and normal to the extruding direction. The samples are, as shown in Figure 3-12, cut in two giving 4 samples, two from each extruded profile. These are then cast in epoxy and grinded and polished as described in chapter 3.3.

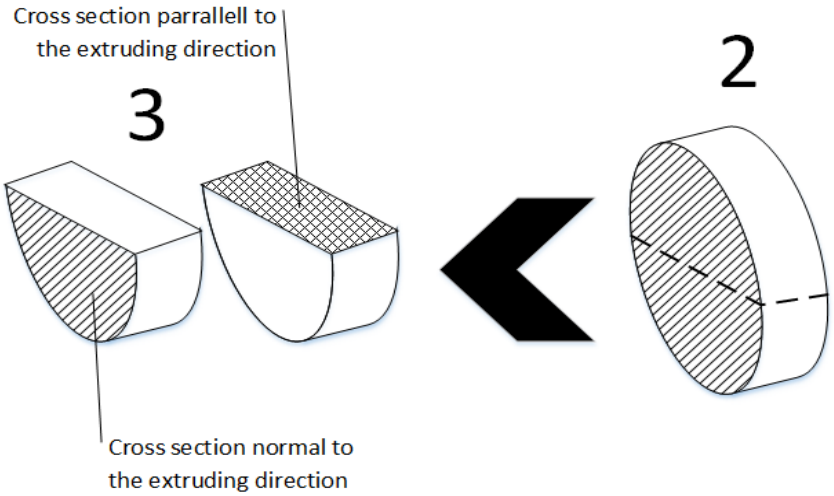

Figure 3-12. An illustration of the following steps of cutting after step 2, see. Figure 3-11 The sample is cut diagonally producing two samples. One is used for examination at cross section parallel to the extruding direction, the other for the cross section normal to the extruder direction.

The hardness measurements are done with a “Qness 10A+” by Norsk Titanium forming a grid over the entire sample surface, giving a total of 144 and 322 hardness indentations on the ϕ20 samples parallel and normal respectively, and 779 and 867 on the ϕ30 samples, parallel and normal respectively. The following microstructural images are produced with the same samples. The samples are re-polished and etched to remove the indentations and surface strain. Polishing and etching are done as described in Sectioon 3.3.

3.2.2 Tensile specimen

The screw extruded samples were cut into nine plates, as illustrated in Figure 3-13, and a tensile specimen was machined out of the plate. The tensile specimens were designed with a length of 8 mm, width of 4mm and thickness 1 mm, illustrated in Figure 3-14. The small scale of tensile specimens are due to the small amount of experimental material, and a need to conserve as much as possible.

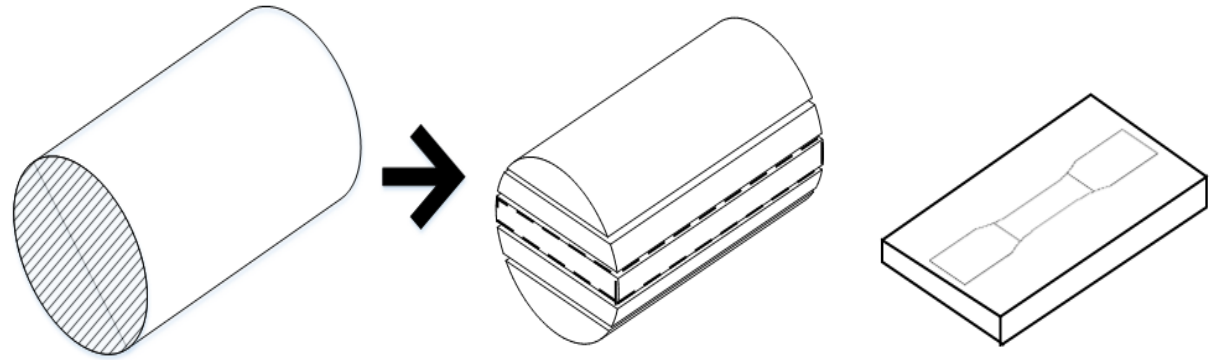

Figure 3-13. The extruded titanium profile is cut in nine plates. Tensile samples machined out of the plates from extruded samples.

The original tensile specimen design had a target area of 4 mm^2, this showed to be a problem since the tensile machine had a max power at 2.5 kN, giving a max pulling strength of 625 MPa. This is not enough as some samples have shown yield strengths well above 625 MPa, therefore, the target area needed to be reduced.

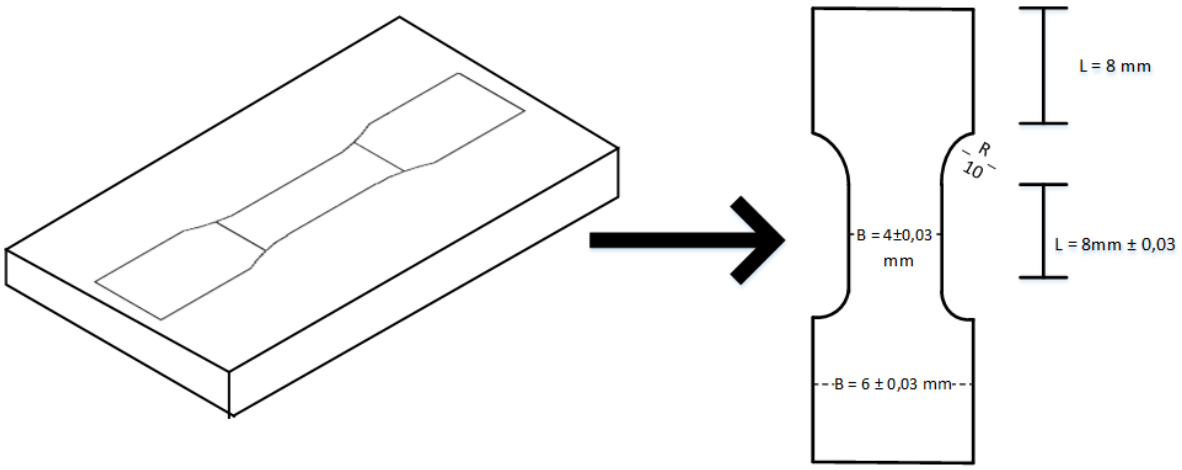

Figure 3-14. To the left, an illustration of the cut out plates from the scew extruded profiles, with the tensile specimen outlined within. To the right the geometry specifics of the tensile specimen.

A misunderstanding at the mechanic's work shop resulted in the tensile specimen illustrated in Figure 3-15. The tensile specimen keeps their original design in the heads, however the tension area was machined down 0.5 mm on just the one side, giving the unusual shape as shown. The difficulty in ascertaining if this geometry is affecting the tensile results are hard, the overall variation in tensile characteristics gave no clear definite behaviour, which again gave no reference field to compare to. The abnormal shape of the tensile specimen is a concern, however the untreated samples showed a similar stress-strain curve compared to earlier tensile test with standardise geometry. Therefore, because of limited test material and time restrictions, the tensile tests were deemed sufficient for the testing purpose.

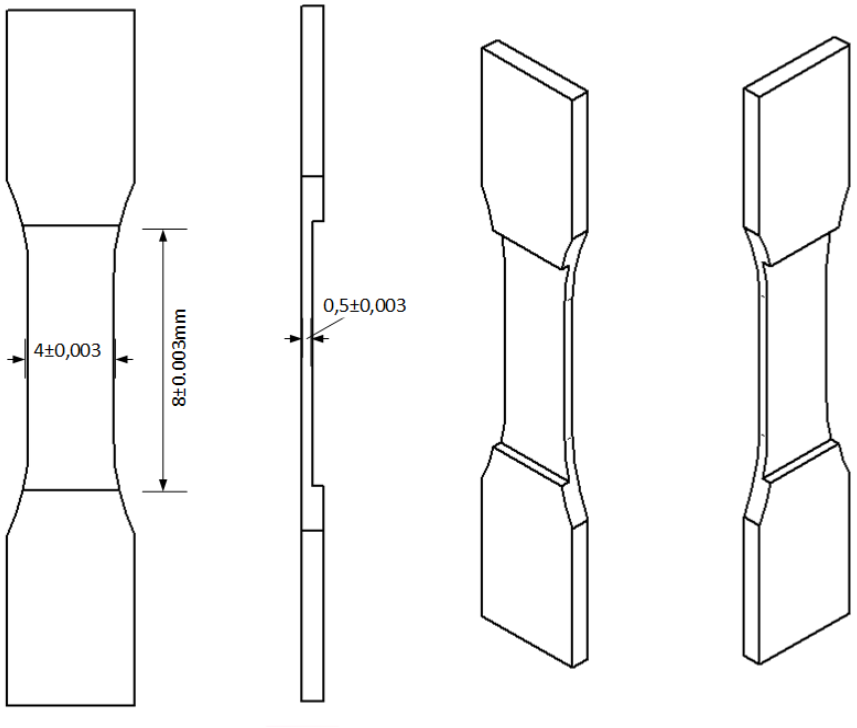

Figure 3-15. Schematic drawing of a tensile test specimen geometry. The tensile specimen has an abnormal geometry with the target area machined down 0.5mm. The dimensions are width of 4mm, length of 8mm and thickness at 0.5mm. The radius is 10° and the heads are 1mm thick.

There are 9 samples each of the extruded profiles of ϕ20 and ϕ30. Three samples from each stock were untreated to give a basis for the tensile data. Two samples from each stock were given a heat treatment of 400°C as described in 3.3.3. Four other samples from each stock were treated to a heat treatment of 560°C, two in argon atmosphere and two in air. The decision to do the heat treatments were based on former tests with other tensile specimens and the testing of none treated specimens. Both batches showing promise, it was interesting to see if any heat treatment would give more tangible results.

The specimen names are made through a system where the first digit indicates which experimental sample the specimen comes from, either ϕ20 or ϕ30. The next digits indicate heat treatment temperature in Celsius and letters describe atmosphere during heat treatment. The under-slash separates the specifications and leads to numbering of samples to separate equally treated samples.

Table 3-2. Overview over tensile specimen, added to give a easy way to understand the labelling of each sample in relation to their specific processing conditions upon screw extrusion

Specimen	***From extruded profile***	***Max temperature***	***Atmosphere***
20_1	ϕ20	N/A	N/A
20_2	ϕ20	N/A	N/A
20_3	ϕ20	N/A	N/A
24Ar_1	ϕ20	400 °C	Argon
24Ar_2	ϕ20	400 °C	Argon
256Ar_1	ϕ20	560 °C	Argon
256Ar_2	ϕ20	560 °C	Argon
256Air_1	ϕ20	560 °C	Air
256Air_2	ϕ20	560 °C	Air
30_1	ϕ30	N/A	N/A
30_2	ϕ30	N/A	N/A
30_3	ϕ30	N/A	N/A
34Ar_1	ϕ30	400 °C	Argon
34Ar_2	ϕ30	400 °C	Argon
356Ar_1	ϕ30	560 °C	Argon
356Ar_2	ϕ30	560 °C	Argon
356Air_1	ϕ30	560 °C	Air
356Air_2	ϕ30	560 °C	Air

Heating of tensile specimen were done with three different schemes. The heat treatment at 400°C was chosen to investigate what effect a small stress reliving process would have on the material, the heat treatment consisted of heating the sample in an alumina boat crucible in argon atmosphere to 400°C and kept there for 12 minutes. They were then removed and quenched. The heat treatments at 560°C are chosen to investigate stress relief at higher temperature and longer times, possibly resulting in recrystallization as well as to observe any difference between heating in air vs argon. Both heating schemes heat the samples up till max temperature, and then held for 1.5 hours. The heat treatment ends with quenching after 1.5 hours holding time at max temperature. Figure 3-16 is included to illustrate the heat treatment of the tensile specimens. Details of furnace, heating rate, quenching and sample setup are presented in Section 3.3.3.

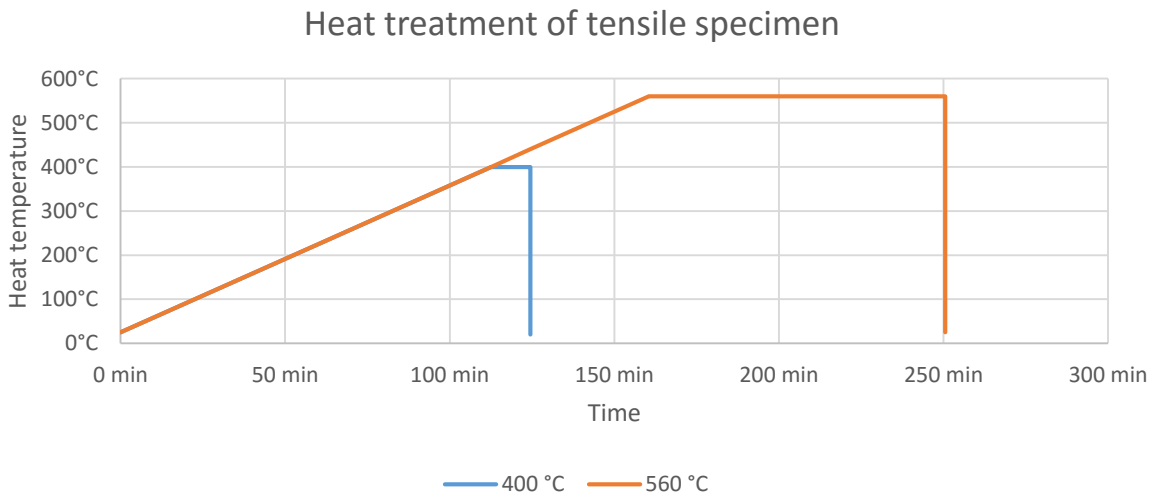

Figure 3-16. Illustration of the heat treatment of the tensile specimen.

Colling in titanium is a concern, because of its low thermal conductivity, too high cooling rate may induce thermal related residual stresses in the material. This was decided not to be an issue as the tensile specimen have a thickness of maximum 1 mm. The samples were stretched at room temperature with a rate of 1mm/min in a Zwick/Roell Z2.5 and "Extensometer". Before stretching the specimen were grinded with a 4000 SiC grid paper to remove any edges in the target area. The machine is fairly new and the internal experience is low, so a few samples were mounted wrong, ending up in giving no valuable data.

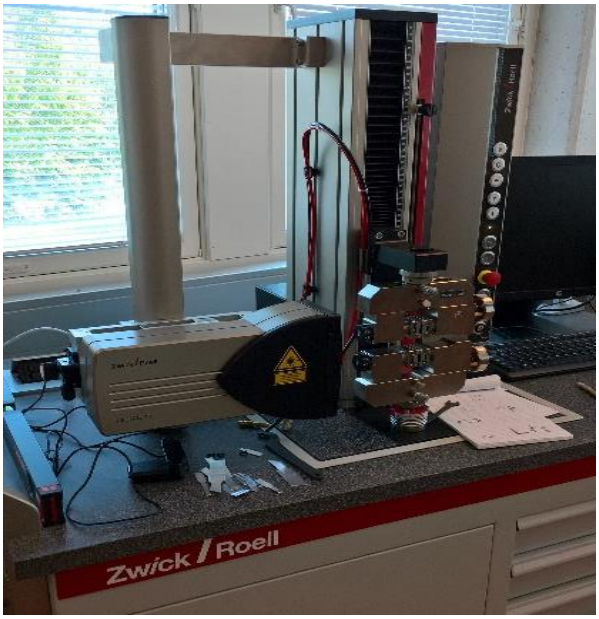

Figure 3-17. Picture of the Zwick/Roell Z2.5 used for tensile testing.

After the tensile tests, the specimens were polished and hardness tested as described in Section 3.3.2 and Section 3.3.4. The hardness measurements were taken at the heads of the tensile tests as illustrated in Figure 3-18.

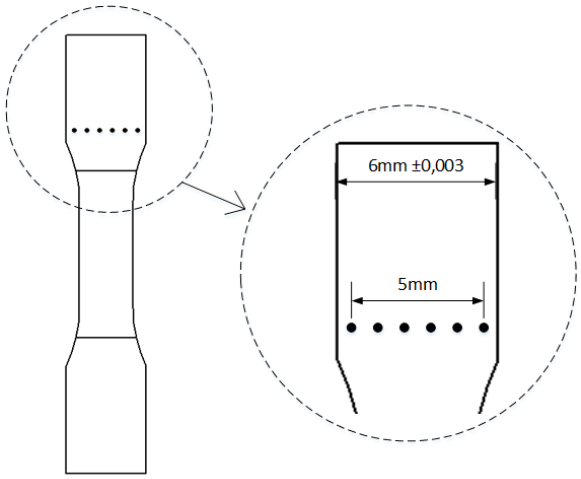

Figure 3-18. Illustration of the hardness measurements on a tensile sample. 6 indentations were taken at the specimen heads, with a space of 1 mm between each indentation.

3.3 Metallurgical treatments

The preparations for both titanium sponge and extruded material were done in accordance to the procedure which have been continuously improved by master students at NTNU (Mathisen, 2012, Eriksen, 2013, Trøan, 2014), and from a basis of titanium preparation found in (Peters et al., 2005) and M.J. Donachie (1988). All images have been taken with a Lumia 650, 8-megapixel camera with lens opening of F/2.2. Polarised images have been taken with a LEICA MEF4M light microscope with a JENOPTIK ProgRes C10plus camera. The epoxy used is made of 25 parts of EpoFix Resin and 3 parts EpoFix Hardener, solidified over 24 hours.

3.3.1 Cutting of Titanium

Cutting of titanium was done with a Struers Discotom-2, cutting blade 20S25, a blade specifically made for ductile materials, with a hardness from 70-700 HV. The cutting was done with water cooling, and manual force control to ensure as low heat build-up as possible.

3.3.2 Grinding and polishing of titanium

The grinding was done in a Struers RotoPol-31 coupled with Struers RotoForce-4. If needed, a grinding surface of 80 SiC was used to grind through the epoxy and remove surface defects. The next step is grinding with 500 SiC and 800 SiC with a force 10 Newton per sample at 150 RPM, co rotation with a continuous water stream. Polishing was done with a Struers TegraPol-31 connected to a Struers TegraForce-5 and TegraDoser-5. The polishing steps were followed as shown in Table 3-2, if the surface was not reflective after the polishing with a MD Largo cloth, the sample was put back into a Struers RotoPol-31 and grinded with 500 SiC and 800 SiC at same settings as shown in Table 3-3 and Table 3-4. Electro polishing would have been a good method for final polishing, however the geometry of the titanium samples made mounting difficult.

Table 3-3, The present grinding preparation steps for titanium.

	COARSE	FINE
GRINDING SURFACE	500 SiC	800 SiC
SUSPENSION	Water	Water
TIME	2 min	2 min
FORCE (SAMPLE HOLDER)	10 N Pr sample	10 N Pr sample
ROTATION	150 RPM, co rotation	150 rotation, co rotation

Table 3-4, The present polishing preparation steps for titanium.

	COARSE	FINE
POLISHING SURFACE	MD Largo cloth	MD chemical cloth
SUSPENSION	9 µm grit DP	90vol%OPS with 10vol%H_2O_2
TIME	10 min	20min
FORCE (SAMPLE HOLDER)	30 N	30 N
ROTATION	150 RPM co rotation	150 RPM Contra rotation

All samples followed the former procedure except for polishing of the tensile specimen, where the samples were held manually using doubled sided bonding tape and manually grinded stepwise from 1200 SiC to 2400 SiC to 4000 SiC.

3.3.3 Heat treatment of titanium

Heat treatment of titanium was done in an Entech Tube furnace with a 2404/2408 Control Setpoint Programmer, in an inert atmosphere, 5.0 Ar (99.999 wt. % Argon). All samples underwent a temperature increase of 200 °C per hour both up and down. The gradient on cooling after 200 °C falls as the furnace struggles with cooling at the rate of 200 °C. The exact cooling rate between 200 °C to 25 °C is not known, but is through observation assumed to be around 150°C per hour.

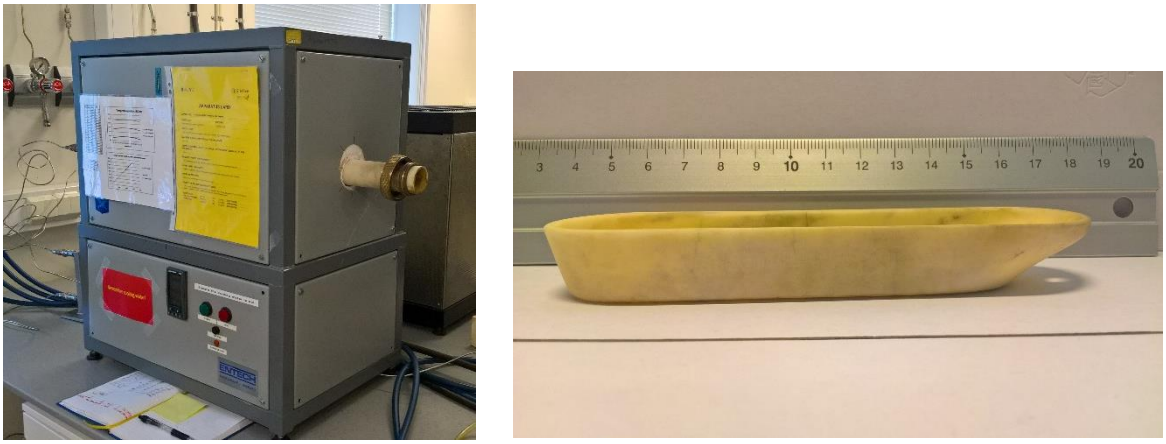

Figure 3-19. Picture of Entech tube furnace to right, which is used in heating in an Argon atmosphere and the sample holder used for all samples are shown to the left.

The heat treatment in air was conducted in a Nabatherm 17 furnace, depicted in Figure 3-20, with the same parameters as indicated above.

Figure 3-20. Nabatherm 17 furnace.

3.3.4 Hardness testing

LEICA VMHTMOT was used, a micro hardness machine with the capabilities to use a force between 5g to 1000g with small indentations. The indentation could be aimed with more accuracy to avoid pores, not fully supported surface or other influencing defects. The hardness testing of the titanium sponge was performed with 50 grams of force per indentation. The indentations spots were not selected randomly, but chosen so as to avoid influencing parameters on the results, however it is based on what is seen through a microscope lens, and underlying geometries and defects are hard to predict.

3.3.5 Elemental chemical analysis

The elemental chemical analysis was carried out, by SINTEF Molab, on the extruded Φ30 and Φ20 mm titanium specimen using an inert gas fusion quantitative analysis for nitrogen, oxygen and hydrogen and an infrared gas analyser to track the carbon content. The gas fusion analysis, also termed melt extraction, involves fusion of the sample at high temperatures. The infrared gas analyser measures trace gases by determining the absorption of an emitted infrared light source through a certain air sample.

3.3.6 Etching of titanium

The etching of titanium was done with a version of the Kroll solution presented in . The Kroll solution has been applicate with good results before, however the specifics of the solutions need to be determined for best possible results. The appropriate amounts of acid should be chosen based on the desired results, hydrofluoric acid attacks titanium and enhances grain boundaries and deformation, the nitric acid brightens the α-phase.

Table 3-5. Overview of composition of the Kroll solution used for etching of titanium. The solution presented as Etching solution on the right is the used composition of the Kroll to etch titanium in this thesis.

Kroll		*Etching solution*
Type	Ti & Ti-alloys	CP-Titanium
Water	90 – 100 mL H_2O	94mL H_2O
Hydrofluoric acid	1 – 3 mL HF (40%)	2mL HF (40%)
Nitric acid	2 – 6 mL HNO_3 (65%)	4mL HNO3 (65%)
Holding time	10 – 40 seconds	20 seconds

It is important to note this solution have a varied response on samples, and great care should be taken in choosing composition and holding time. Etching of titanium has a tendency to highlight deformation if the holding time is too long, and spurious microstructure may show due to strain induced during preparation.

4 Results

The results are presented in two sections, i.e. titanium sponge and screw extruded profiles. The first section focuses on characterisation of titanium sponge, heat treatment and subsequent changes in titanium sponge microstructure and hardness. The investigation into what effect a heat treatment of titanium sponge would have on screw extrusion is presented thereafter.

The section encompassing screw extruded profiles examines and characterises the resulting product of two different screw extrusion experiments. The difference between these profiles are the screw extrusion die openings, φ30 and φ20. The screw extruded profiles are compared, and they demonstrate the effect of die openings as well as the characteristics of the obtained extrusions. A small investigation into the effect of heat treatment is carried through to examine the effect and need for stress reliving in relation to property improvement.

4.1 Titanium Sponge

The sponge being unknown, a former investigation into chemical composition was done by SINTEF explained in chapter 3.1. It has been suggested that the batch labelled MHT-100 Brand might be the received sponge. Therefore, a comparison of the received sponge, MHT-100 Brand and commercially pure titanium is listed in Table 4-1.

Table 4-1. Chemical composition comparison of as received titanium sponge, the MHT-100 Brand and CP-titanium. SINTEF analysis was commissioned before project and done by Universidad Carlos III de Madrid.

Element	*Ti -Sponge – SINTEF analysis*	*Ti-sponge MHT - 100*	*CP Titanium*
Oxygen (wt. %)	0,031±0,005	0,05	0,15 - 0,18
Nitrogen (wt. %)	0,0033±0,0026	0,004	0,02- 0,03
Carbon (wt. %)	0,013±0,002	0,011	0,08
Hydrogen (wt. %)	-	0,001	0,007 - 0,015
Iron (wt. %)	-	0,029	0,18 - 0,2
Titanium (wt. %)	99.95	99,837	99,5

The received sponge has a higher purity than the MHT-100 Brand, and only carbon is above. However, the latter is within one standard deviation. As received titanium sponge are several degrees purer than commercially pure titanium. The size distribution of the primary sponge is calculated by measuring the average size of 228 sponges, the distribution of sponge size is shown in Figure 4-1, showing that a size of 1.5 mm to 2 mm is dominating, and that 87 % of all sample sponges are within 1.5 mm to 4mm.

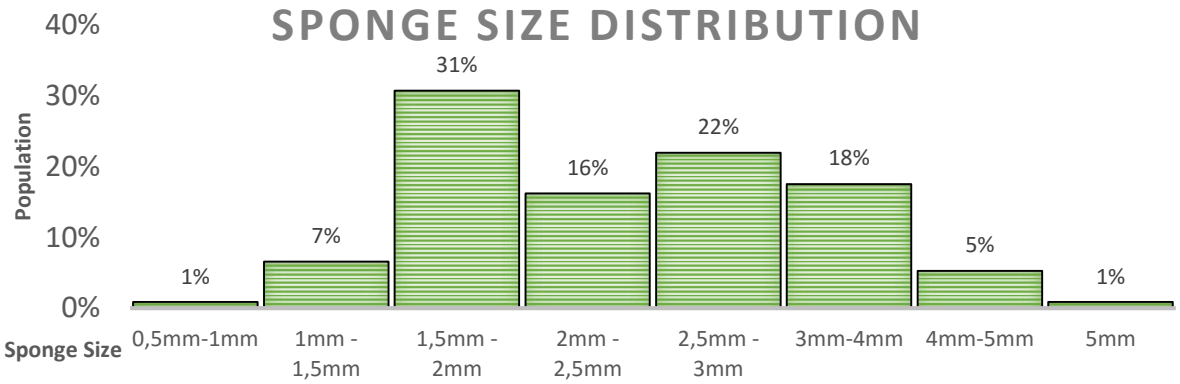

Figure 4-1. The size distribution of the titanium sponge calculated from 228 granulates. The data have been categorised into boxes of 0.5mm

These results give an average size of 2.48 mm and a standard deviation of 0.88 mm, resulting in a normal curve presented in Figure 4-2.

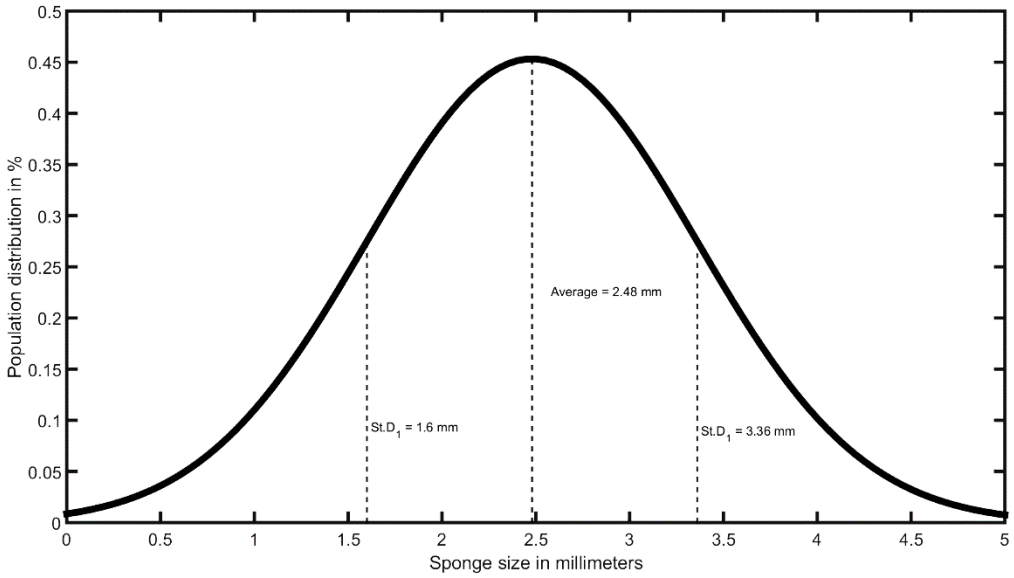

Figure 4-2. Normal curve of size distribution of primary titanium sponge.

The average hardness of the as received sponge was found at 120 HV with a standard deviation at 31 HV, with 61 measurements. The microstructure of the as received titanium sponge has high variation in grain size and deformation twinning, Figure 4-3, at the next page, is included to indicate the microstructure of the as received titanium sponge and show the high degree of variation in microstructure. The average grain size in untreated sponges are 81µm, with a variation at 19µm. This is a fairly low variation, and most likely a lower average, with a higher variation is correct, since the grain size in the most deformed titanium sponge is hard to measure correctly and therefore was not included in the statistics.

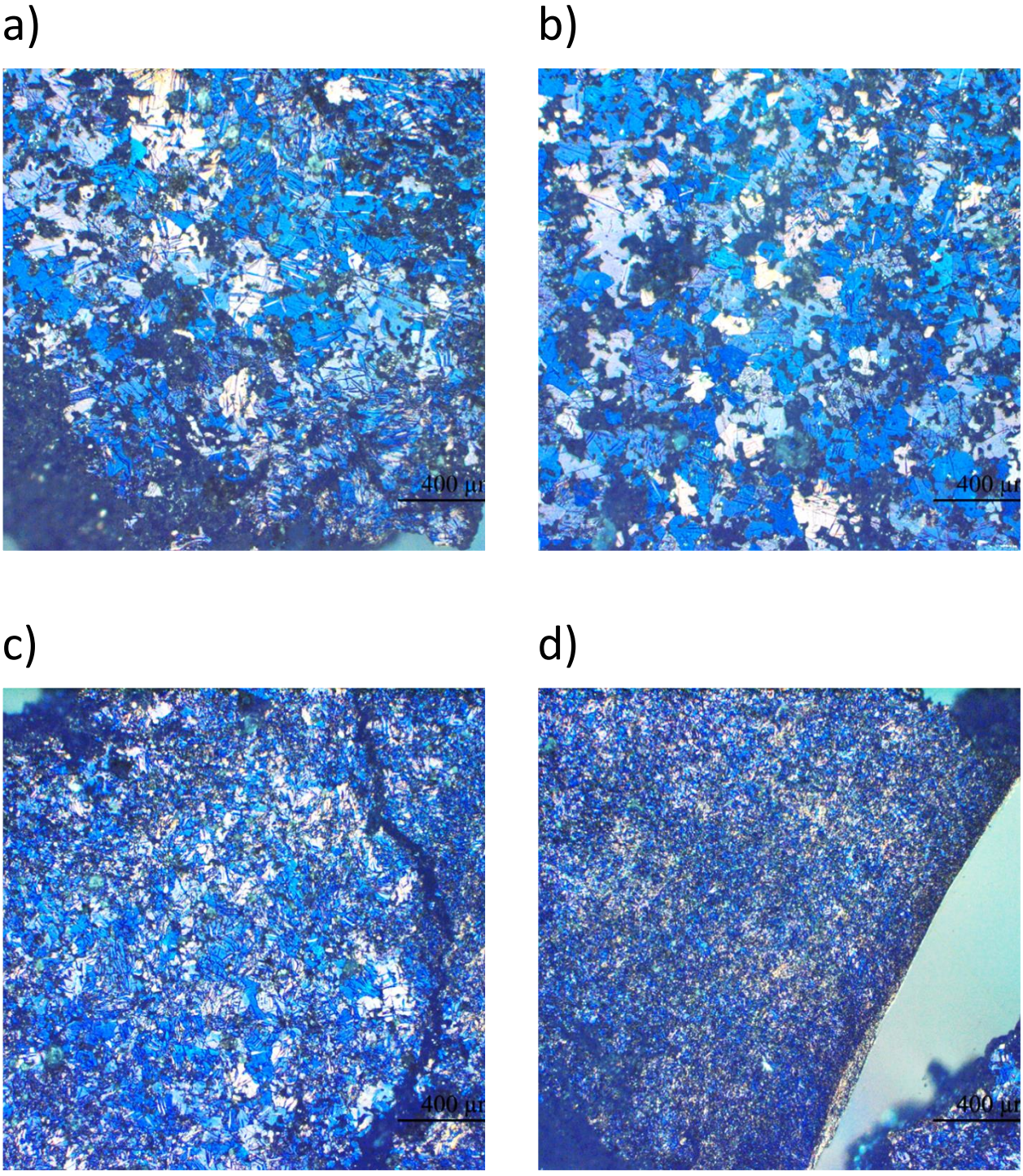

Figure 4-3. Polarized optical light field images of the microstructure of the as received titanium sponge. All micrographs are taken at a magnification of 50X, and all are from untreated sponges. a) & b) are sponges with a low degree of deformation, and twinning deformation, c) & d) shows large degree of deformation overshadowing the grain contrast.

4.1.1 Hardness and Microstructure of heat treated samples at 400°C

The hardness of the heat treated sponge at 400°C/1 hour shows a clear decrease inn hardness of 17 HV, which is a 15 % drop in hardness, to an average hardness of 103 HV, with an standard deviation at 31 HV, 61 hardness indentations. Figure 4-4 shows the characteristic microstructure of the heat treated titanium sponge. The microstructural images show no clear indignation of stress relief in the titanium sponge, any decrease in twinning deformation is hard to quantify through light microscopy. The average grain size is calculated at 102µm with a standard variation at 27µm.

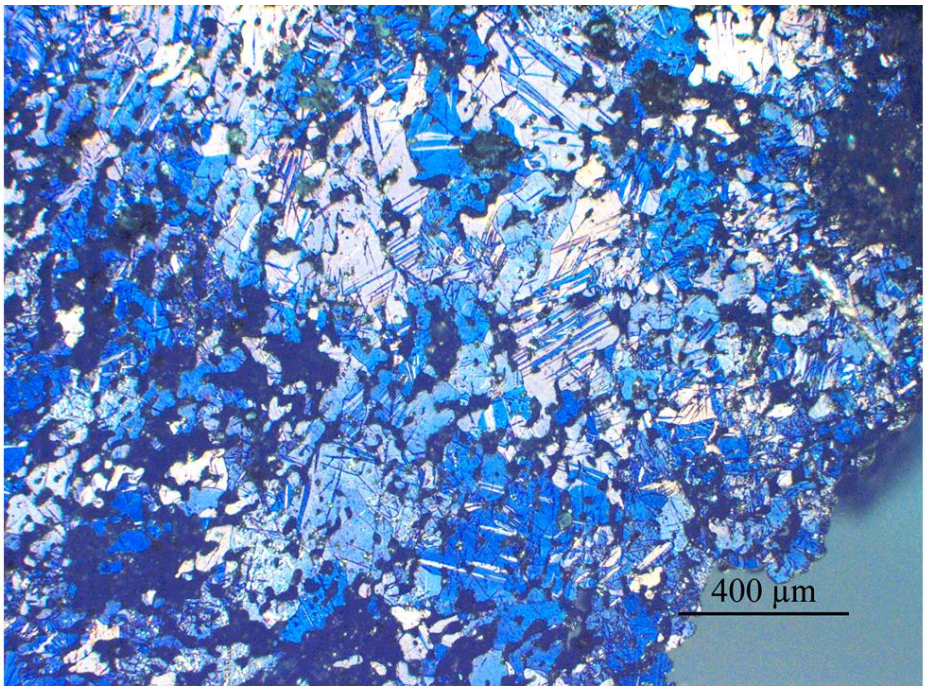

Figure 4-4. Polarized optical light field photo of the microstructure. Characteristic microstructure of titanium sponge heat treated at 400°C. Average size of grains in this picture is 85µm.

4.1.2 Hardness and Microstructure of heat treated sponge at 600°C

Titanium sponge heat treated at 600°C, shows an even clearer drop in hardness of 36 HV, a 30 % drop in hardness. A drop in standard deviation is also recorded from 31 HV to 22 HV, number of hardness indentations are 69. The following microstructural investigation, see Figure 4-5, give an average grain size at 19µm with a standard deviation of 3µm. This is a drop in average grain size of 77 %.

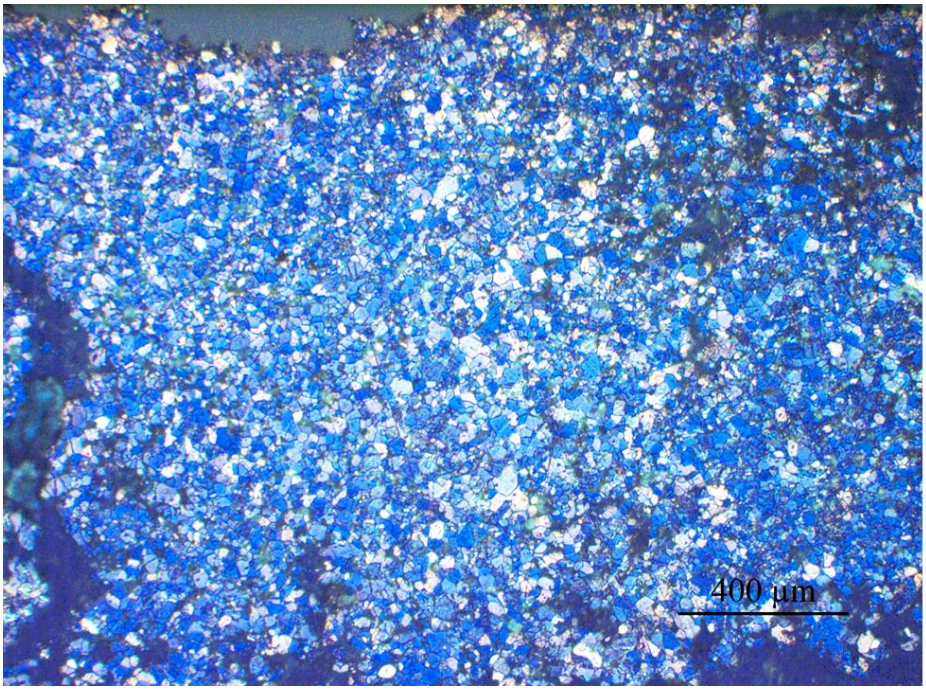

Figure 4-5. Polarized optical light field photo of the microstructure. Characteristic microstructure of titanium sponge heat treated at 600°C. In this figure the average grain size is 17µm.

4.1.3 Hardness and Microstructure of heat treated sponge at 800°C

The titanium sponge heat treated at 800°C shows no decrease in average hardness compared to the untreated sponge, giving an average of 120 HV. However, the standard deviation has increased up to 41 HV, an increase of 32 %, calculated with 63 hardness indentations. Further investigation into the microstructure, see Figure 4-6, follows the development of the heat treatment at 600°C. The grains have grown larger giving an average grain size of 28µm and a standard deviation of 4µm.

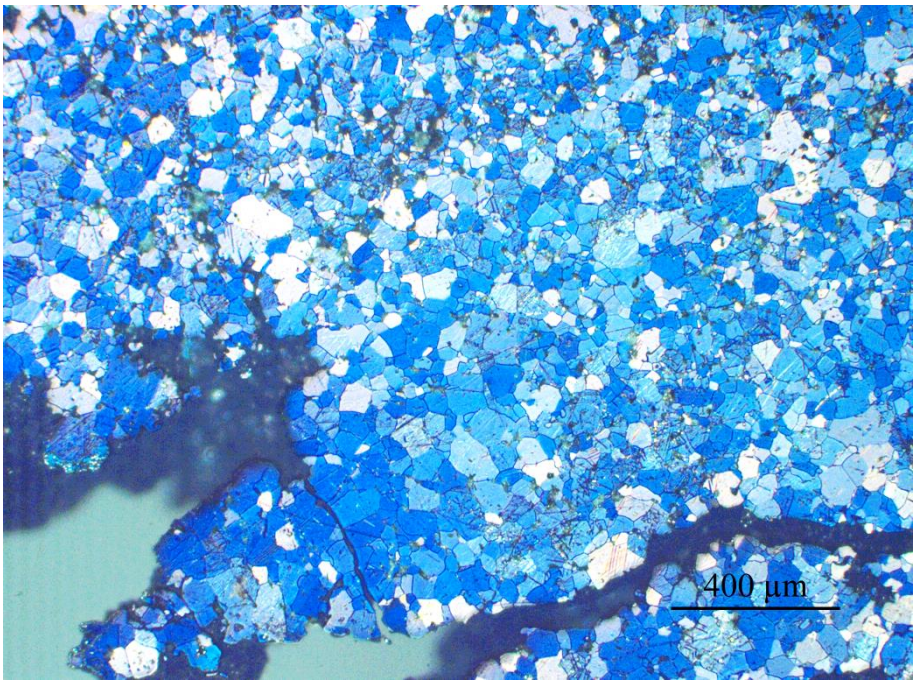

Figure 4-6. Polarized optical light field photo of the microstructure. Characteristic microstructure of titanium sponge heat treated at 800°C. The average grain size in the figure is 31µm.

4.1.4 Overview of the Heat treatment of titanium sponge

Here the heat treatment of both batches of titanium sponge are shown, the titanium sponge with a diameter lower than 4 mm deemed the primary batch, and the titanium sponges above 4 mm in diameter deemed the secondary. Overall the heat treatment of both batches at 400°C and 600°C leads to a decrease in hardness and a decrease in standard deviation, see Figure 4-7. The primary batch had a drop of 30 % hardness and the secondary experienced a drop of 36 % in hardness. However, the results for the 800°C heat treatment are slightly different. The heat treatment of the primary batch experienced no hardness decrease, but a large increase in standard deviation, where the secondary batch did experience a hardness drop of 20% to 109 HV, and no increase in standard deviation at 30 HV, the original standard deviation of secondary batch is 33 HV.

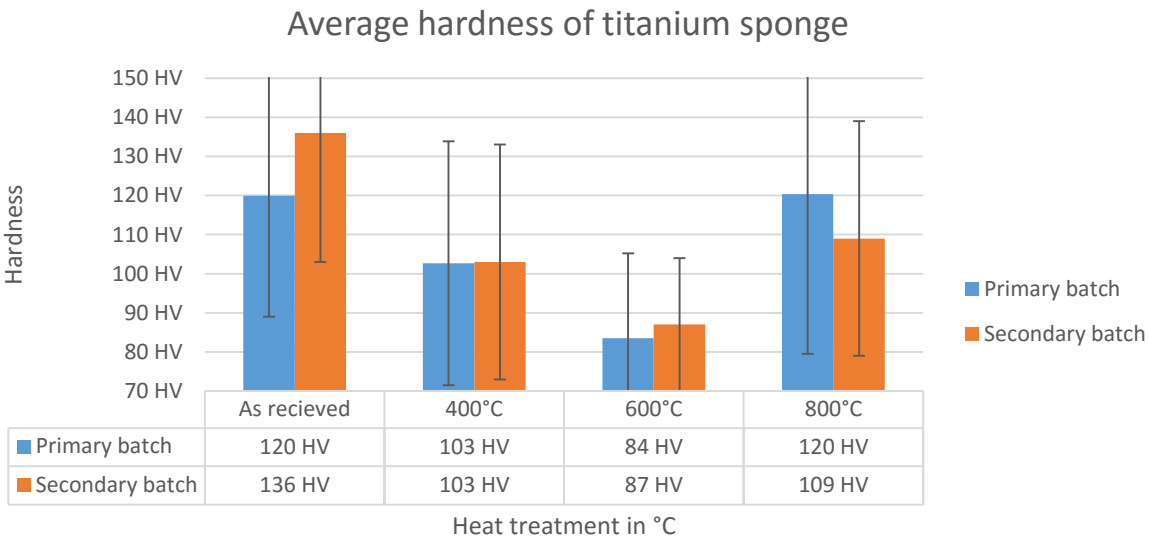

Figure 4-7. Diagram presenting the average hardness and standard deviation of primary and secondary titanium sponge batches. The heat treatments show a similar trend for both.

To summarize the change in microstructure, change after heat treatment of the primary batch of titanium sponge, Figure 4-8 presents the average grain size of titanium sponge. The heat treatment at 400°C gives an increase in grain size. The change in microstructure at a heat treatment of 600°C is a drop in average grain size of 77 % to 19µm with almost equal drop in standard variation of 84 %. The heat treatment at 800°C shows a similar drop in grain size with an average at 28µm and standard deviation at 4 µm.

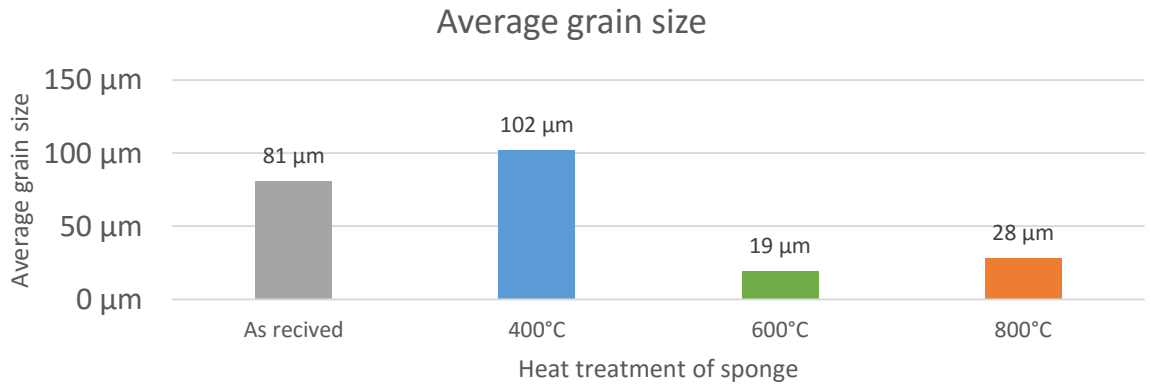

Figure 4-8. Effect of heat treatment on average grain size of primary titanium sponge.

4.1.5 Medium pressure torsion

The results of the medium pressure torsion experiments are compressive disk as shown in Figure 4-9, they are quantified through the amount of consolidation, measured by the maximum depth of the consolidated titanium region in the samples. All samples have undergone an accumulated strain at around $\varepsilon \approx 2.5$ close to the edge.

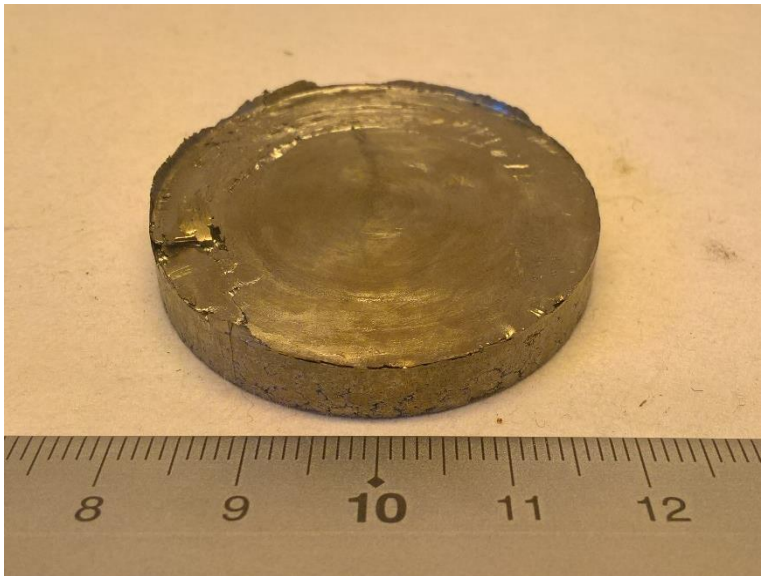

Figure 4-9. Compressive disk produce through medium pressure torsion. Each disk being 40 mm in diameter and height of 5.3 to 5.8 mm. This one is produced with heat treated at 600°C/1 hour at an experiment temperature of 400°C, 5 turns under a pressure of 200 MPa.

Visual observation of the cross section of the samples show that only a fraction of the disk is consolidated titanium, where the rest, mainly centre of the sample and the bottom of the disk are compacted sponge with clear boundaries and porosity. The samples are characterised by two parameters, the input material, i.e. if the titanium sponge had a heat treatment and if yes, at what temperature, and the experiment temperature.

Table 4-2. Overview of density and depth of consolidated area of the medium pressure torsion experiments. The heat treatment column describes the heating scheme for the sponge used, the experiment temperature is the temperature of the equipment during MPT.

Heat treatment	***Experiment Temperature***	***Density of disk (g/cm³)***	***% Density***	***Depth of consolidated area***
None	300 °C	4.35	96.59 %	0.63 mm
None	300 °C	4.28)	95.20 %	1.42 mm
None	400 °C	4.24	94.22 %	1.71 mm
None	400 °C	4.25	94.43 %	1.11 mm
400 °C	300 °C	3.96	88.03 %	1.39 mm
400 °C	400 °C	3.92	87.18 %	1.77 mm
600 °C	300 °C	4.25	94.52 %	1.42 mm
600 °C	300 °C	4.26	94.75 %	0.92 mm
600 °C	400 °C	4.31	95.76 %	0.61 mm

The table data in Table 4-2 are presented in a bar diagram in Figure 5-1. They are placed in accord to the experiment date, going from old to new, left to right. The colour scheme is to separate the different sponges used in the experiments, blue is for as received sponge, green is for heat treated at 400°C and orange is for heat treated at 600°C.

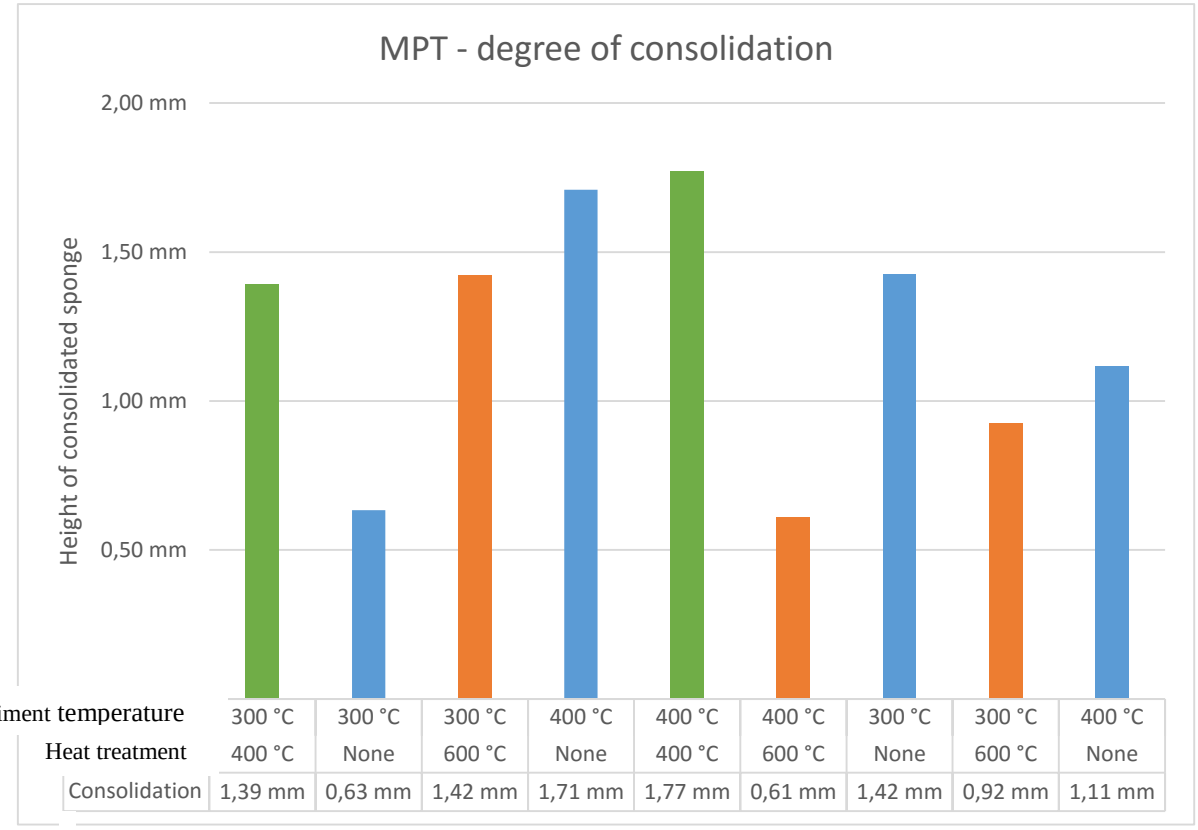

Figure 4-10. A bar diagram of the consolidation data in Table 4-2. The bar diagram is for the amount of consolidation. The data is placed by date of experiment, old to new, left to right. Bars coloured blue are disks from as received sponge, green are disk of heat treated sponge at 400°C/1 hour and orange are disk heat treated at 600°C/1 hour.

The torque needed to hold the piston in place is shown in Figure 4-11. These three line diagrams described the three last experiments, it was assumed the control program for the MTS 311 logged them automatically, as this turned out to not be the case a manual logging was done. All has a high starting effect with a drop in the beginning, and then a gradual increase in torque needed as the number of rounds increase.

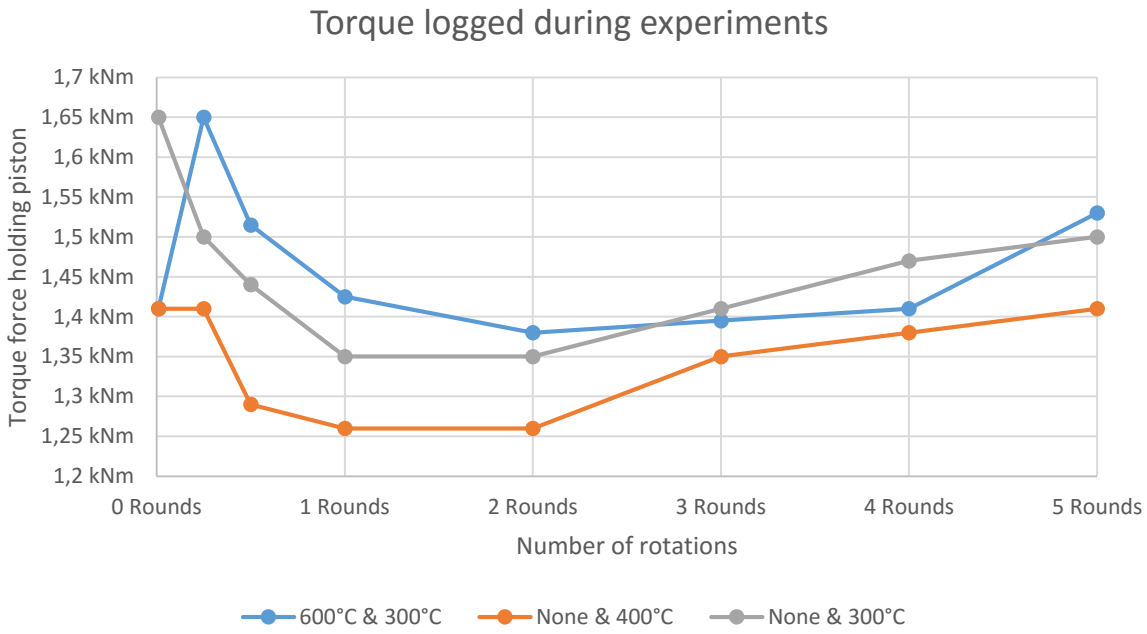

Figure 4-11. Overview of torque forces of three experiments, all showing the same trend of a rise in torque forces as the amount of shear deformation increases.

4.2 Screw extruded profiles

Two screw extruded profiles were chosen, i.e. produced with a die opening of ϕ30 and ϕ20 respectively. Both have been examined in terms of chemical composition, hardness, macro- and microstructure as well as machined to tensile specimen. The hardness measurements serve as an indication of the amount of deformation and homogeneity over the cross section of the profiles. Microstructure images are taken of the cross section, determining grain size and visual degree of deformation. The tensile test are done to find the degree of consolidation within the screw extruded profiles and investigate effect of annealing on the sample material. Several heat treatment schemes are made to determine the necessary steps of post-production treatment.

4.2.1 Chemical composition of screw extruded samples

The elemental compositions are presented below in Table 4-3 and Table 4-4 to show the accumulated contamination during the screw extrusion process. Table 4-3 shows the measured compositions of titanium sponge, both screw extruded samples and commercially pure titanium. Both titanium sponge, and screw extruded profiles are listed with a Titanium content of less than their number, this is to illustrate that only some elements have been measured and there are most likely more interstitial elements decreasing the overall purity. Table 4-4 illustrates the change in composition from titanium sponge to screw extruded samples.

Both screw extruded samples shows a large increase in oxygen and nitrogen. The most noticeable increase is the level of nitrogen, with levels of percentage increase at 5657 % and 3536 % to ϕ30 and ϕ20 respectively. The oxygen increase does not have the same levels increase with a 223 % and 352 % oxygen increase to ϕ30 and ϕ20 respectively. The difference in oxygen and nitrogen increase between screw extruded profiles is unknown as the error range is well below the difference.

Table 4-3. Overview of the chemical composition of the titanium sponge, and finished extruded samples with Φ30 and Φ20, and compared to commercially pure titanium.

Element	***Ti -Sponge***	***Ti -Extruder Φ30***	***Ti -Extruder Φ20***	***CP-Titanium***
Oxygen *(wt.%)*	0,031	**0,1**	**0,14**	0,15 - 0,18
Nitrogen (wt.%)	0,0033	**0,19**	**0,12**	0,02- 0,03
Carbon (wt.%)	0,013	0,01	0,02	0,08
Hydrogen (wt.%)	-	0,0031	0,003	0,007 - 0,015
Iron (wt.%)	-	-	-	0,18 - 0,2
Ti (wt.%)	≤ 99,95	≤ 99,70	≤ 99,72	≥ 99,50

The carbon content has no significant increase through the process. Hydrogen increase cannot be calculated before a new elemental chemical analysis has been done on the titanium sponge. The iron content has not either been measured.

Table 4-4. An overview over the change in oxygen, nitrogen and overall purity between the titanium sponge and extruded material. The change in carbon has been neglected as the difference may very well be measurement inaccuracy.

	Change in wt.% after screw extrusion		***% increase of foreign elements***	
Element	Ti -Extruder Φ30	Ti -Extruder Φ20	Ti -Extruder Φ30	Ti -Extruder Φ20
Oxygen	0,069 wt.%	0,109 wt.%	223 %	352 %
Nitrogen	0,187 wt.%	0,117 wt.%	5658 %	3536 %
Hydrogen	-	-	-	-
Ti	-0,23 wt.%	-0,21 wt.%	-0,23 %	-0,21 %

4.2.2 Hardness of screw extruded samples

Two cross sections per screw extruded profile, φ30 and φ20, were examined in terms of hardness and microstructure. The average hardness and variation is first presented, thereafter the hardness maps and then microstructure. Figure 4-12 is included to illustrate what the samples represent.

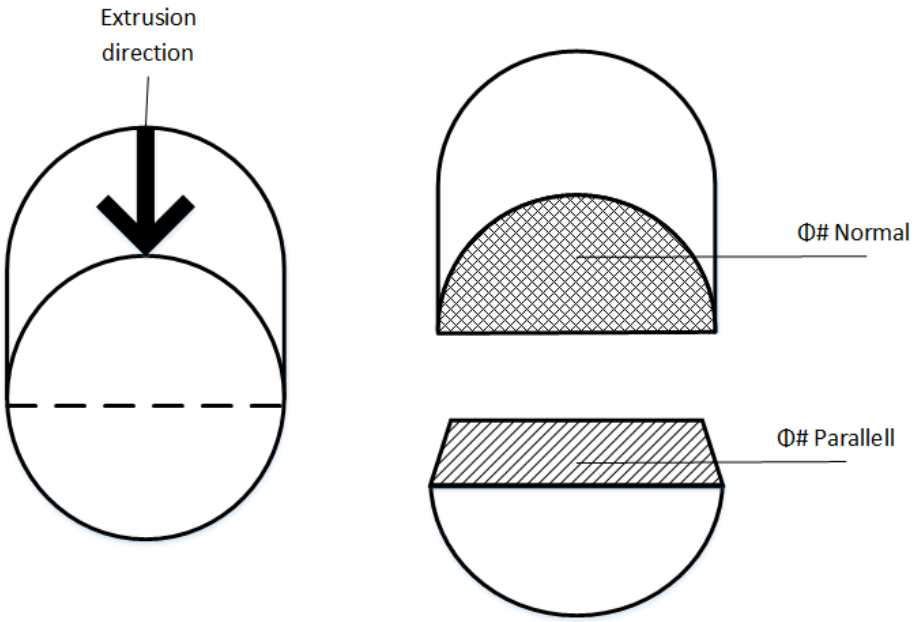

Figure 4-12. Illustration of the cross sections discussed in this section. The samples are, as described earlier, cross sections of the screw extruded profiles, one per sample represent the cross section normal to the extrusion direction and the other represents the cross section parallel to the extrusion direction.

The average hardness and standard deviation of these cross sections are presented in Table 4-5.

Table 4-5. Overview of average hardness, standard deviation and number of indentations on the screw extruded cross section samples.

	φ20Normal	*φ20Parallell*	*φ30Normal*	*φ30Parallell*
Average hardness	190 HV	236 HV	245 HV	251 HV
St. D	40 HV	56 HV	51 HV	51 HV
Number of indentations	322	144	867	779

Separate measurements of cross sections from another position in the screw extruded profiles have been performed earlier in (Meling, 2015), these are shown in Table 4-6. The hardness over the cross sections normal to the extrusion direction reported a different hardness for the samples. The results show a completely different picture, where these results registered the highest hardness in φ20 compared to the φ30.

Table 4-6. The table shows the average, standard deviation and number of indentations for each extruded sample and a reference titanium grade 2 sample. Gathered from (Meling, 2015).

	Grade 2 Ti	*Φ20*	*φ30*
Average hardness	202 HV	336 HV	275 HV
St. D	8 HV	55 HV	57 HV
Number of indentations	9	20	20

The difference in average hardness for the φ20 screw extruded samples is 100 HV compared to the φ20 Parallel and 146 HV compared to the φ20Normal, these differences amounts to twice and tipple the size of the standard deviation. The hardness measurements from φ30 samples shows an average difference of 20 HV, well below their standard deviation.

The hardness grids formerly mentioned and results broken down in
Table 4-5, are shown in Figure 4-13 to Figure 4-16. The purpose of these results are looking at the homogeneity of the screw extruded samples.

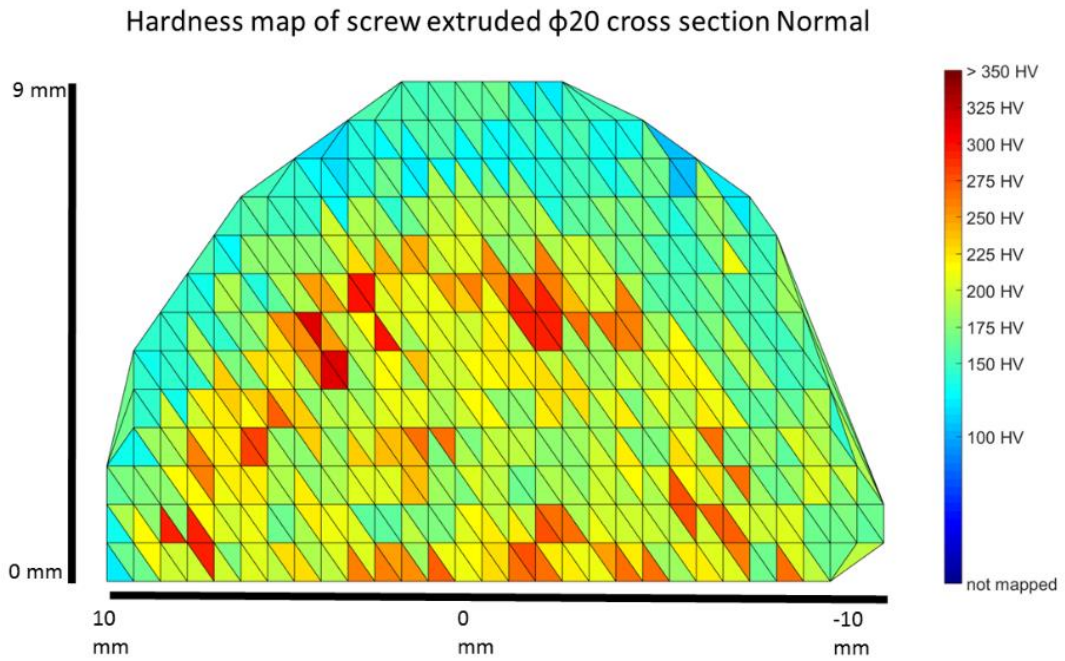

Figure 4-13. A hardness map over the cross section normal and parallel to the extrusion direction of the φ20 sample. 322 hardness indentations in total, giving an average hardness of 190 HV and standard deviation at 40 HV.

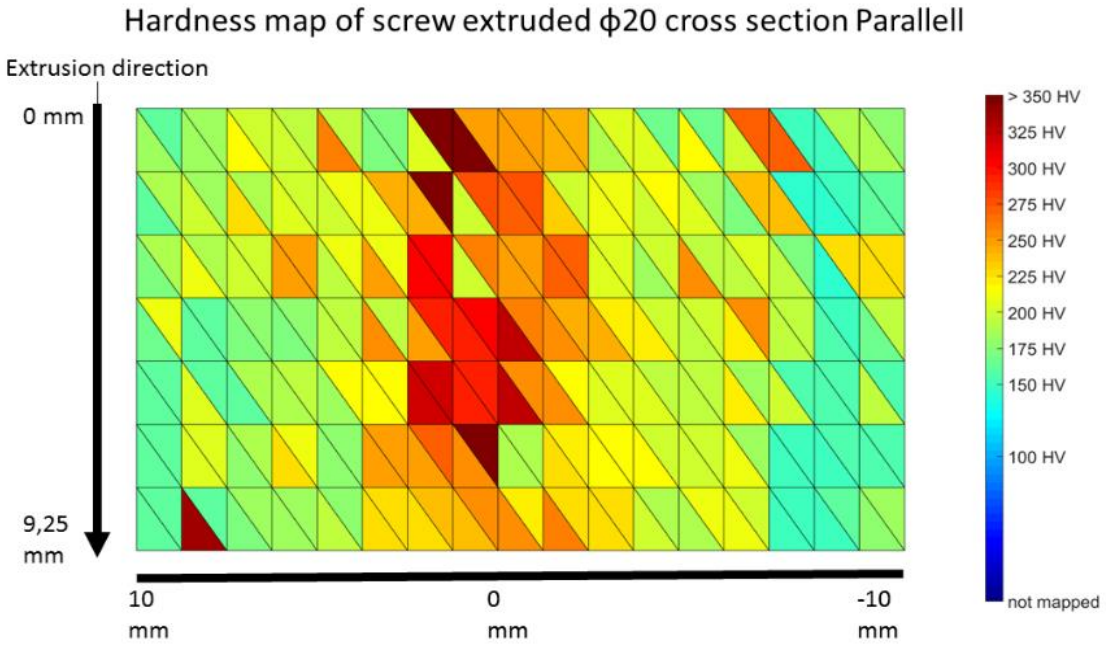

Figure 4-14. A hardness map over the cross section parallel to the extrusion direction of the φ20 sample. 144 hardness indentations in total, giving an average hardness of 236 HV and standard deviation at 56 HV.

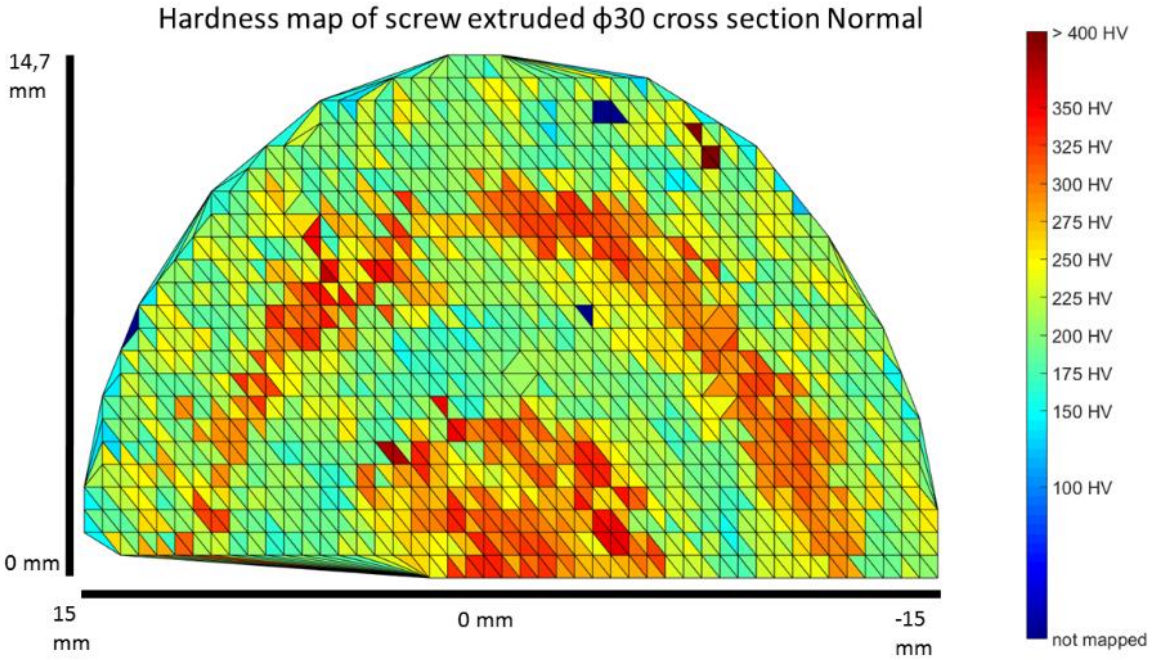

Figure 4-15. A hardness map over the cross section normal to the extrusion direction of the φ30 sample. 867 hardness indentations in total, giving an average hardness of 245 HV and standard deviation of 51 HV.

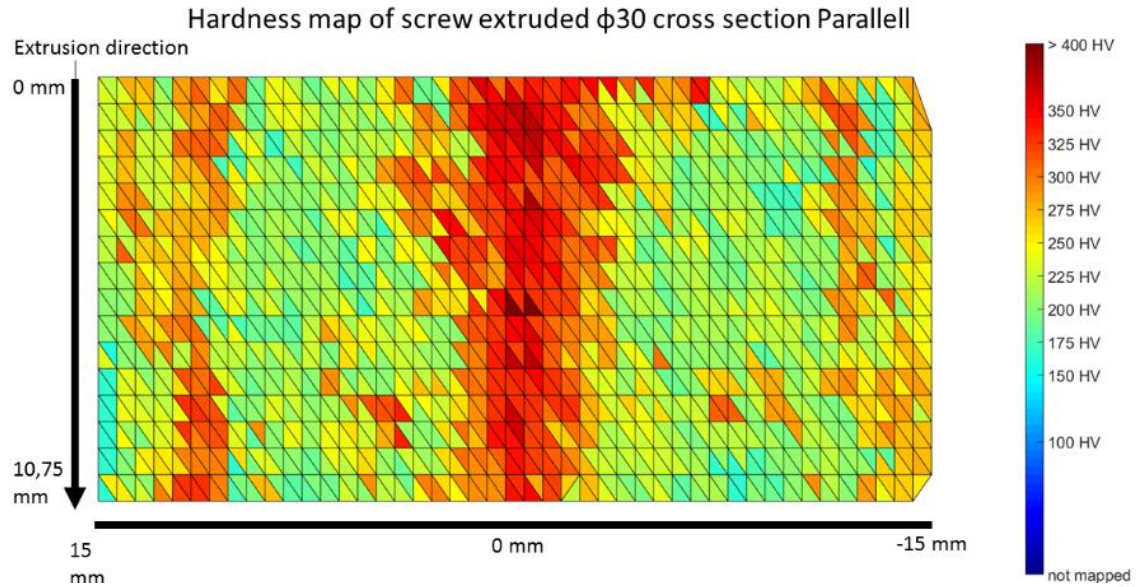

Figure 4-16. A hardness map over the cross section parallel to the extrusion direction of the φ30 sample. 779 hardness indentations in total, giving an average hardness of 251 HV and standard deviation at 51 HV.

The indentations were generally asymmetrical, not uncommon for titanium because of the anisotropy in the material. However almost all were longer in the extrusion direction, indicating some weakness along this direction.

4.2.3 Microstructure of screw extruded samples

Microstructural images of both screw extruded samples are shown below, showing characteristic microstructure of the samples. Macro imaging of the cross sections are placed in Appendix B.

Looking at the microstructure, visually all shows the same characteristics, a large variation in grain size and deformation. There are no clear distinct areas where one current microstructure is prevalent. Figure 4-17 illustrates this point, showing the edge of the ϕ20 sample. There are paths of different sizes, in grains and deformation, indicating a relationship with degree of deformation and recrystallization. This large variation in grain size make any calculation of the average grain size slightly irrelevant as it does not explain the microstructure, a range of grain size is rather used to illustrate the difference of the regions.

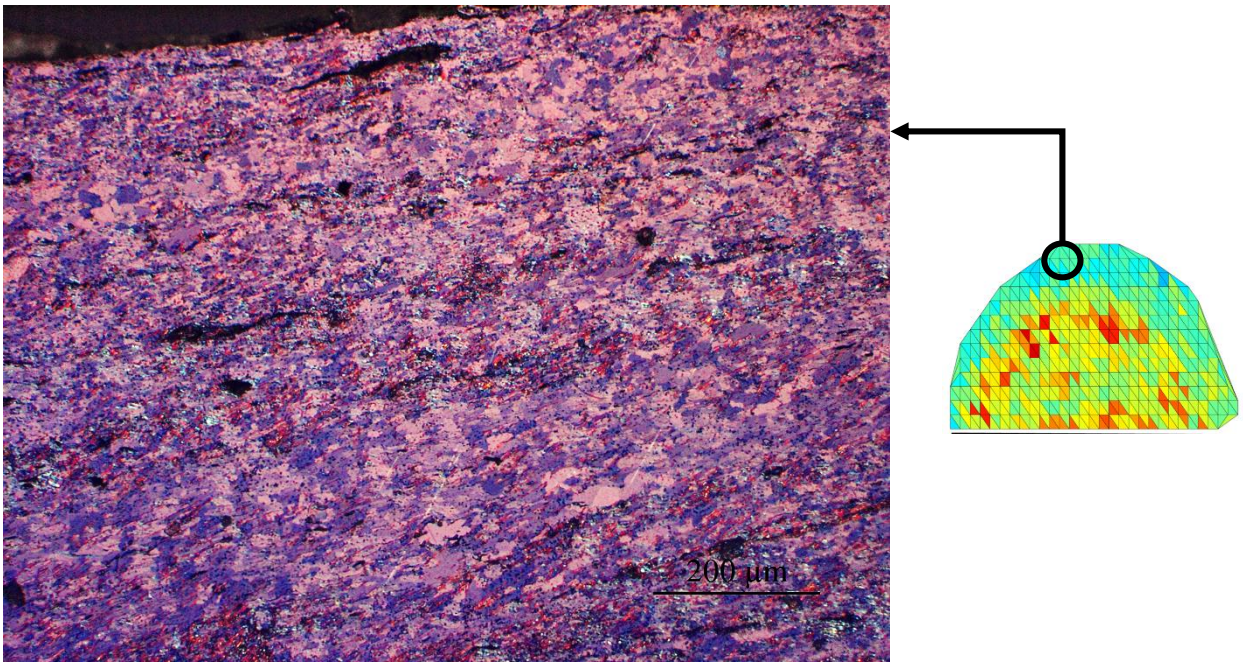

Figure 4-17. Polarised light emission field image of the φ20 Normal sample. Notice the dark areas, they are caused by the etching, getting severely etched due to the extra surface area from deformation. The position of the image is indicated on the hardness grid to the right, area in the picture shows a hardness of 125HV to 150HV.

Generally, the edge showed the largest grains, with the largest found to be 135µm, generally the range of grain size along the edge is around 10µm to 100µm, spread around in pockets of equally sized grains. The range of grain size decreases moving inwards with both samples, showing the same variation in some areas with large grains and some smaller, indicating different growth basis. Both samples had a general range of grains at roughly 10 to 70µm. Figure at the next page is the ϕ30 Normal cross section, showing this range of grain size.

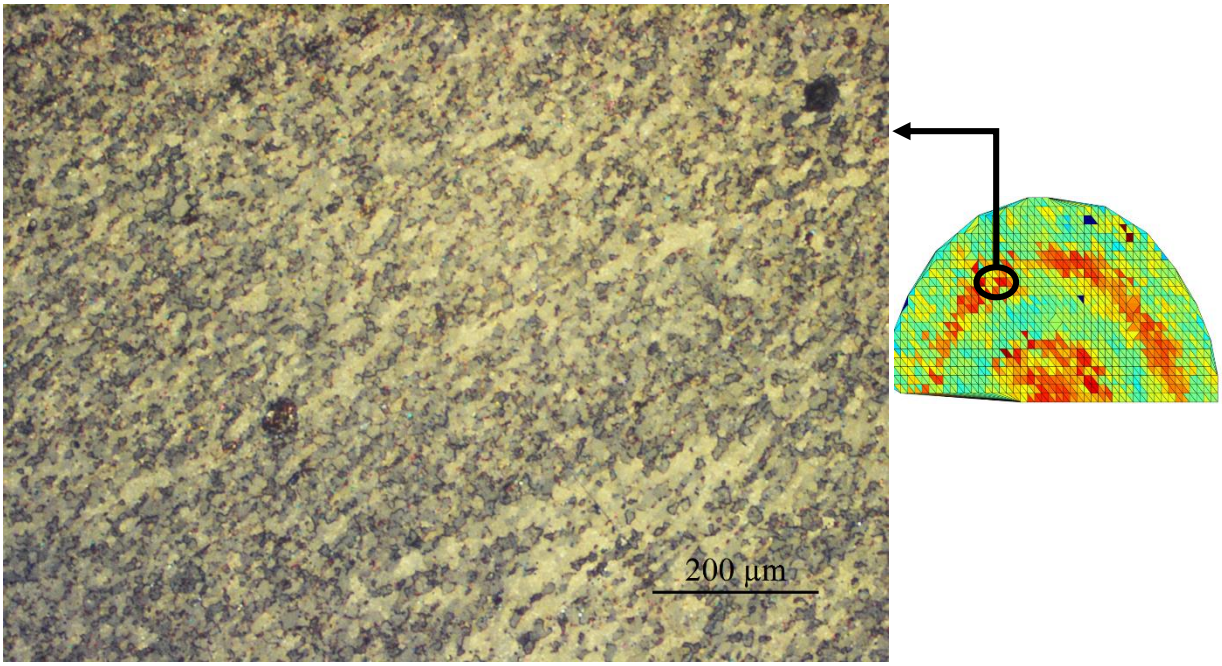

Figure 4-18. Polarised light emission field image of the φ30 Normal sample. The position of the image is indicated on the hardness grid to the right, area in the picture shows a hardness of above 300 HV.

Moving to the next soft region, Figure 4-19, illustrates the microstructure in both φ20 and φ30. All show a less degree of deformation, and smaller range in grain size, range of grains observed is 10 - 50µm.

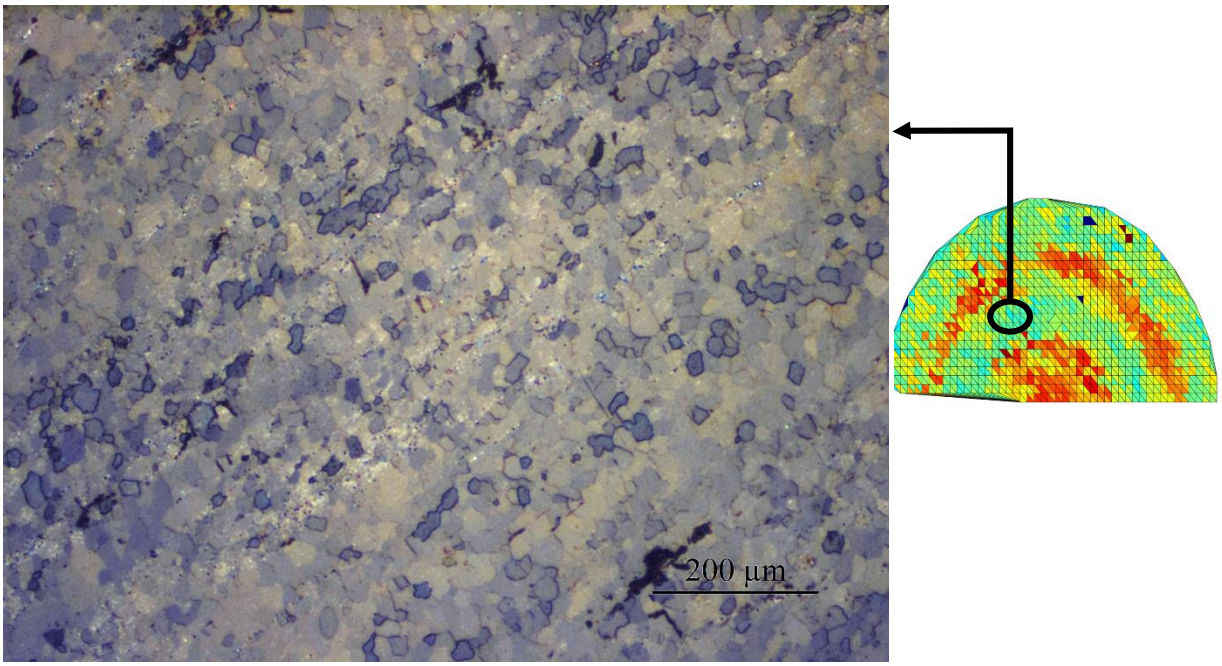

Figure 4-19. Polarised light emission field image of the φ30 Normal sample. The position of the image is indicated on the hardness grid to the right, area in the picture shows a hardness of 175 – 200HV.

At this point, examining the cross sections of φ20 and φ30 have showed similar microstructure tendencies in the edge and inwards towards the centre in hardness area. However, in the centre of the samples it is hard to distinguish as the deformation often overshadows any microstructure and images with descriptive microstructure hard to find. The general description is a varying degree of deformation, with large variation in grain sizes. Figure 4-20 is included to show deformation and microstructure side by side of φ20 and φ30.

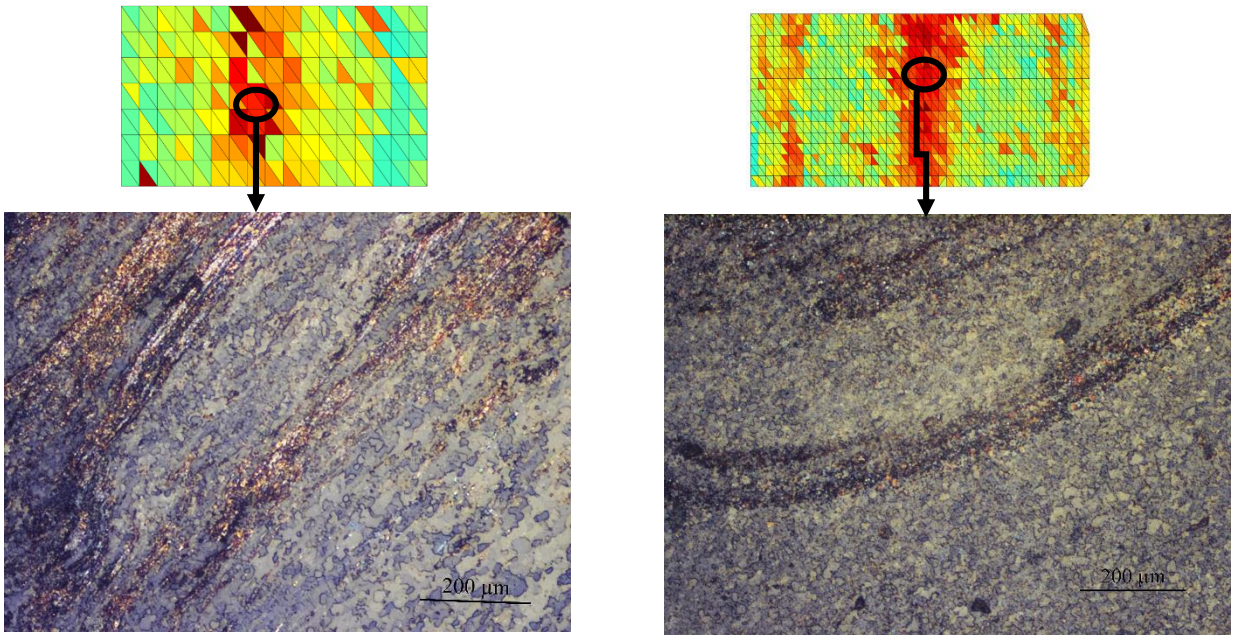

Figure 4-20. Polarised light emission field image of the φ20 and φ30 parallel samples. The position of the image is indicated on the hardness grid to the right, area in the picture shows a hardness of above 300 HV. In this figure the grain size of the φ30 sample is lower than for the φ20, however this is not necessarily characteristic for either samples

4.2.4 Tensile tests

Several of the tensile specimen failed in producing valid data as describe in chapter 3.2.2. Those that did are listed below in Table 4-7 and shown in stress strain diagrams in Figure 4-21 for ϕ30 and Figure 4-22 for ϕ20. The specimens are characterised based on hardness measurements on the heads, yield strength (YS), ultimate tensile strength(UTS), elongation at fracture (ε_f) and the measured E-modulus. Table 4-7 is designed in mind to serve as an overview of the tensile data.

Table 4-7. Overview of hardness and tensile data from tensile specimen.

Specimen	***Hardness***	***YS***	***UTS***	$\boldsymbol{\varepsilon_f}$	***E-modulus***
20_14	428 HV	829 MPa	837 MPa	0,9 %	128 GPa
20_3	318 HV	586 MPa	745 MPa	5,1 %	164 GPa
24Ar_2	324 HV	0 MPa	614 MPa	1,1 %	24 GPa
256Air_1	361 HV	0 MPa	704 MPa	0,9 %	94 GPa
256Air_2	296 HV	0 MPa	911 MPa	1,5 %	47 GPa
256Ar_1	384 HV	0 MPa	527 MPa	0,9 %	70 GPa
256Ar_2	362 HV	0 MPa	630 MPa	0,7 %	96 GPa
30_3	210 HV	0 MPa	413 MPa	0,3 %	218 GPa
30_4	218 HV	387 MPa	487 MPa	11,6 %	99 GPa
34Ar_1	178 HV	0 MPa	449 MPa	0,8 %	77 GPa
34Ar_2	235 HV	0 MPa	443 MPa	0,5 %	88 GPa
356Ar_1	196 HV	405 MPa	432 MPa	1,3 %	60 GPa
356Ar_2	257 HV	462 MPa	536 MPa	6,5 %	65 GPa
356Air_1	225 HV	422 MPa	532 MPa	7,5 %	229 GPa
356Air_2	259 HV	478 MPa	581 MPa	2,2 %	224 GPa

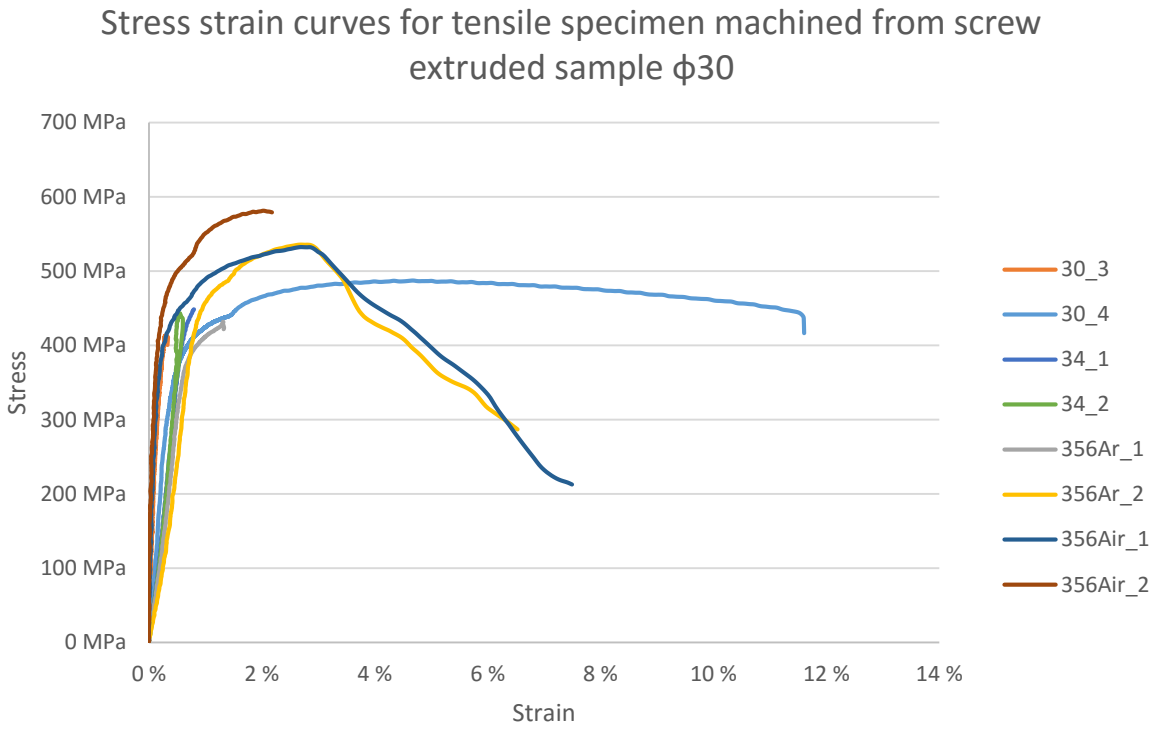

Figure 4-21. Tensile stress strain curves for tensile specimen machined from screw extruded sample φ30

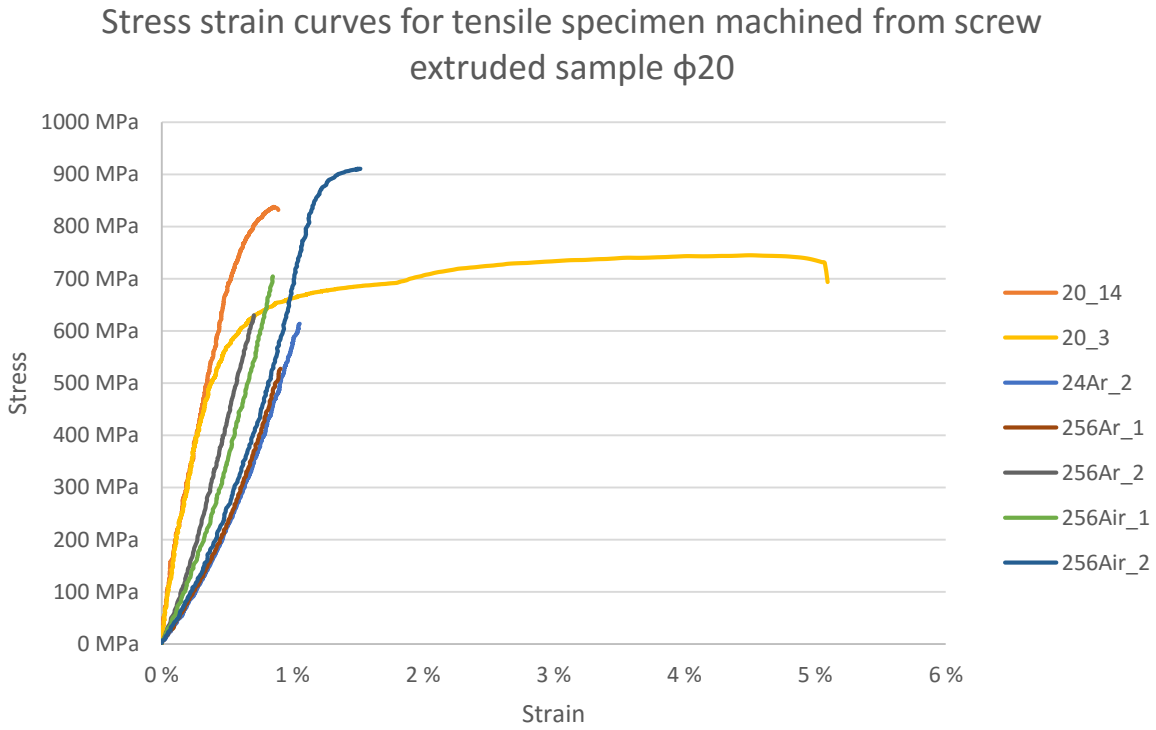

Figure 4-22. Tensile stress strain curves for tensile specimen machined from screw extruded sample φ20

4.2.5 Fractography

Four tensile specimen were chosen to represent the total set of specimens. The two most ductile samples, one from each extruded profile. One tensile specimen showing normal tensile behaviour, but had a brittle fracture, and one representing those that showed an abnormal tensile curve. The SEM images were taken to identify fracture surfaces as well as any clear indication of fracture initiations from defects such as pores, cracks or inclusions. The first presented images, in Figure 4-23, are from the 30_4 sample, the sample with the longest elongation at 11.6%.

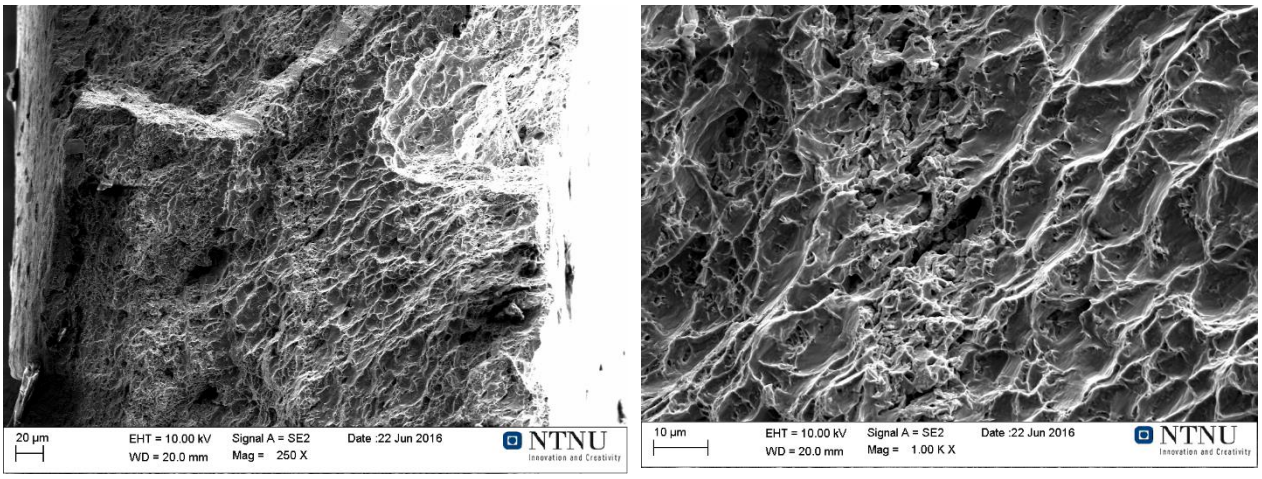

Figure 4-23. SEM images from the sample 30_4, with a UTS of 487MPa and elongation of 11.6%. The fracture surface shown in the images are characteristic for the samples, showing a surface with cavities in the range of 2 - 20µm. The fracture surface has been identified as intergranular with signs of cleavage.

Next image, Figure 4-24, is from the most ductile sample of the ϕ20 set, 20_3, with an UTS of 745MPa and an elongation of 5.1%.

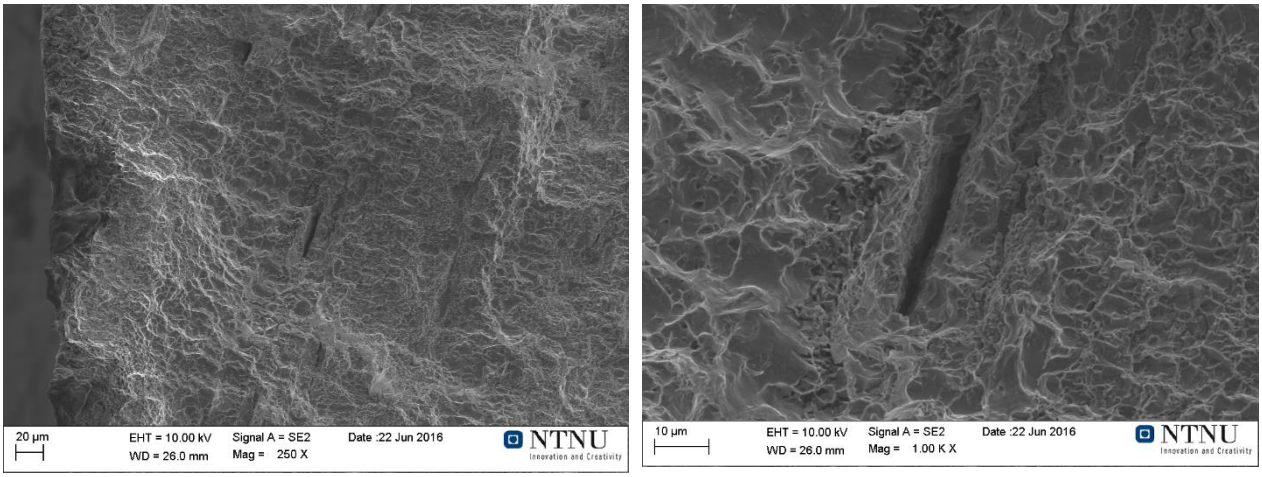

Figure 4-24. SEM images from the sample 20_3, with a UTS of 745MPa and elongation of 5.1%. The fracture surface indicates a quasi-ductile fracture with signs of intergranular fracture and shear. The crack observed in the figure are identified as a secondary crack.

The images in Figure 4-25 show another untreated sample from the screw extruded ϕ30 profile, the 30_3. The sample had a strong elastic region with the Young's modulus measured at 218GPa, fracturing without yield at a UTS of 413MPa and elongation of 0.3%.

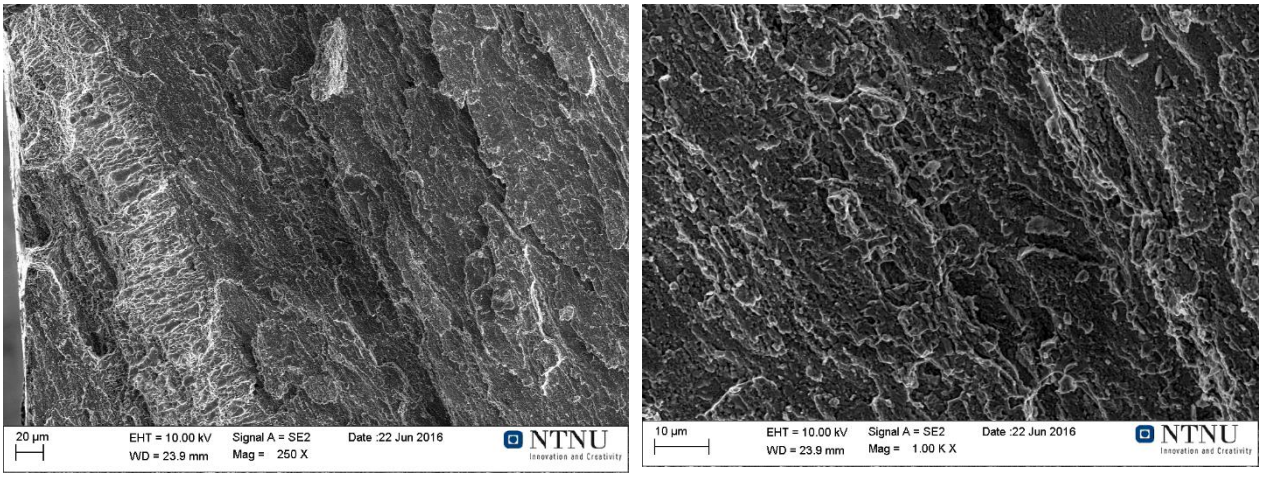

Figure 4-25. SEM images from the sample 30_3, with a UTS of 413MPa and elongation of 0.3%. The identified general fracture pattern is shear.

Figure 4-26 are taken of 24Ar_2, heat treated at 400°C/0.1 hours. This specimen showed a Young's modulus at 24GPa with no yield. The UTS at 614MPa and elongation at fracture of 1.1%.

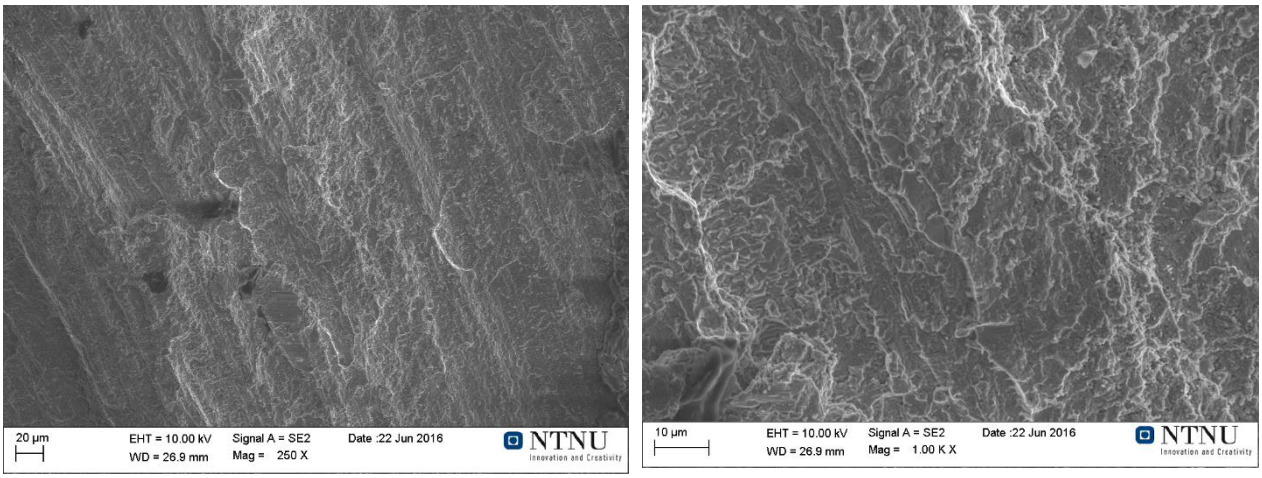

Figure 4-26. SEM images from the sample 24Ar_2, with a UTS of 614MPa and elongation of 1.1%. The fracture surface shows large shear regions with small pockets of intergranular fracture.

5 Discussion

The discussion will focus on answering the questions stated in the introduction. This means, (1), can heat treatment of titanium sponge be an optimisation of the screw extrusion process and, (2), to what degree is the already produced material within industry specifications?

5.1 Effect of heat treatment on titanium sponge

To answer the first questions, the characteristics of titanium sponge found in an earlier report will be presented. Thereafter, the effect of three different heat treatments on sponge characteristics and finally tests in MPT device to examine any difference in consolidation between the differently treated sponges. This discussion will focus on the primary titanium sponge, as the secondary titanium sponge served as a reference group for the heat treatment.

The MHT-100 Brand of sponge is showing similar chemical composition as the received titanium sponge. Higher oxygen and nitrogen content and lower in carbon, but within one standard deviation. The chemical composition given for the MHT-100 Brand is a maximum limit. It's uncertain if the received sponge is the brand MHT – 100, regardless the sponge has a high degree of purity with a low degree of variation and will serve well as a starting point for production of CP titanium or titanium alloys. The low levels of oxygen, nitrogen and carbon puts the titanium sponge into the category of high purity titanium. The theoretical hardness from the interstitial elements is calculate to be an increase of 29 HV, any other direct effect on the material is low as the composition is well below CP titanium.

The average hardness of the primary sponge is reported at 120 HV and the microstructure show an equiaxed microstructure with average grain size at 81µm. The high standard deviation indicates an inhomogeneous distribution of deformation which can also be seen in the microstructural images. The microstructural images show a large degree of deformation twinning, sometimes overshadowing the grain contrast. This microstructural deformation variation most likely comes from the production where the titanium sponge is first in the form of a large cake, and then crushed down to the desired size.

Using the theoretical hardness equations and hardness basis for pure titanium given in chapter 2.2.2 the theoretical hardness of the titanium sponge is 129 HV, 7.5 % higher hardness than measured. This theoretical hardness only accounts for the interstitial hardening effect, neglecting the deformation which also would contribute. The fact that the measured average hardness is 7,5% below the theoretical hardness level indicates that the porosity and geometry of titanium sponge have an effect on the hardness indentations. This leads to the conclusion that the hardness results may not be directly comparable with other measurements and should only be compared internally. Another source to the large standard deviation is the anisotropy of titanium. With the average grain size being 81µm and the average hardness indentations taken at a 50 gram of forces range from 25µm to 40µm with a HV range at 60 to 150 HV. This shows that most hardness indentations were most likely within one grain, not giving and average of hardness of several grains but for only one, as well as the local degree of twinning varies a lot and will also effect the measurements.

Another aspect of the received primary sponge batch is the size distribution. The primary sponge size distribution rapports an average of 2.48 mm and a standard deviation of 0.88 mm. It is unknown if any variation in size of titanium sponge will affect the screw extrusion process, however this specific inquiry is beyond the scope of the thesis.

5.1.1 Heat treatment of sponge at 400°C

A heat treatment at 400°C in titanium is considered a low stress relief temperature because of titanium's low self-diffusion of below 10^{-19} m/s^2. Normally for CP titanium the stress relief temperature range lies between 480°-595° C, with holding times 0,25-4 hours respectively. The holding time of 1,5 hours is decidedly lower than the suggested 480°C at 4 hours. This indicates that the any stress relief at 400°C should not be significant, however since titanium sponge is a lot purer than CP titanium, this may not be the case.

The microstructure examination for 400°C show no clear indignation of stress relief in the titanium sponge, however any decrease in twinning deformation is hard to quantify through light microscopy. A grain growth was recorded, with an average grain size of 102µm an increase of 26 %, as well as a drop in hardness of 15 %. This drop in hardness is produced through two effects, a larger grain size, which according to Hall-Petch, does cause a loss in hardness and strength, as well as some form of stress relief, however to what degree both contribute is not known.

Another important aspect is the standard deviation which experience no definite drop. The local variation in deformation and indentations only effecting single grains at the time is still in effect, as well as the porosity influence on the hardness measurements.

5.1.2 Heat treatment of sponge at 600°C

Titanium at 600°C has a self-diffusion rate of 10^{-18} m/s^2, still considered small, however, the literature puts this temperature above normal stress relief treatments and the expected effect should be noticeable. The microstructural images show a clear recrystallization of the microstructure with a drop of grain size from 81µm to 19µm, a drop of 77 % in grain size. Any of the former deformation twins seen in the microstructural images from untreated and heat treated at 400°C can no longer be seen. The small grain size may be accounted from the extreme deformation twinning, as the former stored deformation energy has been released and the recrystallization starts at grain boundaries and deformation. This significant drop in grain size should give a hardness increase, however a drop of 30% in hardness is registered. It therefore seems that the stress relief overshadows any strength increase in from the smaller grain size. This is in accord with the literature where it is reported that any heat treatment and subsequent microstructure change will not lead to any noticeable strength increase in alpha and near-alpha alloys.

The drop in standard deviation from 30 HV to 20 HV is probably caused by removal of the local deformation and smaller grain size, where now the indentations impacts several grains. The still large standard variation of 20 HV does show the impact the porosity has on the indentations.

5.1.3 Heat treatment of sponge at 800°C

Titanium at 800°C has a self-diffusion rate of 10^{-16} m/s^2 and is higher than any industry stress relief scheme found. This heat treatment continues the trend from the 600°C treatment with recrystallization and reports larger grains with an average size of 28µm. As earlier discussed the former results and theory indicates no noticeable direct strengthening effect through any change in microstructure, this coupled with the expected large stress relief effect would indicate a lower average hardness. This is not the case, where the average hardness stays the same at 120 HV. The microstructural images do not show any high levels of deformation, and the expected stress relief does seem to have occurred, therefore there must be another effect influencing. A possible explanation, may lie in the large increase in diffusion rate and standard deviation. At this temperature, diffusion can have a large effect in diffusion of contamination elements, and assuming the heat treatment process is less clean than formerly stated, interstitial elements may be the reason for the hardness increase. The stress relief have resulted in hardness drop, however the interstitial contamination of oxygen, nitrogen and hydrogen may lead to a clear increase, as only an increase of 0,1 wt. % of oxygen or nitrogen can give a hardness increase of 60 HV and 50 HV respectively. This may indicate a contamination in the heat treatment and, even though it is most obvious in the heat treatment at 800°C, will also have affected the sponge treated at 400° and 600°C.

This can be supported by the hardness results from heat treatment of the secondary batch, where larger titanium sponge, above 4mm in diameter, have experience the same heat treatment. The heat treatment at 800°C of the secondary sponge shows an average hardness of 109 HV, a drop of 20 %, but with an increased standard deviation of 38 HV. If the interstitial elements are the cause of the high hardness in the primary batch they would have a slightly different effect on the secondary batch. The reasoning being that these sponges are much larger, and therefore the travel length of the diffusing interstitial elements is longer and the overall surface area of the sponges in heat treatment is lower. The secondary batch would have a relative high amount of interstitial elements in and close to the surface of the sponges, however deeper in the sponges less contamination would occur. As the stress relief have occurred in all of the sponge there would be areas with low contamination and a low hardness, and areas with high contamination and high hardness. The general drop in average hardness from the stress relief, together with the increased standard variation may be proof of this hypothesis.

5.1.4 Summary of heat treatments

Based on the assumption that the microstructure has little to no effect on the hardness a stress relief have been registered at all heat treatments. All heat treatments were effective of reliving stresses, however the heat treatment at 800°C showed that a greater care is needed in selection of heat treatment processes, and the currently used tube furnace is not atmospheric closed enough for stress reliving of titanium.

The heat treatments also showed that the titanium sponge have a recrystallization temperature below 600°C indicating that the titanium will undergo recrystallization during the current parameters for the screw extrusion. If the grain size of titanium sponge and screw extruded material is not important the heat treatment at 600°C does result in the lowest hardness and may be the easiest sponge to consolidate. However, if there is a wish to have more control over the grain growth, the heat treatment at 400°C may be more favourable. The deformation during screw extrusion however may be so large as any former microstructure will have little effect on the eventual recrystallization during consolidation in the screw extrusion process.

5.2 Effect of heat treatment on degree of consolidation

At this stage in development of the screw extrusion process the toll on the equipment used in screw extrusion is too high. Equipment are damaged and constant machining and grinding has to be done to removed cold welded titanium. The thought behind heat treatment of titanium sponge is reducing its hardness and therefore easing consolidation and pressure conditions in the screw extruding process. Two parameters are presented earlier, the titanium sponge and the temperature. The titanium sponge was the as received sponge, and two other differently heat treated sponge, at 400°C/1 hour and 600°/1 hour. This parameter is the important one as this is the indication if consolidation will increase with a lower hardness in sponge. The temperature parameter is added as a control parameter serving the function of checking the experiments and measuring method of increased consolidation. The idea being that at higher temperatures the pressure conditions is lower, diffusion higher and consolidation easier. To reiterate, the sponge parameter is the indicator on effect in the screw extrusion process, and temperature is the reference group.

The medium pressure torsion experiments are experimental research as a lot of the work was adapting the procedure to the needs for titanium, as earlier research were only done with aluminium. Titanium being significantly harder, with higher melting temperature, and the corrosion resistance, made the research difficult. Because of the time restrictions, compromises were needed such as the inability to mount any cooling directly on the MTS 311 and production of new holders was not possible. The main setbacks are a lack of temperature control and a sample section at 40 mm.

The temperature problem arises because the connection between holders and loading cells are solid steel with a relative high thermal conductivity. The max temperature of the loading cells are roughly 150°C, which made heating of equipment in the MTS 311 possibly damaging for the loading cells. This impacted the experiments by lowering total experiment time as too long times could lead to overheating of the loading cells, and any direct heating during the experiments was not possible. The lack of in situ heating caused a lack of control of temperature and number of rotations possible as the heat in the piston and compression disk could sink below target temperature. Measuring of the temperature was not possible as the equipment needed to be hot mounted into the MTS 311, removing the ability to place thermocouples inside the piston. All these temperature problems influenced experiments, as the target temperature for the piston would sink quickly, influencing consolidation and torque needed to shear deforme the sample.

The sinking of temperature leading to higher torque leads to the next problem, force restrictions. Due to sample section size of a cylinder with a diameter of 40mm, the maximum compressive forces are only at 400 MPa and the max torque forces of 1,6kN to hold the piston is inadequate. There were several times the compressive forces needed to be lowered, resulting in less sticking, leading to less torque needed to resume rotation. The original parameters planned for the experiment was, the two formerly mentioned, input material(sponge) and temperature variation, the third being number of rotations. However, the low temperature and low max torque made rotations above 5 rounds difficult, resulting in weak academic results.

A third source of error may be in the heat treatment of sponge. The difference in the analytical heat treatments and those with the purpose of creating sponge for the MPT process were the amount of sponge per heat treatment. The increased amount may give a varied response to the heat treatment as any investigation into a filled alumina boat regarding temperature distribution and chemical contamination is lacking.

Another important notice is that after several experiments were done, the piston started to show damage, from grinding of the piston to remove deformed areas and cold welded titanium. This enlarged the clearance between piston and sample holder walls, resulting in material build up between piston and the walls during experiments, deviating from the experimental parameters specified when Fredrik Widerøe (2011) validated the procedure in his article. It's difficult to ascertain if this material builds up affected the experiment, and at what time it started to influence the results. Below in Figure 5-1, all experiments done after the experiment with heat treated sponge at 400°C and an experiment temperature at 400°C are removed.

The results shown are the ones that shows positive correlations with increased consolidation, and are closest to expected results. Looking first at none heat treated sponge, the consolidated depth increases with higher experiment temperature, with an increase of 166 %. The same correlation can be seen with sponge heat treated at 400°C, where an increase in experiment temperature leads to 32 % deeper consolidated area. Examining the parameter titanium sponge, the same positive correlations can be seen. A change to 400°C heat treated sponge leads to an over 105 % increase in consolidated area, and with sponge heat treated at 600°C the consolidated area is 119 % deeper.

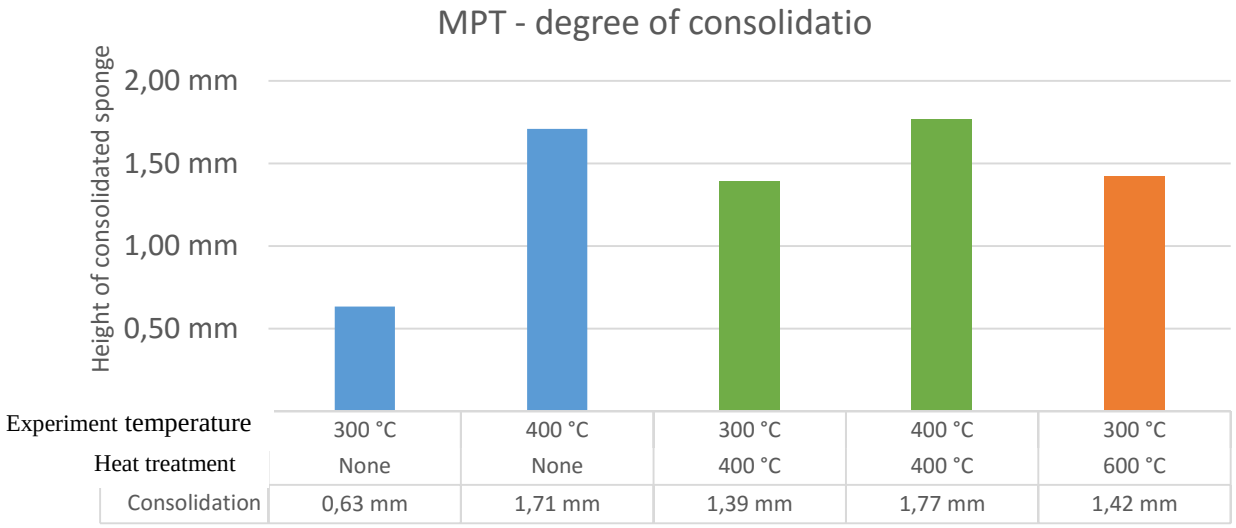

Figure 5-1. A bar diagram of the consolidation data in Table 4-2. Same figure as Figure 4-10 where the four last experiments have been removed. Bars coloured blue are disks from as received sponge, green are disk of heat treated sponge at 400°C/1 hour and orange are disk heat treated at 600°C/1 hour.

Remember these are results separated from others as all correlations disappears when all results are considered. All results are shown in Figure 5-2, sorted by categories. There is one test with heat treated sponge at 600°C and experiment temperature at 300°C showing a lower consolidated depth than for non-treated sponge at experiment temperature of 300°. Another test where an increase of experiment temperature minimises the depth of consolidated area. The last experiment done, heat treated sponge at 600°C and experiment temperature at 400°C, expected to have the largest consolidated area, shows the lowest consolidation depth

Either the characterisation method is unsuitable for this process by being inaccurate or higher temperature and/or lower hardness in sponge does not have a direct connection with the depth of the consolidated area. The third source of error may be insufficient heat treatment of sponge, resulting in a sponge with different characteristics than the former analysed sponge.

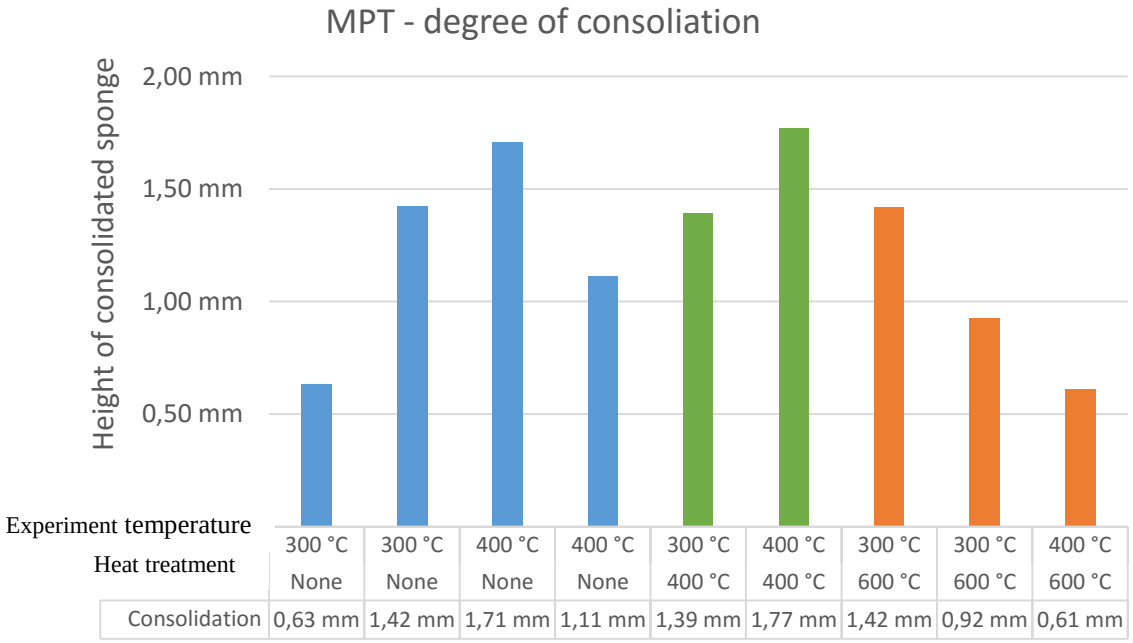

Figure 5-2. Medium pressure torsion data from Table 4-2 , presented by category. Bars coloured blue are disks from as received sponge, green are disk of heat treated sponge at 400°C/1 hour and orange are disk heat treated at 600°C/1 hour.

The reason for choosing to present data with some removed is that all data that contradicted expected results are done after one specific experiment, and perhaps at that time the material build up along the walls started to have an effect on the experiments or the tube furnace became contaminated or less closed.

A quick discussion of the torsion can reflect on the trend showing a quick drop in force, and then a gradually increase. This may be from the sponge being relatively free to move in the beginning, where the rotations and shear results in movement and shifting of the sponge. The more rotations, results in less possible movement, and more deformation in the sponge. Interesting mentioned is that the depth of consolidated area varies along the diameter where the centre and edge has the lowest amount, and 10 % of radius away from edge is often the deepest. This is an effect of the pressure conditions in the test area, and revolves around

whether the sponge is sticking to the piston, die walls or move freely. Equation 1 indicates that the largest deformation should be at the edge, however this is not the case where gliding along the die walls is more prominent. Therefore, the area closest to the die wall, but not touching, experiences the highest shear, and the sponge close to the wall moves with the wall.

5.3 Characterisation of the screw extruded profiles ϕ30 & ϕ 20

Tackling the second question the discussion will begin with the chemical composition of the screw extruded profiles and the change from titanium sponge. After this, with hardness testing and microstructural imagining the homogeneity of the sample, microstructure and degree of deformation will be investigated. The last section will focus on tensile testing of tensile specimen machined out from the screw extruded profiles, with the intent to examine the degree of consolidation of the product and determine, together with the hardness and microstructure results, what after treatments are needed.

5.3.1 Chemical composition of screw extruded profiles

The degree of contamination during experiments are interesting as contamination elements such as oxygen, nitrogen, carbon and hydrogen have a large influence on titanium's characteristics. The interstitial element concentrations of these elements are high due to titanium's HCP lattice, were the atoms easily place them self and diffuse between prism and basal planes. The experiments are done in air, and at a high temperature so a large increase in these elements is expected, however to what degree is uncertain. A small effect is considered if the screw extruded profiles are within commercially pure titanium, and no direct steps are required. A large increase in contamination is when the levels are clearly above CP specified levels and development into screw extrusion in inert atmosphere needs to be done.

The chemical composition shows a large increase in oxygen and nitrogen, small increase in carbon and an unknown increase of hydrogen. The hydrogen increase is important since hydrogen severely embrittles titanium, however the increase cannot be calculated before data on hydrogen levels in the titanium sponge are known. If the titanium sponge is the MHT-100 Brand the hydrogen levels is reported at 0,001 wt. % giving an increase of 300% in both cases. The level of 0,003 wt. % of hydrogen is still within the commercially pure titanium with levels at 0,007-0,015.

The possible hydrogen increase of 300 % is comparable with the oxygen level increase of 223% and 352% of samples φ30 and φ20 respectively. This addition of oxygen puts the extruded samples close to the CP grade of titanium, where the range is 0,15 to 0,18 wt. % The relative high increase of nitrogen samples φ30 and φ20 are harder to explain. In terms of the φ20 sample, the solution may be in the merely the order of magnitude lower nitrogen content than the oxygen in the primary sponge, as the levels of nitrogen and oxygen are comparable where 0,14 wt. % oxygen and 0,12 wt. % are 0,42 at. % and 0,41 at. % respectively.

The φ30 sample on the other hand has a nitrogen level that is twice as large as oxygen, putting it 500 % above CP specified limits. Nitrogen, being an alloying element with similar effects as oxygen, are often omitted in titanium alloys as the oxygen is strengthening enough and the loss in ductility needs to be limited. The high levels of both oxygen and nitrogen should severely increase hardness and strength and lower the ductility.

The reason for the increase in hydrogen, oxygen and nitrogen is most likely a result of the process is done in air, letting large amounts of oxygen, nitrogen and hydrogen diffuse into the material. The general purity level of the screw extruded samples are more than acceptable in commercially pure titanium, however the nitrogen levels are too high. A more robust control of the degree of contamination is needed, and some development into doing the process in an inert atmosphere should be done. One method already tested out is filling the chamber with argon before beginning of the experiment. The heavier than air argon will remain in the chamber, hopefully severely diminishing the oxygen, nitrogen and hydrogen contamination. An EDS investigation into precipitation of brittle and hard titanium phases have not been done due to the general low level of elemental contamination.

5.3.2 Hardness and microstructure of the cross sections

The first subject to tackle is the different average hardness results found of the cross sections of the φ20 sample. Because of the large difference, knowing where the cross sections samples are taken from the extrusion sample is necessary. As indicated in Figure 5-3 the cross sections are cut from different sections of the screw extruded profile.

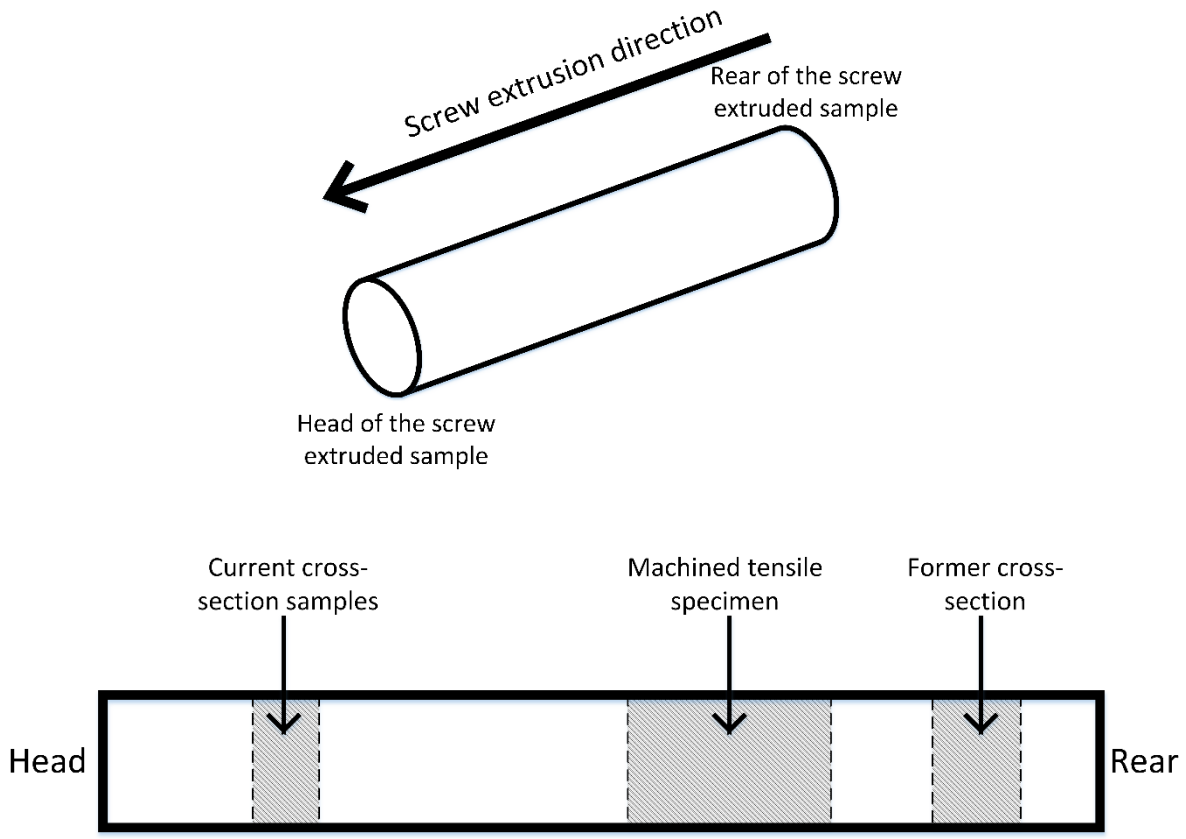

Figure 5-3. The figure illustrates where the samples are taken. Length and exact positions are not given as they are not known. The gaps between the shaded areas are sample material that have been used for other purposes.

As the process is still in early stages and continuous production has not been achieved, different sections of the screw extruded samples may have experienced different max temperatures and holding times, this most likely resulting in different degrees of deformation,

stress relief and precipitation. The variation does undermine the characterisation of the screw extruded samples, as it clearly has different hardness along the screw extrusion direction, hinting to that most likely the degree of consolidation, microstructure, precipitation and chemical composition may also vary. The φ30 sample showed no significant difference in average hardness as both were within each standard deviation, however, some inhomogeneity as seen in the φ20 needs to be expected. This discovery, showing a probable variation in characteristics along the screw extruded profile, will hopefully diminish when a continuous process is achieved, but it also stresses a possible need for cutting of the head and rear of the samples.

Assessing the variation in characteristics in the short length, the examination of the cross section maps parallel to the extrusion direction does not show any significant variation. Both show a highly deformed centre with less deformations at the sides. At the φ30, there is a noticeable increase in deformation at the edge of the sample, however, this is not seen in the φ20 sample. There may be a number of reasons for this, first one being that the samples are taken from different places at the screw extruded samples and the exact temperature and holding time of these section are not known. The φ20 samples cross sections are close to the head of the screw, giving it a longer time to consolidated and perhaps therefore the deformation would be lower. The section of the φ30 sample may have had less holding time within the chamber causing more deformation. Another reason may be with the difference in die diameter, where φ30 die diameter gives a less homogenous distribution of deformation, resulting in larger variation of deformation and thereafter recrystallization, giving the four distinct areas, where the φ20 samples only has the three.

Both cross sections Normal to the extrusion direction show a similar correlation with high deformation in the centre, a softer region and then a highly deformed region. However, it comes across more clearly that there is a fourth area close to the edge with the lowest hardness in both samples. Both cross sections Normal to the extrusion direction shows a lower average hardness than their parallel cross sections. The reason for this lies in the surface area of each formerly mention hardness sections. The Normal cross sections have a larger degree of edge surface compared to their parallel partners, and with this area being at a general lower hardness, reflects this in the lower average hardness.

The internal area with the highest hardness is an area closest to the screw, perhaps giving larger pressure conditions and faster speeds, consolidating the sponge at a higher rate causing more deformation and less stress relief. The area just outside seems to be of a slower moving region causing less deformation. The third area and fourth is most likely one area, but with a different degree of recrystallization. The reasoning behind this is based on earlier research into the flow patterns in screw extrusion (Widerøe and Welo, 2013). Where Widerø identified two specific regions in the extruded profiles, diving the extruded profiles into centre and edge, centre being fast moving material with a lower amount of deformation, the edge is formed by slower moving material with a higher degree of deformation from the process. The fourth area, edge and third area may be the same slow moving, highly deformed area.

The different degrees of recrystallization may be explained by the variation in deformation occurring at the edge, giving good conditions for a recrystallization, areas with less deformation would have less recrystallization and high hardness. Another possibility may be the large temperature gradients, due to titanium’s low thermal conductivity. However, the temperature profile within the chamber, zone 2, is hard to predict, measure or numerically calculate. Therefore, knowing if there is a temperature gradient within the screw extruded

samples when exiting the die is difficult. The cooling in air when leaving the die and formation of oxide surface is neglected as the depth of the oxide layer at those temperatures is fairly low, with oxide layers formed at 650°C are measured to be less than 0,05mm (M.J. Donachie, 1988). The discussion and conclusions of these maps relating to the process engineering of screw extrusion is exciting but outside the scope of this thesis.

Looking at the calculated hardness data, shown in Table 5-1, based on the chemical composition there are similar tendency showing that the measured hardness for the φ30 sample is close to the theoretical hardness. Considering the range of hardness at the measure maps it can be observed areas with very high and hardness and other areas with low hardness. The high hardness may be explained by a high local deformation, however the low hardness values between 150 HV to 225 HV may indicate a severe local variation in chemical composition. The same observation can be done with the φ20 sample, where some hardness levels are measure down to 150 HV indicating the same local variation. The general lower average hardness found in the φ20 compared to the theoretical data show, that more than likely the chemical composition varies both locally and globally along the screw extruded profile.

Table 5-1. Measured hardness data compared to calculated hardness based on theoretical equations in chapter 2.2.2

	φ20Normal	*φ20Parallell*	*φ30Normal*	*φ30Parallell*
Average hardness	190 HV	236 HV	245 HV	251 HV
Calculated hardness	257 HV		263 HV	

Moving to microstructural images of the cross sections. It should be mentioned that variation do apply, especially in such inhomogeneous samples as these screw extruded profiles, however the same trend was spotted. The general description of the samples, from the microstructure, is that a variation in degree of deformation and pockets of equally sized grains are spread out. The largest grains and largest range of grains can be seen at the edge, indicating that the growth basis for recrystallization was largest at the edges, at the same time showing a large variation in the growth basis. This indicates that the samples have the largest deformation in edge, with clear local variation. Further inwards, a drop in grain size and grain size range is observed showing a lesser degree of deformation and subsequent recrystallization. The centre of the cross sections had a microstructure which was hard to determine, the overall deformation, as well as some strain induced microstructure from preparation, overshadowed the microstructure, making it difficult to find any distinct microstructure and connection. The overall tendency was a high rate of deformation, interspersed with recrystallization to varying degrees in between a clear flow pattern which can be seen in Appendix B from the macro graphs of the samples.

5.3.3 Tensile properties

The hardness indentation of the cross sections in the former subsection does predict a high variation in the tensile data as the tensile specimen are from different sections along the cross section of one sample. From the hardness mappings, the φ30 should show a larger variation in properties as the hardness range in the φ30 cross section range from 124 HV to 426 HV. The screw extruded φ20 with a lower average hardness and range of data 107 HV to 312 HV,

should give a more homogenous sampling data. The also large variation in grain size and deformation spotted in the microstructural investigation indicates that no clear definitive tensile properties can be found. The microstructural images show a large variation in grain size and deformation. The likelihood for brittle specimens are large, with expected fracture manners such as shear and cleavage. The heat treatments will hopefully be an indication if annealing will be effective treatment. Any flaws in the microstructure images was not spotted, however cracks in the size of 1µm or smaller would be hard to detect.

Out of the total 18 tensile specimens machined out, 15 gave valid tensile data, two failed in the heads and one during application of gripping tension. The intention of these tensile samples was to examine the degree of consolidation. An interest was to see if anyone could experience yielding and plastic deformation or if just all had brittle failure. The overall picture when looking at the tensile data, where 8 of 15 didn't have a yield point, is that nothing conclusive can be determined of the specific tensile strength and ductility, however, it shows a clear need for after treatment of screw extruded profiles. The samples show a large variation in properties, where many experienced no yield and some showing plastic deformation. There are also several specimens deviating heavily from the theoretical Young's modulus of titanium, with a registered range of Young's modulus from 24 GPa to 229 GPa. The general image is that the tensile specimens are indeed very brittle and the elastic region for most specimen achieve fracture when one certain flaw reaches critical shear stress.

The two most reliable parameters in this test are the hardness and ultimate tensile strength, an overview of the average data is shown in Table 4-5. The tensile specimens are easily separable through hardness as it can be observed that the hardness of the φ30 have a hardness range of 178 HV to 257 HV, with an average hardness of 222HV. This is one standard deviation within the average hardness of the cross sections shown in Table 4-5. It should be noted that 6 of the samples giving the average of 222 HV have been heat treated, which may be the reason for this slightly lower average hardness.

Table 5-2. Overview of average hardness and UTS of the tensile specimen.

Tensile specimen	***Avg. HV***	***St. D***	***Avg. UTS***	***St. D***
φ20	354 HV	42 HV	710 MPa	124 MPa
φ30	222 HV	26 HV	484 MPa	56 MPa
Grade 1	122 HV	-	240 MPa	-
Grade 2	200 HV	-	340 MPa	-

The average hardness of the ϕ20 is much higher than the measured values in Table 4-5, and more comparable with the values in Table 4-6, where the average hardness of the φ20 sample is 336 HV, within one standard deviation. Table 4-6 being results from a former rapport of testing the same material(Meling, 2015). These are also heat treated, however, in this case the tensile specimens have a higher average hardness. It should therefore be concluded that the section of the screw extruded sample made from the tensile specimen do not have the same characteristics as the cross sections that are examined for hardness.

Evaluating the data in Table 5-2, comparing the average hardness and average UTS to Grade 1 titanium, shows hardness in the φ20 is 290% higher than for grade 1, similarly the UTS is 296% higher than for grade 1. The same tendency can be observed with the φ30, showing a hardness at 182% compared to grade 1, and a UTS 200% higher than grade 1. This does indicate a clear relation between hardness and ultimate tensile strength, and if the specimens were more stable maybe yield strength as well. Finding such relations and determining empirical equations are very interesting, however due to the geometry of the samples and the general low control of the specimen's properties this is neglected.

Looking into SEM, the four samples were chosen to represent the different behaviours seen in the tensile specimens. The two ductile samples were investigated as the degree of plastic deformation was not expected. Both samples showed similar modes of fracture with a general intergranular manner and small signs of cleavage and/or shear. The sampled 20_3, untreated tensile specimen from φ20, also showed secondary cracks arrested. The two others were chosen for their characteristic tensile curve. 30_3 showed a large Young's modulus at 218GPa and no plastic deformation, reasons for this behaviour was not discovered, although the fracture mode was identified as shear. The last on, had an uncommon tensile curve with a Young's modulus at only 24GPa and then an expected mix of elastic and plastic deformation. The reason for the odd behaviour was not understood through fractural analysis as only signs of large shear regions interspersed with small regions of intergranular fracture was detected.

The high deformation, local and global variation in characteristics and fairly brittle fracture indicates a material, not as expected with large flaws, but with such high deformation and interstitial contamination that any dependable ductile behaviour is not present. To counter this, the process need to develop a cover atmosphere during the screw extrusion, stopping large influx of contamination elements such as oxygen, nitrogen and hydrogen. Another countermeasure to achieve a more ductile behaviour is after treatment. The heat treatment of the tensile test proves that annealing not enough. Some sort of compression while heating at high temperatures is needed. Good control of atmosphere and temperature is needed during screw extrusion and a controlled machining of surface may be needed if an oxidised surface is created.

6 Summary and conclusion

Will a heat treatment of the as received titanium sponge caused a drop in hardness and consequently ease consolidation of sponge in screw extrusion? And, to what extent does the screw extruded profiles satisfy industry qualifications?

The answer to the first question is complicated, where the heat treatments do indicate a loss in hardness and occurrence of recrystallization with heat treatments at and above 600°C. Whether this causes easier consolidation of sponge in screw extrusion is more unclear. The results were inconclusive, even though some showed a positive correlation, the lack of more samples and better control over parameters overshadows the possible correlation.

Regarding the second question, the answer is no. There is a large increase in contamination elements, and even when oxygen and hydrogen are within the limits, the nitrogen levels are too high. A development within screw extrusion in a protective atmosphere is needed. It is also a need for post treatment of the screw extruded profiles, as they are heavily deformed and inhomogeneous across their cross sections. Annealing is proved, through tensile testing, not to be enough as there are too many flaws, leading to a need for deformation at high temperature levels, compacting the material, deforming it and causing recrystallization.

- Heat treatments of titanium sponge leads to a stress relief of titanium sponge, causing lowered hardness at all tested temperatures. Recrystallization of the microstructure is registered after heat treatments at and above 600°C.
- The tube furnace used may not be fully sealed letting contamination elements into the heat treatment atmosphere and diffusing into the titanium. This is most prevalent at 800°C.
- The medium pressure torsion experiments are deemed inconclusive because of lack of control over parameters. A more vigorous study, with permission and time to modify the MTS 311 is needed.
- Development into screw extrusion in an inert atmosphere is needed as the nitrogen and oxygen levels of the screw extruded profiles are too high. If various grades of titanium and other alloys are to be developed, better control of contamination is needed.
- Hardness and microstructure examination of the screw extruded samples uncovered a large degree of variation locally and globally along the screw extruded profiles. Some variation will decrease with achieved continuous production, however after treatments of the samples are needed.
- The tensile test supports the need for after treatment, showing brittle behaviour in almost all samples. The heat treatments of the tensile specimen also indicate that annealing is not sufficient, as compressive deformation to close cracks and flaws are also needed.

7 Future work

Future work, industry is interested in highly ductile Titanium thread with specific chemical compositions. The recommended future studies are a study into a heat treatment of titanium sponge, verification of a correlation between decrease in hardness of titanium sponge and ease of consolidation, and a more homogenous screw extruded profiles with controlled chemical composition.

The titanium sponge heat treatment should focus on achieving a heat treatment capable of heating more than maximum 35 grams of sponge at a time, in a homogenous manner with a more protective atmosphere than provided by the used tube furnace.

The verification of a positive correlation between heat treatment of sponge and ease of consolidation should be continued with a new set of equipment and built-in cooling on the MTS 311, giving more control over parameters, making heating to temperatures such as 600°C or more possible.

Achieving a more homogenous screw extruded profile can be achieved by developing a protective atmosphere in the screw extruding chamber, removing the contamination of oxygen, nitrogen and hydrogen. A development of screw extrusion at increase temperatures would also clearly ease the consolidation and give a more homogenous sample. Finally, investigations into after treatments of screw extruded profiles should be examined and evaluated.

8 References

ASHBY, H. J. F. M. F. 1982. *The plasticity and Creep of metals and Ceramics, Chapter 6* [Online]. http://engineering.dartmouth.edu/defmech/. [Accessed 18.06 2016].

BOYER, R., WELSCH, G. & COLLINGS, E. W. 1994. Materials Properties Handbook - Titanium Alloys. ASM International.

CONRAD, H. 1981. Effect of interstitial solutes on the strength and ductility of titanium. *Progress in Materials Science,* 26**,** 123-403.

ERIKSEN, L. 2013. *Combined EBSD-Investigations and In-situ Tensile Tests of a Direct Metal Deposited Ti6Al4V-Alloy.* Master thesis, Department of Material Science and Engineering, NTNU.

FREDRIK WIDERØE, T. W., HARALD VESTØL 2011. A new testing machine to determine the behaviour of aluminium granulate under combined pressure and shear. *International Journal of Material Forming,* 6**,** 199-208.

HANDBOOK, A. 1990. Properties of Pure Metals, Properties and Selection: Nonferrous Alloys and Special-Purpose Materials, . *ASM Handbook, ASM International.*

HANDBOOK, A. 2015. Al (Aluminum) Binary Alloy Phase Diagrams, Alloy Phase Diagrams. *ASM Handbook.* ASM International.

LIU, Z. & WELSCH, G. 1988. Effects of oxygen and heat-treatment on the mechanical properties of alpha and beta titanium-alloys. *Metallurgical Transactions a-Physical Metallurgy and Materials Science,* 19**,** 527-542.

M.J. DONACHIE, J. 1988. Titanium: A Technical Guide. *ASM INTERNATIONAL.* ASM International.

MATHISEN, M. B. 2012. *In-Situ Tensile Testing Combined with EBSD Analysis of Ti-6Al-4V Samples from Components Fabricated by Additive Layer Manufacture.* Master thesis, Department of Material Science and Engineering, NTNU.

MELING, J. I. 2015. Characterisation of titanium sponge and extruded material from screw extrusion of Titanium sponge. Project report, NTNU: Department of Materials Science and Engineering.

METALPRICES.COM. 2016. *Aluminium and Titanium prices, metalprices.com* [Online]. www.metalprices.com: Argus Media. Available: https://www.metalprices.com/ [Accessed 18.06 2016].

PETERS, M., HEMPTENMACHER, J., KUMPFERT, J. & LEYENS, C. 2005. Structure and Properties of Titanium and Titanium Alloys. *Titanium and Titanium Alloys.* Wiley-VCH Verlag GmbH & Co. KGaA.

REISO, O., WERENSKIOLD, J. C., AURAN, L., ROVEN, H. J. & RYUM, N. 2006. *Ekstruder for kontinuerlig ekstrudering av materialer med høy viskositet.(Screw extruder for continuous extrusion of materials with high viscosity).* Norway patent application 20065308.

ROVEN, H. J. 1985. Materialtekniske aspekter ved sveising av titan og titanlegeringer. *SVEISETEKNIKK***,** 93-99.

SIBUM, H. 2005. Titanium and Titanium Alloys – From Raw Material to Semi-finished Products. *Titanium and Titanium Alloys.* Wiley-VCH Verlag GmbH & Co. KGaA.

SKORPEN, K. G., MAULAND, E., REISO, O. & ROVEN, H. J. 2014. Novel method of screw extrusion for fabricating Al/Mg (macro-) composites from aluminum alloy 6063 and magnesium granules. *Transactions of Nonferrous Metals Society of China,* 24**,** 3886-3893.

TRØAN, E. N. 2014. *Effect of Solution Annealing on Plasma Weld Deposited Ti-6Al-4V Characterized by In-Situ Tensile Testing Combined With EBSD.* Master thesis, Department of Material Science and Engineering, NTNU.

WIDERØ, F. 2012. *Material flow in screw extrusion of aluminium.* PhD thesis 2012:183, Department of Engineering Design and Materials, NTNU.

WIDERØE, F. & WELO, T. 2013. Using contrast material techniques to determine metal flow in screw extrusion of aluminium. *Journal of Materials Processing Technology,* 213**,** 1007-1018.

WILLIAMS, J. C., BAGGERLY, R. G. & PATON, N. E. 2002. Deformation behavior of HCP Ti-Al alloy single crystals. *Metallurgical and Materials Transactions A,* 33**,** 837-850.

ZHILYAEV, A. P. & LANGDON, T. G. 2008. Using high-pressure torsion for metal processing: Fundamentals and applications. *Progress in Materials Science,* 53**,** 893-979.

Appendices

A. Temperature profile of compression disk

The temperature profile is calculated using Fourier's second law, see equation 2. The equation is adapted to the MPT by dividing the MPT titanium disk into a matrix of 50 by 400 nodes, where the distance in every direction is 1 mm, see Figure A-1. Its aimed at calculating the temperature distribution in the cross section of the compressive disks.

Figure A-1. An illustration of the MPT disk matrix. Every intersection is a node, including the edge of the box.

Formel A-1. The general heat transfer law. α is material specific coefficient.

$$\frac{du}{dt} - \alpha\nabla^2 u = 0 \tag{2}$$

The heating of the sponge before full contact between wall and piston is neglected as this calculation is to determine the minimum holding time before torsion, and therefore, any extra heating will not work against us. The calculations begin when the piston is at max load, 50 tons, and the titanium sponge and sample wall have approximately full contact. It is assumed that at the beginning of calculations that the edges of the MPT disk have the same temperature as the steel sample holders and piston. Any generation of heat as a result of compressive stress or torsion is neglected. Equation 3 shows the two dimensional equation that is used.

Formel A-2. The heat transfer law for two dimensional heat transfer. k is thermal conductivity, ρ is density and C_p is specific heat capacity.

$$\frac{dT}{dt} = \frac{k}{\rho C_p}\left(\frac{dT^2}{dx^2} + \frac{dT^2}{dy^2}\right) \tag{3}$$

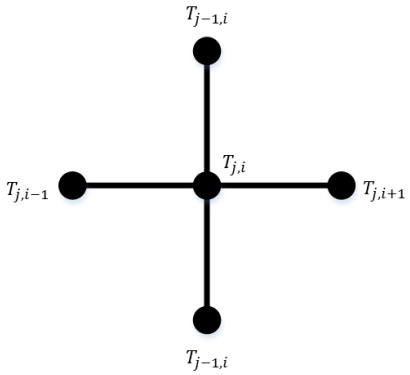

Figure A-2. Illustration of node relationships.

Equation 3 is the final equation, finding the next temperature step based on surrounding temperature.

Formel A-3. Equation used for calculation of the heat transfer. The temperature placement are indicated in Figure A-2.

$$T_{j,i}^{t=0+dt} = T_{j,i}^{t=0} + \frac{k * dt}{\rho C_p * dx^2}\left(T_{j,i+1} + T_{j,i-1} + T_{j+1,i} + T_{j-1,i} - 4 * T_{j,i}\right) \quad (4)$$

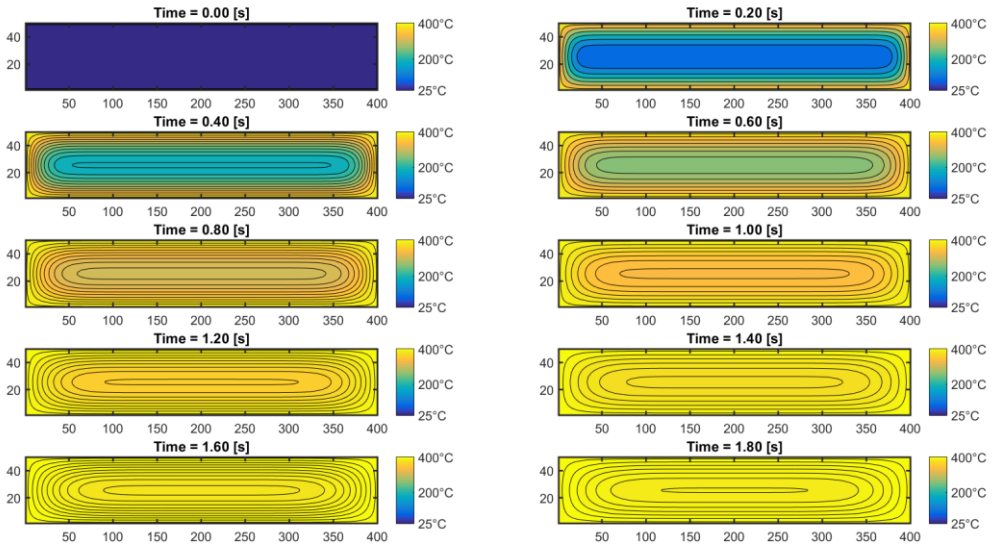

Figure A-3. Temperature profiles for the cross section over time.

B. Light emission field images of the cross sections.

These pictures are Macrographs of the cross sections. Notice the flow patterns that are revealed from etching. The hydrofluoric acid attack protruding geometries, and often in titanium enhances deformation very clearly when the deformation is to the large degree as from screw extrusion. The dark areas and lines show high levels of deformation and coincides with the high hardness from the grid maps in chapter 4.2.2.

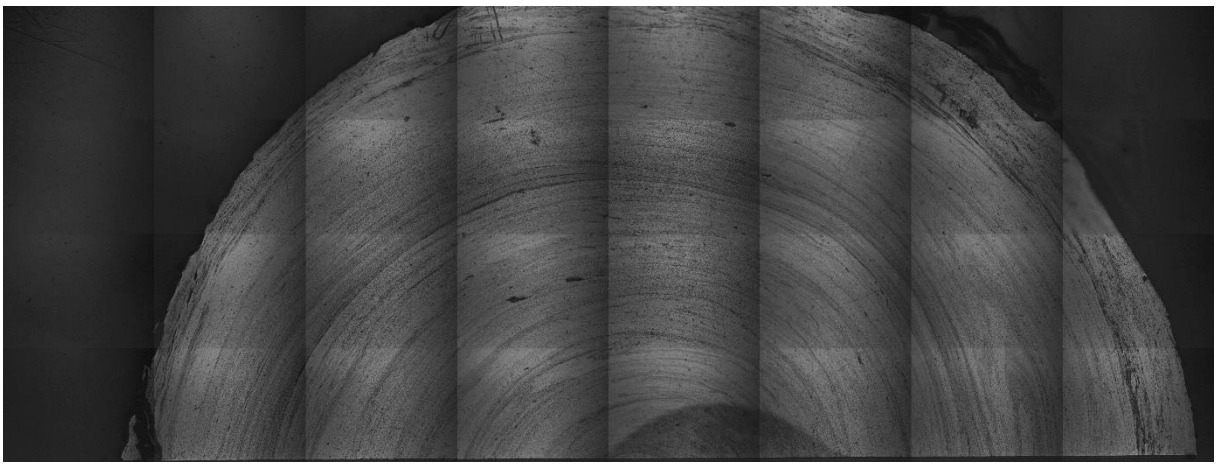

Figure B-1. Overview picture of the cross section normal to the extrusion direction. Sample φ20.

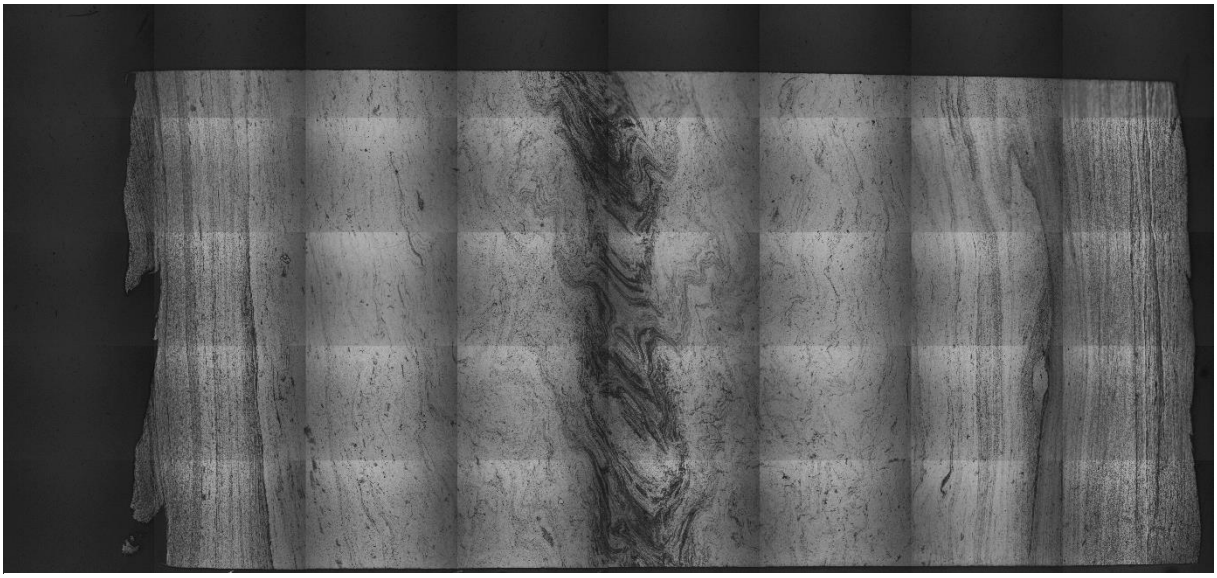

Figure B-2. Overview picture of the cross section parallel to the extrusion direction. Sample φ20.

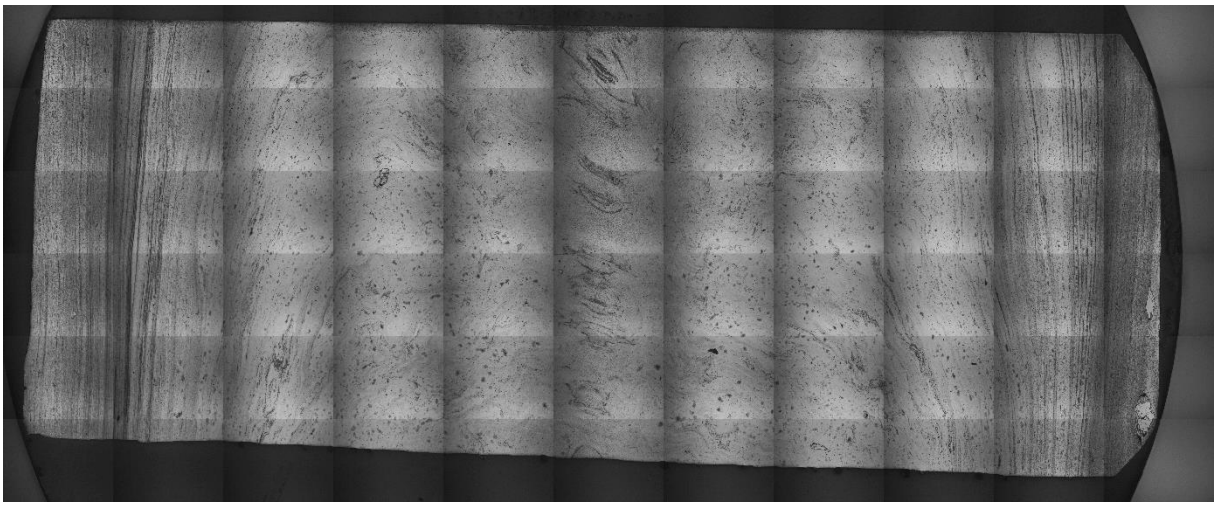

Figure B-3. Overview picture of the cross section parallel to the extrusion direction. Sample φ30.

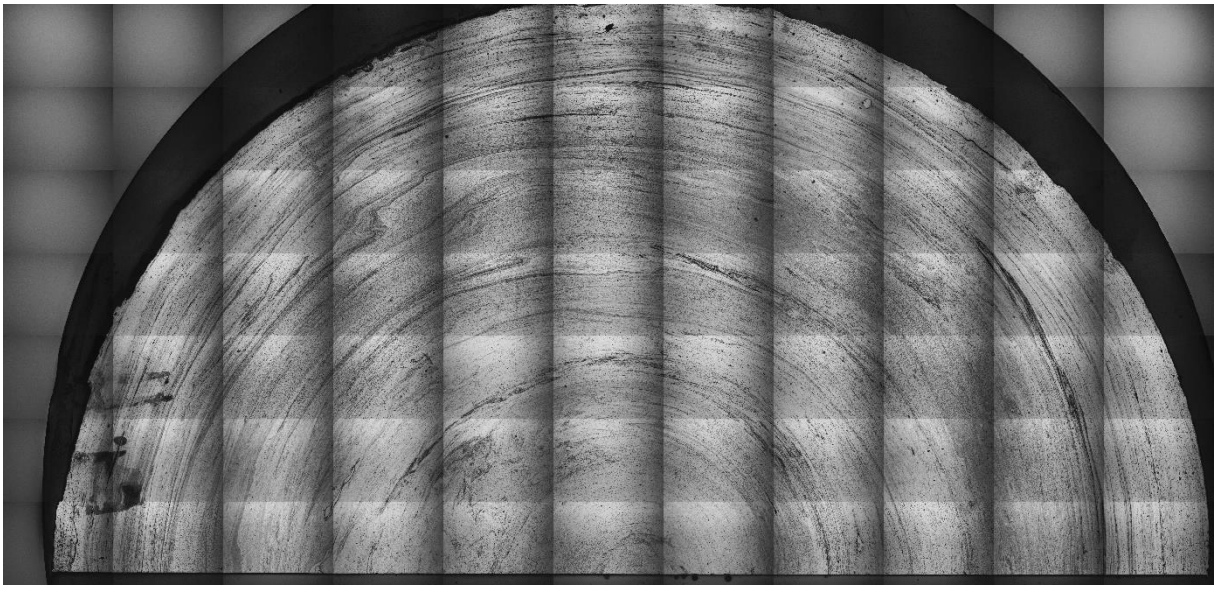

Figure B-4. Overview picture of the cross section Normal to the extrusion direction. Sample φ30.